Seismostratigraphy of Late Quaternary Sediments and Lake Level History, Eastern Lake Erie

by

Gordon Cameron

Submitted in partial fulfillment of the requirements

for the degree of Master of Science

at

Dalhousie University

Halifax, Nova Scotia

August 1991

DALHOUSIE UNIVERSITY

DEPARTMENT OF GEOLOGY

The undersigned hereby certify that they have read and recommend to the Faculty of Graduate Studies for acceptance a thesis entitled "Seismostratigraphy of Late Quaternary Sediments and Lake Level History, Eastern Lake Erie."

by Gordon Cameron

in partial fulfilment of the requirements for the degree of Master of Science

Dated _____

Supervisor: _____

Readers: _____

_____

_____

D A L H O U S I E U N I V E R S I T Y

DATE August 26, 1991

AUTHOR Gordon D.M. Cameron

TITLE Seismostratigraphy of Late Quaternary Sediments and Lake Level History, Eastern Lake Erie.

Department or School Geology Dept.

Degree MSc Convocation Fall Year 1991

Permission is herewith granted to Dalhousie University to circulate and to have copied for non-commercial purposes, at its discretion, the above title upon the request of individuals or institutions.

TABLE OF CONTENTS

List of Figures

Page

List of Tables

Abstract

Seismo- and lithostratigraphic analysis of unconsolidated sediments in the Long Point area of eastern Lake Erie reveals two stratigraphic sequences. The lower sequence forms a wedge of material, thickest in the centre of the basin (ca 50 m), which thins shoreward where it commonly pinches out against an overlying regional unconformity. This lower sequence comprises glacial drift and stratified proglacial and postglacial sediments. The upper sequence forms a continuous wedge-like cover, up to 40 m thick in the centre of the basin, which thins shoreward. The upper sequence (Holocene in age) consists of laminated or massive muds, muddy sandy lag and contains, in places, relict brown and gray beach sand at ca 20 to 30 meters below datum (m.b.d.).

Port Huron Ice reached Long Point Bay between 12.5 and 13 ka depositing glacial drift on the basin flanks and bedrock highs while delivering fine-grained sediments to deeper portions of the basin. Ice retreat about 12.5 ka lowered lake levels and allowed drainage over the Niagara escarpment. Lake levels were probably maintained above present lake level by high volume flow over moraine crests on the escarpment until 10.5 ka when Upper Great Lakes waters were diverted away from the Erie basin. Lake levels rose (from a low of 30 m.b.d.) throughout much of the Holocene Epoch. The Nipissing flood (ca 5 ka) renewed Upper Great Lakes flow and temporarily raised lake levels ca 5 meters above datum (m.a.d). Water levels continued on an upward trend after falling ca 10 m.b.d. (ca 3.9 ka).

Acknowledgements

Special thanks is extended to Dr. C.F.M. Lewis of the Geological Survey of Canada (GSC) at the Atlantic Geoscience Centre (AGC) for his guidance and generosity throughout this project. Without his initiative and expertise this thesis would not have been possible.

A special word of thanks to Dr. D. Scott of the Centre for Marine Geology at Dalhousie University, who supervised this project and willingly gave his time and expertise. I would also like to thank Dr. T.W. Anderson of the Geological Survey of Canada for financially supporting this project. I also appreciate his helpful efforts and expertise in processing and evaluating the pollen data.

The help, advice and support from the staff of the Atlantic Geoscience Centre is greatly appreciated. In particular, I would like to extend special thanks to Kate Moran and Harold Christian for allowing access to their excellent geotechnical laboratory facilities and for their patience, time and expertise. I would like to acknowledge Russ Parrott for the generous use of his computer and Gary Sonnichsen for technical expertise. I also wish to thank Kevin Robinson, Kenny Asprey and Donnie Clattenburg for allowing access to the sedimentology laboratory facilities at the AGC. Thanks also to Wayne Prime for computer access.

I would like to thank the Department of Geology at Dalhousie University and its staff, graduate and

undergraduate students. I would particularly like to thank Ron Boyd for constructive input and discussions. I greatly appreciate Francine McCarthy's work with the palynological data. I also would like to thank Dr. Larry Mayer for his generosity in allowing access to his laboratory facilities at the Oceanography Department at Dalhousie University. I would like to acknowledge Janice Marsters for her help and guidance with the velocity and geotechnical measurements. I also extend many thanks to C. Younger for her guidance and hard work with core processing.

I would like to thank Mr. J.J. Godawa, Jim Grass and John Bowlby of Ontario Hydro for access to and discussions of the Lake Erie Cable Crossing data.

I would like to acknowledge the entire staff, officers and crew of C.S.S. Limnos of the Centre for Inland Waters for their assistance and cooperation in data collection. I would like to thank A. Zeman of National Water Research Institute for sharing his 1987 C.S.S. Limnos cruise so that acoustic profile and sediment cores could be collected for this study. I would like to thank Dr. R.L. Thomas of National Water Research Institute (presently Great Lakes Institute, University of Windsor) who kindly arranged for collection of an additional piston core and echo sounding data in 1990.

A last but very special word of thanks goes to Darcy Johns for her help in the preparation of this manuscript and

for her love, patience and good humour during this project.

Chapter 1

BACKGROUND

General and Objectives:

Situated on the Canadian/United States border, Lake Erie is the southernmost of the Laurentian Great Lakes (fig. 1.1). The lake dimensions are approximately 141 kms along the east-northeast axis and about 34 kms at maximum width. The present lake surface (datum) stands at 173.3 meters above mean sea level (m.a.s.l.). The Detroit River brings major inflow (approximately 5000 m^3/s) from the Upper Great Lakes to the western basin of Lake Erie and the Niagara River carries the discharge (approximately 5600 m^3/s) from eastern Lake Erie into Lake Ontario. A bedrock sill at the head of the Niagara River is the principal control of lake level.

The evolution of the Erie basin, throughout the Late Quaternary, has been attributed to glacial processes, isostatic rebound, Upper Great Lakes drainage diversions, climatic changes and changes in lake levels (Hough, 1958, 1966). The present model of lake history, as outlined by Calkin and Feenstra (1985), has evolved principally from onshore geomorphological evidence. Raised beach ridges, wave-cut cliffs, terraces and lake outlet elevations are used as principal indicators of previous lake levels. The correlation of these indicators with glacial-margin features, such as moraines, has clarified a succession of

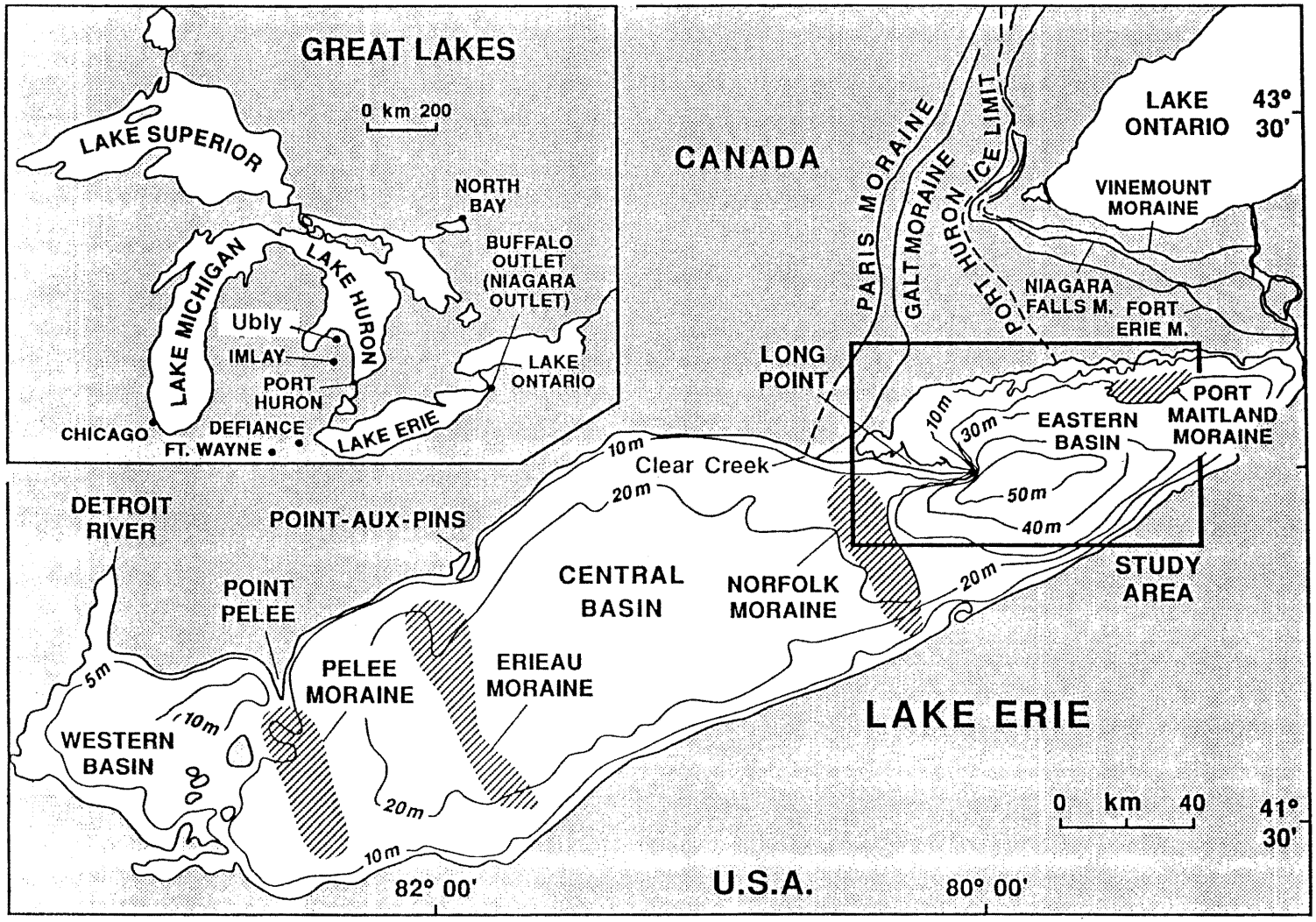

Fig 1.1 Lake Erie setting and bathymetry.

proglacial and nonglacial lakes, with water planes of varying elevations, above and below the present lake level.

A Late Quaternary geological record exists in the offshore areas of central and western Lake Erie. Here, stratigraphic and sedimentological evidence in the offshore record events which influenced the evolution of the Erie basin. This history has never been validated by a study of the eastern basin which contains a thick sequence of sediments with indications of former low lake levels (e.g. buried unconformities) according to a preliminary investigation by Coakley and Lewis (1985). The objectives of this thesis are:

(1) To interpret acoustic profile data and establish an overall seismostratigraphy for the eastern Erie basin.

(2) To analyze sediment and physical properties from a suite of piston and gravity cores. To apply this analysis to the development of sediment lithology and physical properties facies and to correlate these to the seismostratigraphy.

(3) To provide a time frame using a radiocarbon-dated pollen stratigraphy.

(4) To use these data to interpret the lake level history and to provide a model for the evolution of the eastern Erie basin during the Late Quaternary Period.

Geological Setting

Lake Erie is the shallowest of the Great Lakes with an average depth of 17.5 m. The lake is divided into three

major basins, western, central and eastern by cross-lake terminal glacial moraines (Sly and Lewis, 1972), (see fig. 1.1). The deepest point in the lake is 64 metres and is found in the eastern basin, just east and south of Long Point (fig. 1.2).

Much of the lake bottom (approximately 58%) is covered with postglacial muds which accumulated as offshore deposits; these show a distribution similar to deep-water lakes (Thomas et al., 1976). Nearshore zones are generally associated with wave-eroded platforms on glacigenic material and bedrock which are commonly veneered with coarse lag deposits. Major sand deposits have accumulated in the littoral transport zone in large spit features such as Long Point (Coakley, 1985). Known offshore sand accumulations are restricted to the eastern margin of the Norfolk moraine (Thomas et al., 1976). However, investigations through this study have recognized an additional offshore sand body in the eastern basin; detailed discussions follow in subsequent chapters. Erosion of the shore bluffs surrounding the lake, particularly the northshore of the central basin, has been the main source of sediment supply for the postglacial lake basin sediment fill (Gelinas and Quigley, 1973; Lewis, 1984; Rukavina and Zeman, 1987).

Subbottom sediments consist of glacial drift overlain by what many have described as glaciolacustrine deposits (Kick, 1962; Wall, 1968; Sly and Lewis, 1972; Lewis et al.,

1973). These deposits will be discussed further in the following chapters.

Bedrock Geology:

Sequences of Paleozoic sedimentary strata lie beneath the Lake Erie basin and unconformably lap onto dense crystalline rock of the Canadian Shield. The Erie basin is eroded primarily into shales and carbonates of Middle Devonian age, except in the western portion of the lake where Silurian-aged carbonates are important (Hough, 1958). The lake basin mostly follows along strike of a simple bedrock structure with southward dipping beds (Hough, 1958). In the western portion of the lake the dip of the rock strata swings westward reflecting the structural changes of the Michigan basin (Hough, 1958).

Faulting is believed to have played a minimal role with major faults being limited to areas east of the basin (Coakley, 1985). It is generally believed that weathering and erosion through the drainage of a mature river system and subsequent glacial scour played a central role in shaping the underlying bedrock and basin geometry (Hough, 1958). However, seismic data from this study suggest that structural elements may have played a greater role in the basin's evolution than previously believed. Findings of displacements along fractures by Sandford et al. (1985) and an hypothesis of an extension of the St.Lawrence rift zone by Adams and Basham (1989) also suggest that structural

elements have and continue to influence this basin. Structural findings and their possible implications for the Quaternary section will be discussed in Chapters 2 and 4.

Previous Work:

Early studies of the processes within the lake were concerned with the shoreline (Mosely, 1904; Wilson, 1908; Kindle, 1933). They focused on accretionary shoreline features, such as Point Pelee, and proposed a simple littoral-drift mode of formation. Other early studies dealt with shore erosion, chronology of the western basin, shore processes and bottom materials and current studies (Wood, 1951; Ross, 1950; Pincus, 1953; Hartley, 1968).

Lewis (1966) was the first to study the unconsolidated sediments of Lake Erie as a whole. He integrated evidence for low lake stages into a history of early lake levels, developing an explanation and chronology for these events. He assigned an approximate age of 12,500 y.B.P. to this initial low lake stage (Early Lake Erie). He linked the location of four major accretionary forelands with three cross-lake ridges which he identified as glacial moraines. Further studies by Lewis and others yielded additional stratigraphic, chronological, geotechnical, sedimentary and general geological understanding of the lake basin (Lewis et al., 1966; Lewis et al., 1973; Sly, 1976; Sly and Lewis, 1972; Creer et al., 1976; Fritz et al., 1975).

Other important studies focused on subbottom reflectors

and their geological significance (Wall, 1968; Hobson et al., 1969). Wall (1968), concentrating on the central basin, outlined several key reflectors and concluded that the origins of the Lake Erie basin favoured fluvial erosion. Hobson et al. (1969), working in the western basin, described seismic reflection evidence for a pre-glacial fluvial drainage system and glacial features within the lake.

Sediment distribution studies were conducted by Thomas et al. (1976) in the offshore areas, Rukavina and St.Jacques (1971, 1978), St. Jacques and Rukavina (1973) in the nearshore. Coakley (1977) focused on nearshore sediment studies at Point Pelee and interpreted it (and possibly other forelands in the lake) as a relict feature influenced by modern sediment transport.

A recent study by Coakley (1985) centered on the major forelands along the north shore of Lake Erie (Long Point, Point Pelee, and Pointe aux Pins). He applied sediment analysis and other physical data from a suite of boreholes to the interpretion of the postglacial history of these accretionary landforms and the lake. He concluded that these forelands formed under persistent erosion and shoreward transgression due to the influence of rising water levels in the lake, in a manner analogous to the barrier islands of the U.S. east and south coasts, He also proposed that the lake level curve is more complex then was

originally suggested by Lewis (1969). Coakley and Lewis (1985) and Barnett (1985) both propose new lake level curves for Lake Erie.

Late Quaternary History of the Erie Basin:

The Erie basin had the earliest and one of the most complex successions of the glacial Great Lakes (Calkin and Feenstra, 1985). Two major periods of ice advance which affected the Lake Erie basin during the later part of the Late Quaternary were the Port Bruce and Port Huron Stadials (fig. 1.4). These stadials were separated by one period of general ice margin recession, called the Mackinaw Interstadial (Dreimanis and Karrow, 1972).

The northeast-southwest orientation of the lake basin, bounded by the Allegheny Plateau to the south, repeatedly deflected the continental ice flow (Erie Lobe) westward along the trend of the lake. Deposition from the glacial environments played a major role in determining the type and character of the sediments found in the basin. Another factor which affected sediment character was variation in lake water levels controlled by glaciation or glacio-isostatic rebound of natural outlets.

When the continental ice entered the Erie basin at its northeastern end, the Niagara outlet was blocked causing a rise in lake level. The advancing ice would increase the level and extent of glacial lakes throughout the Erie and Huron basins. The presence of lakes fronting the glacier as

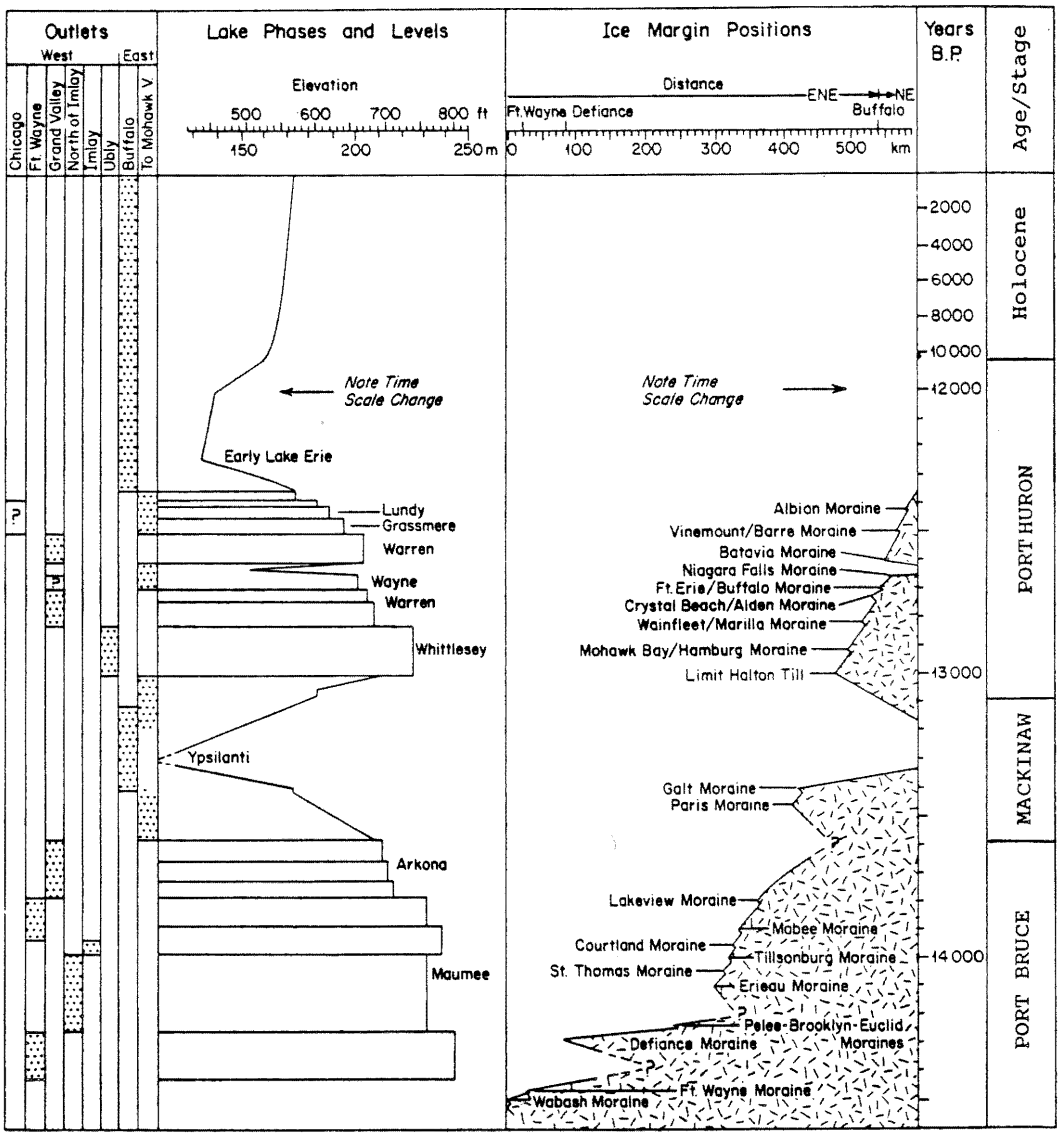

Fig 1.4 Correlation of lake phases and ice barriers in the Lake Erie basin (after Calkin and Feenstra, 1985).

it advanced or retreated in the Erie basin, allowed for the deposition of glacial (till) and glaciolacustrine sediments (Barnett, 1983).

The last major ice re-advance, during the Port Bruce Stadial (fig 1.4) occupied much of the Erie basin, leaving only fragmentary or buried evidence of earlier lake successions. However, younger sequences deposited during the Port Bruce Stadial and Mackinaw Interstadial and during and following the Port Huron Stadial, have recorded successive lake histories (Barnett, 1985).

Lake Maumee evolved ca 14,500 y.B.P. as the ice margin retreated northward from the drainage divide between the Erie basin and the Ohio-Mississippi valley. Various phases of Lake Maumee drained westward through different outlets as the ice margin fluctuated; further ice retreat led to Lake Arkona phases at slightly lower levels (fig. 1.4). Fluctuating ice positions of the Erie Lobe created numerous moraines while depositing Port Stanley Drift during this time.

Lake Arkona features are well developed on Port Bruce sediments and probably were formed during the initial stages of ice retreat during the beginning of the Mackinaw Interstadial (Barnett, 1985). A possible readjustment in the Erie Lobe, during the initial stages of the Mackinaw Interstadial, has been interpreted by Barnett (1985) to be responsible for glacial re-advance and the formation of the

Wentworth Till and the Paris and Galt Moraines (Fig 1.1). Continental ice retreat into Lake Ontario basin, during the Mackinaw, caused a reversal in drainage direction eastwardly, resulting in a drop in lake levels and the development of non-glacial, low Lake Ypsilanti.

At ca 13,000 y.B.P. the Port Huron re-advance reversed the drainage direction eastward and formed Lake Whittlesey. The Port Huron advance (Fig 1.1) deposited the Halton Till (Fig 1.4) but reached only into the eastern portion of the Lake Erie basin. Ice-marginal retreat in the Huron basin and consequent westward drainage, resulted in lower levels of Lakes Warren and Wayne. Transient west-draining early Lake Algonquin was preceded by ephemeral glacial Lakes Grassmere, Lundy, and Dana (fig. 1.4). Retreating Port Huron ice exposed the Niagara Peninsula which allowed the water level of glacial Lake Dana to lower and end the glacial influence in the Erie basin (Coakley, 1985). This event marked the beginning of the Early Lake Erie Phase, dated by Sly and Lewis (1972) at ca 12,500 y.B.P. However, pollen ages suggest that this event could be younger (Coakley and Lewis, 1985).

The evolution of Early Lake Erie to the present lake has been influenced by changes in outlet, varying inflow from the upper Great Lakes and deceleration of rebound of the Niagara outlet and climate (Calkin and Feenstra, 1985). Initially, Coakley and Lewis (1985), suggest that Early Lake

Erie consisted of three sub-lakes, with the easternmost as low as 40 metres below present lake datum. Differential glacio-isostatic uplift of the Buffalo outlet brought lake levels to within 20 or even 10 metres of the present level by 10,500 y.B.P. (Lewis, 1969; Coakley and Lewis, 1985). Diversion of Lake Algonquin waters away from Early Lake Erie at ca 11,800 y.B.P. and again about 10,500 y.B.P., due to ice retreat exposing lower outlets to the north, slowed rising Erie levels (Lewis and Anderson 1989).

Return of outflow of the upper Great Lakes to Erie basin, ("Nipissing floods") at ca 5 Ka, initiated higher lake levels, up to 5 meters above present levels, by 3.5 Ka (Barnett, 1985; Coakley and Lewis, 1985). Barnett (1985) suggests that lake levels may have risen to 5 meters above present levels. Coakley and Lewis (1985) suggest that a 5 meter rise in lake level above present levels could have occurred during the Nipissing flood. Evidence found during this study suggests an alternate lake history, which will be discussed in some detail in Chapter 4.

Methods of Study

Introduction:

High frequency (14 kHz and 7 kHz) acoustic profiles, along ca. 300 km of ship's track, were collected during cruise 87-01-003, in eastern Lake Erie, (fig. 1.3). The cruise was initiated by scientists from the Canada Centre for Inland Waters (CCIW), aboard the C.S.S. Limnos, in 1987.

Ground truthing was accomplished using Alpine piston and Benthos gravity coring systems. Six gravity (7 cm inside diameter of liner) and six piston cores (6 cm inside diameter of liner) were collected from seven coring stations (fig. 1.2 and table 1.1). One additional Alpine piston core was taken in 1990 from the study area (cruise 90-01-003 from CCIW) to verify some aspects of the interpretation of the earlier data. A hyperbolic Loran C positioning system (position accuracy within 10 meters) was used for navigation.

Acoustic and seismic data from 1961, 1963 and 1967 were also used. Additional high resolution acoustic profile data, from a 1980-82 cable crossing project, were kindly provided by Ontario Hydro. Also recent acoustic data from cruise 90-01-003 (initiated from CCIW in 1990) were utilized. Borehole data from Long Point, collected by the University of Toronto (Lewis, 1966), have been referenced to provide additional ground-truthing (fig. 1.2).

Laboratory facilities were made available by the Atlantic Geoscience Centre (AGC) at the Bedford Institute of Oceanography (BIO) and the Centre for Marine Geology and the Oceanography Department, both at Dalhousie University.

Field Work:

Coring was conducted by the crew of the C.S.S. Limnos using the onboard Alpine piston coring system triggered by a lump weight. Benthos gravity coring was accomplished

separately, often at the same coring station as the piston cores (table 1.1). Following core recovery, piston cores were cut into 1.5 m sections, capped, labelled, taped and sealed to prevent moisture loss. They were stored upright in a refrigerated onboard facility and carefully trucked standing upright under cool and vibration-dampened conditions by the author, to Bedford Institute of Oceanography (B.I.O.) in Dartmouth, Nova Scotia where they were stored upright in cool (4^0C) conditions.

A Raytheon 7 kHz profiling system and a Kelvin-Hughes MS26B echosounder (14 kHz) provided acoustic profile coverage throughout the survey area (fig. 1.3).

Acoustic Reflection Data:

High resolution acoustic and seismic data, with approximately 1400 line kms of coverage, constituted the reflection coverage in the study area (fig. 1.3). Early acoustic data collected in 1961 and 1963, onboard the C.C.G.S. Porte Dauphine, consist of Kelvin-Hughes MS26B echogram profiles. A somewhat later seismic survey, conducted from the same vessel in 1967, yielded profiles of lower resolution but higher penetration, all of varying quality. These data were generated by a 400 joule, surface-towed EG&G boomer. Recent data were collected in 1987 aboard C.S.S. Limnos using a 7kHz profiling system, driven by a Raytheon PTR-106A transciever, combined with a Raytheon DE-719RTT recorder. This instrumentation was married to a

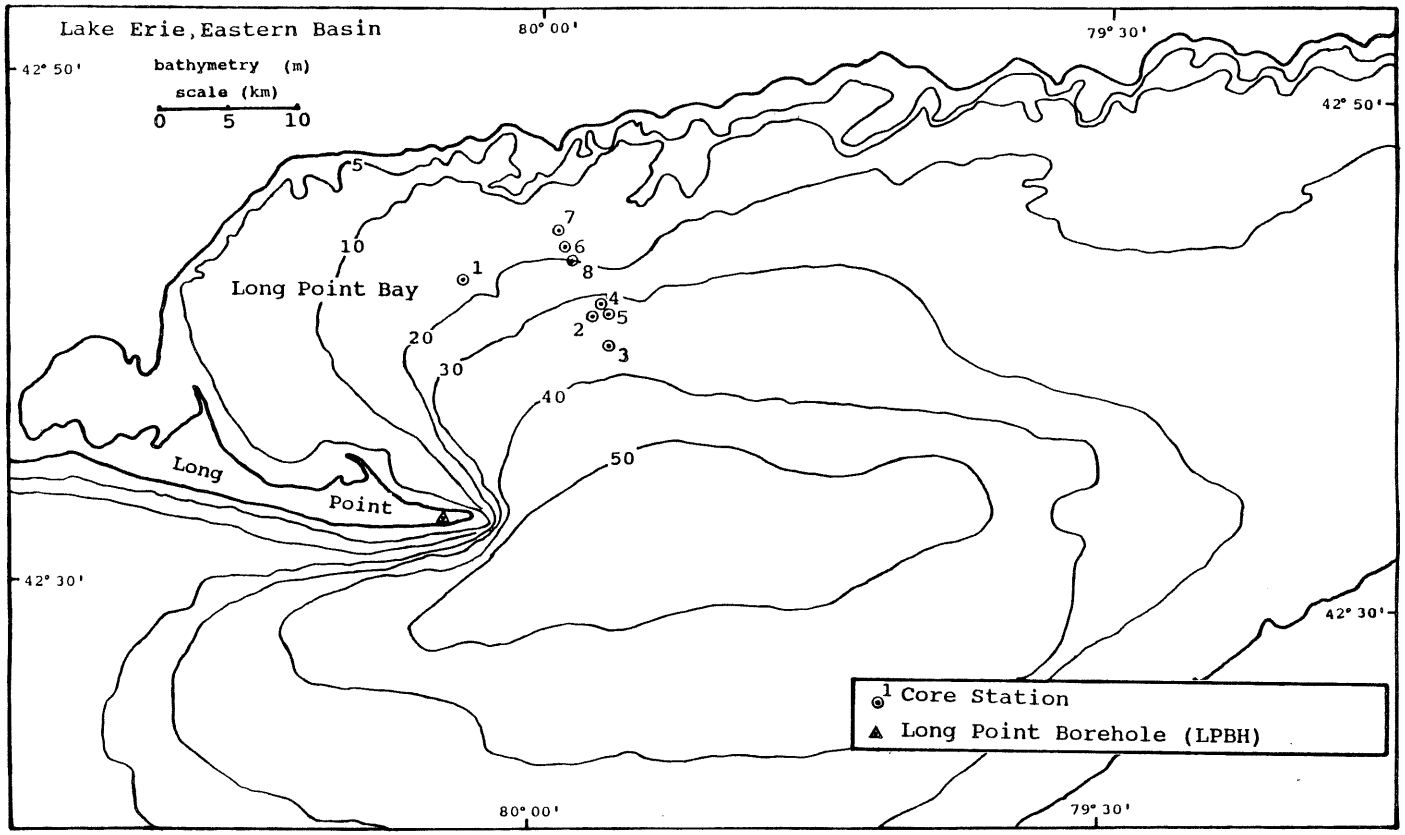

Fig 1.2 Bathymetry and core station map (See Table 1.1 for cores taken at each station).

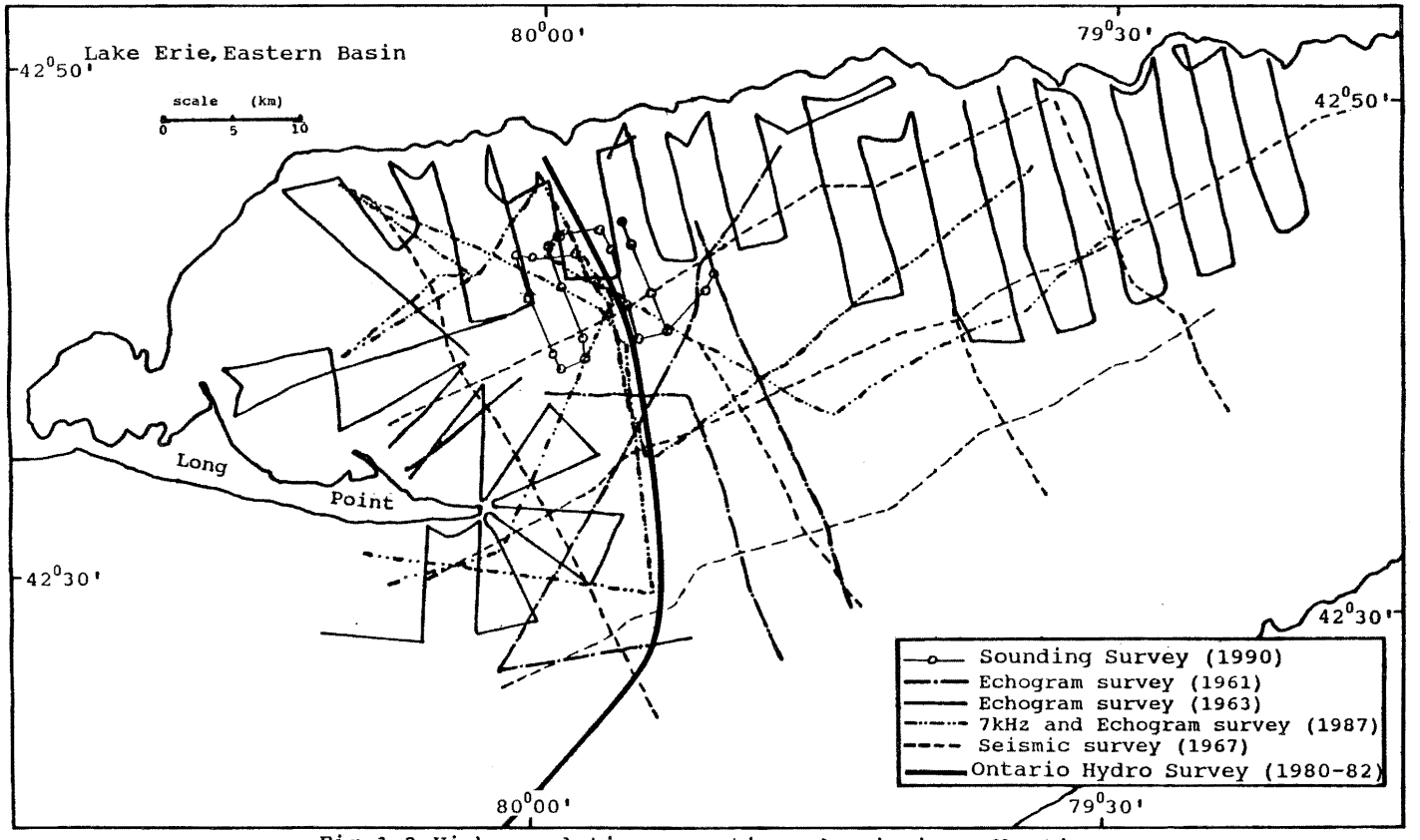

Fig 1.3 High resolution acoustic and seismic reflection coverage over study area.

compatible cone transducer, which was side mounted onboard ship, approximately 2 m below lake level. A permanently mounted shipboard Kelvin-Hughes MS26B echosounder (14 kHz) provided excellent continuous profiles throughout the survey area. Acoustic data from an Ontario Hydro survey yielded excellent cross lake profiles of high resolution and penetration. Sounding data from cruise 90-01-003, collected onboard the C.S.S. Limnos in 1990, provided additional information.

This acoustic and seismic data base was utilized in constructing a seismo-stratigraphy for the study area. The nature and geometry of the seismo-stratigraphy is demonstrated in a series of representative profiles and isopach maps (figs.2.2-2.11). Interpretion of reflection data and recognition of seismo-stratigraphic units and facies followed measures outlined by Mitchum Jr. et al. (1977). The velocity of sound, supported by the physical properties analysis, was assumed to be approximately 1500 m/sec. and applied to the 1967 seismic data (1 cm equals 10 milliseconds of one-way time) and all other acoustic data. All acoustic and seismic track lines, ground-truthing, bathymetry and isopach maps were originally plotted on a 1:400,000 scale Mercator hydrographic base chart published by the Canadian Hydrographic Service.

Laboratory Procedures:

All piston and gravity cores underwent whole core

x-raying and physical properties analysis upon arrival at the Atlantic Geoscience Centre (AGC) and Dalhousie University, less than a week after their collection from Lake Erie. Physical properties analysis on all cores was completed less than a month after the cores where collected from Lake Erie. These cores were kept in cold storage at both localities during analysis. All cores currently are being held in the cold storage facility at Dalhousie University. Whole core x-raying allows for nondestructive scanning of cores for internal structures. The cores were split lengthwise and photographed using core processing facilities at Dalhousie University.

Peak and remoulded undrained shear strength measurements were collected using the AGC computerized Wykekam-Farrance minivane, usually in the working half of the core. The procedure consists of inserting a minivane apparatus into the sediment and applying a rotational stress. Shear strength values are given in kilopascals (kPa).

Velocity measurements were collected, usually in the archive half, using the Dalhousie Digital Sediment Velocimeter (DSV). The DSV apparatus consists of a Compaq microcomputer, a Nicolet 320 digital storage oscilloscope, an HP8116 function generator, an APC digital thermometer and carriage with four acoustic transducers. P-wave velocities were measured by applying known sound frequencies (10 Hz),

across a fixed distance (approximately 6 cm) in the sediment, through longitudinally mounted transducers. All velocities were corrected for bottom water temperatures (table 1.1), gathered at various locations in the lake by bottom thermometers during the 87-01-003 cruise by personnel from the Canadian Centre for Inland Waters (CCIW).

Shear strength and velocity measurements were collected down core at 10, 20, or 25 cm intervals (see appendices). Water content and bulk density samples were collected, usually at similar intervals and locations down core as the velocity measurements. Samples were extracted and placed in hermetically sealed bottles for processing at AGC.

Careful laboratory procedures were followed to determine sample volume, weight and water content. Volumes were determined by transferring sampled sediment to small tare vials of known weight. These vials were placed in calibrated chambers of a Penta-Pycnometer apparatus. Volumes were then determined employing Archimedes Principle of fluid displacement using helium gas and known chamber volumes. The samples were oven dried at 40^0 C, for twenty-four hours and then reweighed. Bulk density was calculated by dividing sample wet weight (g) by sample volume (g/cm^3). Water content is the ratio of the weight of water to the weight of dry sediment, expressed as a percentage (%). All physical property data were entered into a geotechnical data base at AGC. Computer data manipulation and plots were

generated using the Sigmaplot program.

Detailed lithological descriptions of all piston and gravity cores were accomplished following methods outlined by Mudie et al. (1984). The core descriptions documented colour (Munsell Colour Chart), internal structures and lithology of sediments.

Grain Size:

To document the texture of various lithological units recognized within the lake stratigraphy, a complete grain size analysis was carried out on twenty-five samples taken from seven of the Alpine piston cores. The procedures used in the analysis are outlined as follows:

1. Samples (2 x 5cm) were first prepared by dispersing the sediment in a Calgon solution for forty-five minutes.
2. Coarse fractions (less than 4.25 phi) were separated from the fines (greater than 4.25 phi) using a 63 micrometres (microns) sieve.
3. Sand and coarse silt size sediment (-1.0 to 4.25 phi) were separated from the gravel fraction (less than -1.0 phi) using a 2mm mesh sieve. The sand and coarse silt size fractions were then separated using standard dry sieving techniques, at .5 phi intervals (Folk, 1974).
4. The silt-clay fractions were analyzed using a Sedigraph 5000D particle analyzer.

All grain size analysis work was carried out at the sedimentology laboratory at the AGC. The resulting phi

values were entered into the AGC computer grain size data base. Computer-generated histograms (relative frequency percentage), cumulative relative frequency curves and pie diagrams (%) plots were generated. Standard parameters such as mean, standard deviation, skewness and kurtosis were also generated (see appendix).

Pollen Analysis:

Sixteen subsamples from core 3 were analysed for pollen content. Six 5 ml sediment subsamples were taken from core 6 (2 subsamples) and 9 (4 subsamples). These samples were treated with warm 10% HCl to dissolve carbonates, 10% KOH for 5 minutes in a hot bath to remove colloids, and then sieved at 15 micrometres (microns) to remove clays.

Samples were then treated with HF for 2 hours in a hot water bath to remove silicates and acetolysis for 5 minutes in a hot water bath to breakdown cellulose. Samples were then stained with saffrinin and mounted in glycerine gel. Pollen concentration was estimated by spiking samples with plastic microspheres, 25 um in diameter. Pollen and spores were counted at a magnification of 300 x; 200 pollen grains were identified per sample. The complete analysis was performed by Francine McCarthy at the laboratories of Dalhousie University.

Table 1.1 Piston and Gravity Core Statistics

Sta #	Core #	Core Length(cm)	Water Depth(m)	Water Temp(C)	Lat(N)	Long(W)
1	PC-1	433.5	17	12	42 42 12	80 03 47
	GC-1	105	17	12	42 42 12	80 03 47
2	GC-2	98	33.5	7	42 40 50	79 56 48
3	PC-3	873	39.6	5	42 39 41	79 56 02
	GC-3	122	39.6	5	42 39 41	79 56 02
4	PC-6	804	33	7	42 41 14	79 56 21
	GC-6	127.5	33	7	42 41 14	79 56 21
5	PC-7	476	33.5	7	42 41 11	79 56 24
	GC-7	126.5	33.5	7	42 41 11	79 56 24
6	GC-8	26	19	13	42 43 52	79 58 35
7	PC-9	306	17.5	12	42 44 12	79 58 37
8	PC-10	314	21		42 43 11	79 58 25

Chapter 2

SEISMIC STRATIGRAPHY

Introduction:

Two distinct seismic sequences (numbered 1 & 2) have been recognized within Lake Erie's eastern basin. The nature of these Late Quaternary sediments are portrayed in a suite of acoustic profiles (figs. 2.1-2.11). These profiles also illustrate the stratigraphic relationships found between seismic sequences 1 and 2; seismic sequence 1 everywhere underlies sequence 2 and therefore is chronologically older. The extent and thickness of each seismic sequence, within the study area, are disclosed in figs. 2.12 and 2.13 respectively. Both overlie a strong regional reflector (R1), which outcrops on the lakebed near the northwest shore of Lake Erie, above the 10 m isobath (figs. 1.2 and 2.13).

Reflectors:

The regional R2 reflector, commonly an erosional unconformity in the study area, stratigraphically separates seismic sequences 1 and 2. The lakeward extent of the erosional unconformity is mapped in fig. 2.12; southward beyond this boundary the R2 reflector appears to be a non-erosional surface. This reflector, is a flat planar surface, which cuts into the underlying strata of seismic sequence 1, truncating many seismic horizons, (fig. 2.2 and

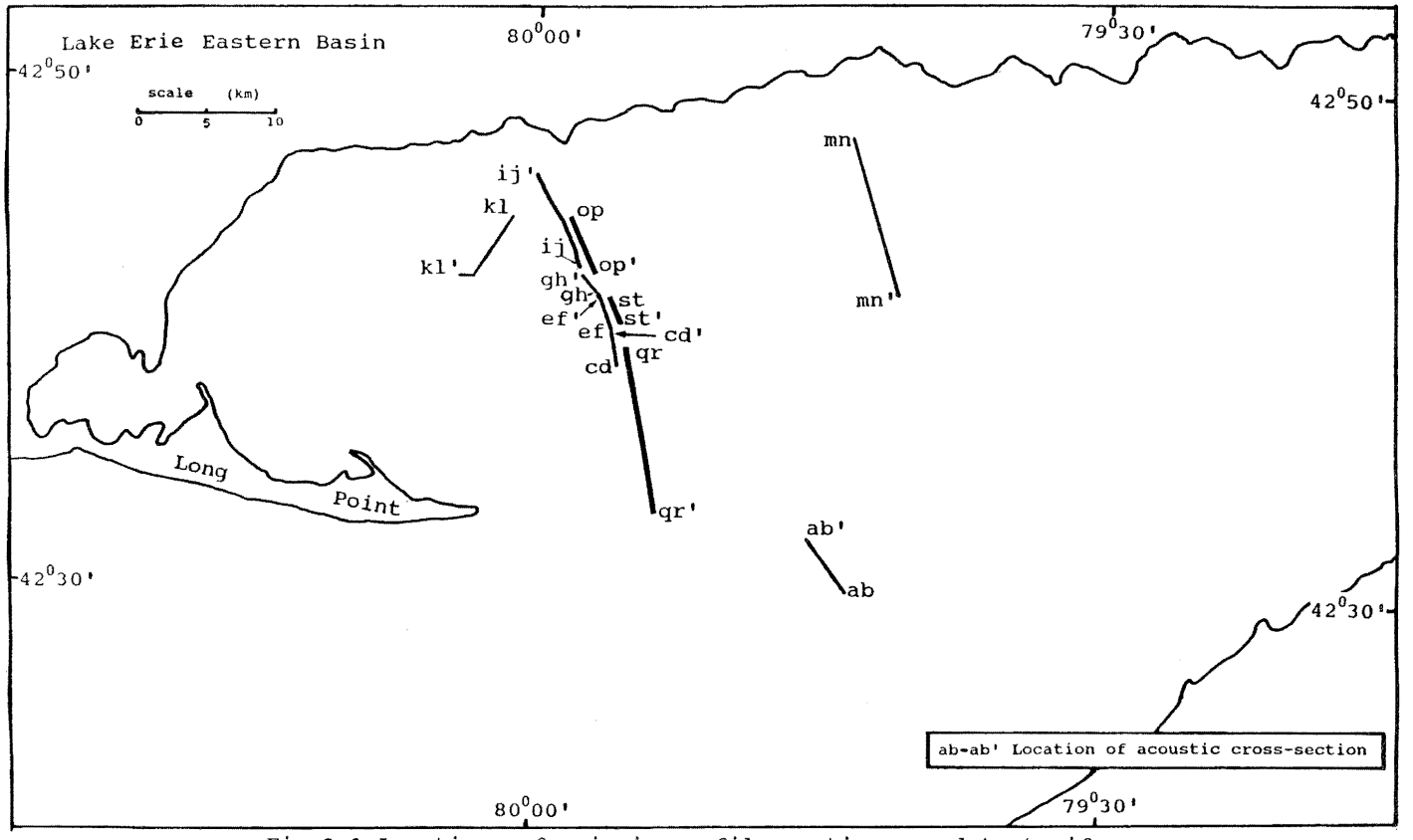

Fig 2.1 Locations of seismic profile sections used to typify basin features.

2.4-2.7 and 2.7a). The maximum water depth at which erosion occurs is approximately 39 meters below lake level. The R2 reflector can be traced deeper as a conformable reflector through the basin, with a maximum depth of 95 m below lake level (fig. 2.8).

Generally strong and continuous in nature (figs. 2.3, 2.6, 2.8 and 8a), the R1 reflector is considered to be the Paleozoic bedrock surface (see Sanford, et al., 1985 for Paleozoic bedrock). A steep-sided, north-facing feature, continuous for many kilometres (approx. 80 km), rises as a northeast-southwest trending prominent bedrock feature, below the unconsolidated lake sediments (figs. 2.8, 2.8a and 2.12) in the centre of the basin. Associated with this structure is a surface expression (step) on the lake bed and related flexure of seismic reflectors (R2), several meters in magnitude (figs. 2.8 and 2.8a). This could imply the presence of relative vertical movement suggesting structural bedrock control and recent vertical movement along this bedrock feature. Alternatively, the bedrock feature could be erosional in origin and flexure of the reflectors could be due to differential sedimentary compaction.

Seismic Sequence 1:

Seismic sequence 1 lies between major reflectors R1 and R2 and is overlain by seismic sequence 2 (figs. 2.2-2.11). Sequence 1 forms a wedge of material, thickest in the centre of the basin (approx. 50 m), thinning shoreward and often

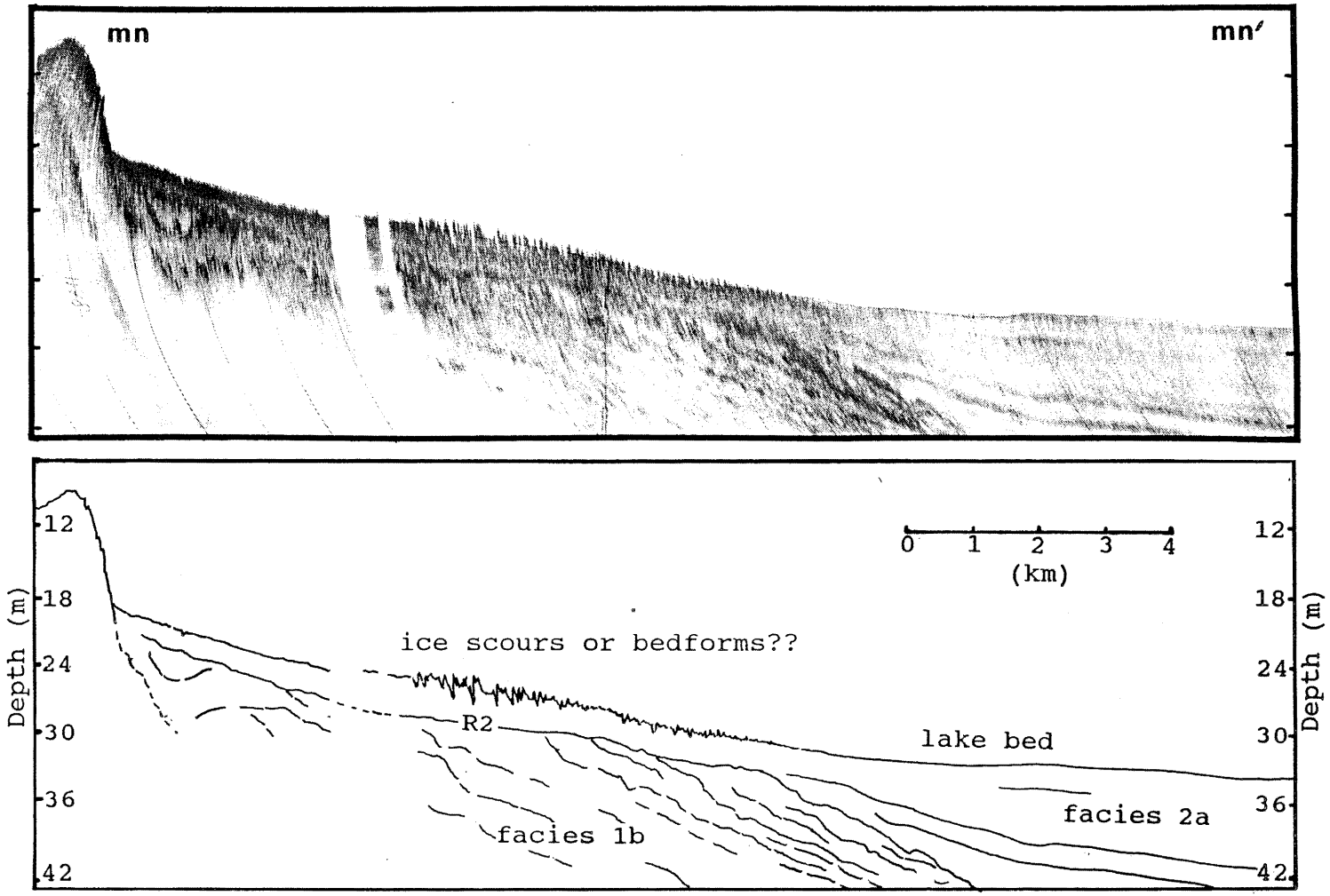

Fig 2.2 Echogram profile with line interpretation showing the relationship of facies 1b, reflector R2, facies 2a and possible ice scours or bedforms on the lake bed.

pinching out against R1 (figs. 2.12-2.13). Sequence 1 is subdivided into two seismic facies on the basis of acoustic character. Seismic facies 1b overlies or appears adjacent to and interfingers with facies 1a (figs. 2.3, 2.6, 2.8 2.8a and 2.10).

Facies 1b generally exhibits many high-amplitude parallel coherent internal reflections. Individual reflections may vary in intensity from weak to strong in the horizontal direction. The distinctive packet of strong coherent reflections that characterize facies 1b in the offshore areas of the basin, changes from a strongly conformable character, in the lower portion of the section, to a slightly less conformable style (figs 2.8 and 2.8a), with onlap on the basin flanks, higher in the section (figs. 2.6, and 2.10). Facies 1b thins shoreward, pinching out against R1 or facies 1a; its upper surface is truncated in places by an unconformity (R2 reflector; figs. 2.2-2.7, 2.7a and 2.10). The unconformity (R2) is developed on the flanks of the basin. This unconformity represents an episode of erosion which has carved a platform and notch into acoustic sequence 1. Wavy and somewhat contorted reflectors occur where underlying bedrock slope surfaces are steepest (figs. 2.3, 2.6 and 2.10). These wavy reflectors do not reflect bedrock topography. Bright or reflection-free areas occur within facies 1b (figs. 2.4 and 2.11).

Facies 1a generally is massive in nature, with spotty

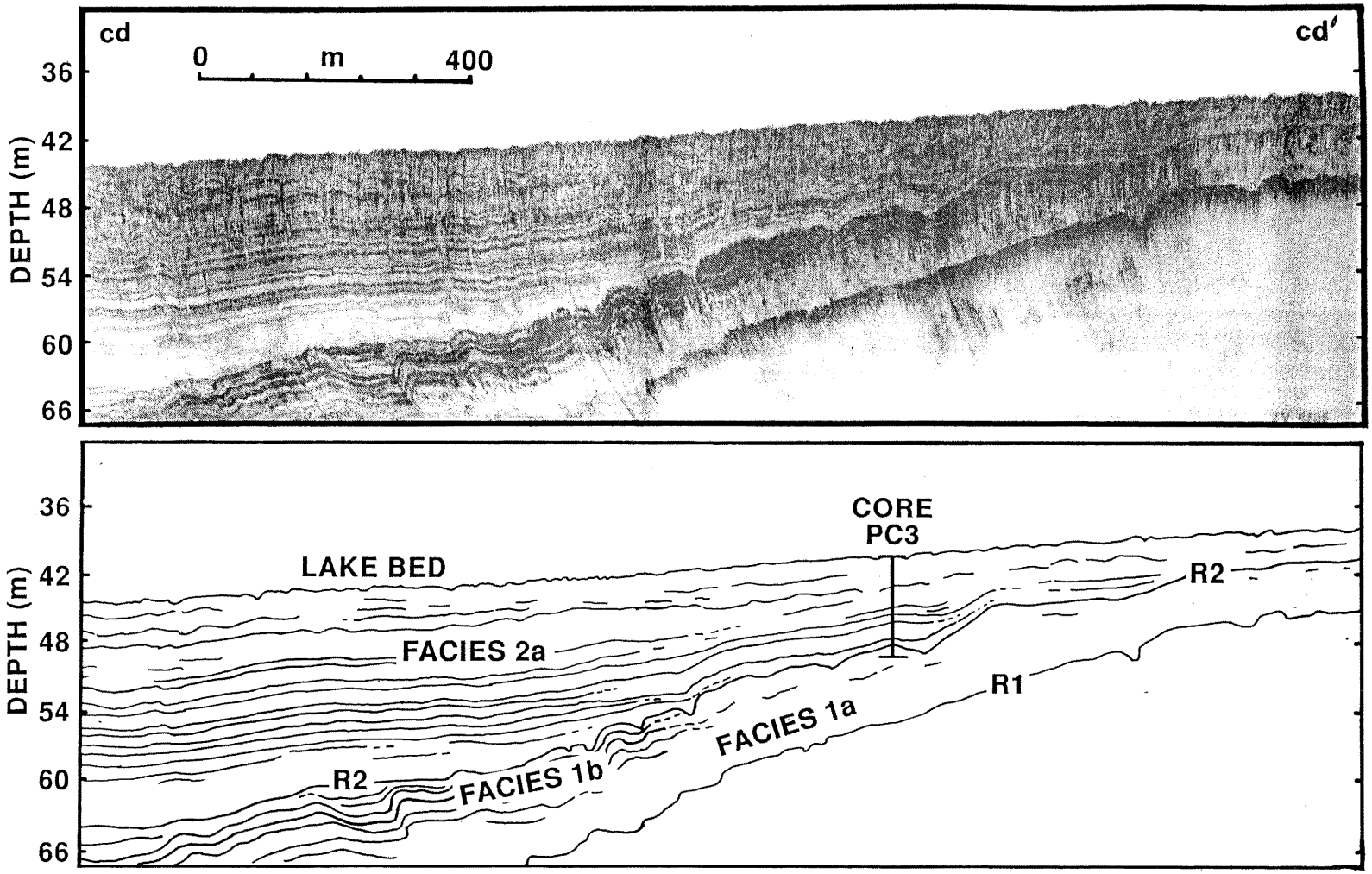

Fig 2.3 Echogram profile with line interpretation showing facies 1a interfingering with facies 1b downslope.

and chaotic internal reflections, often with a distinct surface reflection (figs. 2.3, 2.4, 2.6, 2.8, 2.8a and 2.10). This facies is the lowermost member of sequence 1, underlying or adjacent to and interfingering with facies 1b. Facies 1a is in contact with and unconformably overlies the Paleozoic bedrock. Occurrences of facies 1a are limited to the basin flanks, (figs. 2.3, 2.4, 2.6 and 2.10), with only small isolated occurrences found deeper in the basin (figs. 2.8 and 2.8a). This facies has been eroded in areas along the flanks of the basin (figs. 2.4 and 2.6).

The interfingering relationship of facies 1a with 1b is best seen in figures 2.3 and 2.10. Seismic reflectors from the lower section of facies 1b terminate within facies 1a (fig. 2.3). Isolated occurrences of facies 1a found deeper in the basin may not display this relationship.

Seismic Sequence 2:

Seismic sequence 2 is the uppermost sequence of the unconsolidated sediment section found in the eastern basin. The R2 reflector forms the lower boundary separating the lower sequence 1 from sequence 2. The lakebed offers the upper bounding surface, overlain by as much as 60 m of water. Sequence 2 is up to 40 m thick in the centre of the basin and forms a continuous wedge-like cover which thins shoreward (fig. 2.13). Seismic sequence 2 has been subdivided into seismic facies 2a, 2b and 2d.

Thick accumulations of facies 2a (as great as 40 m)

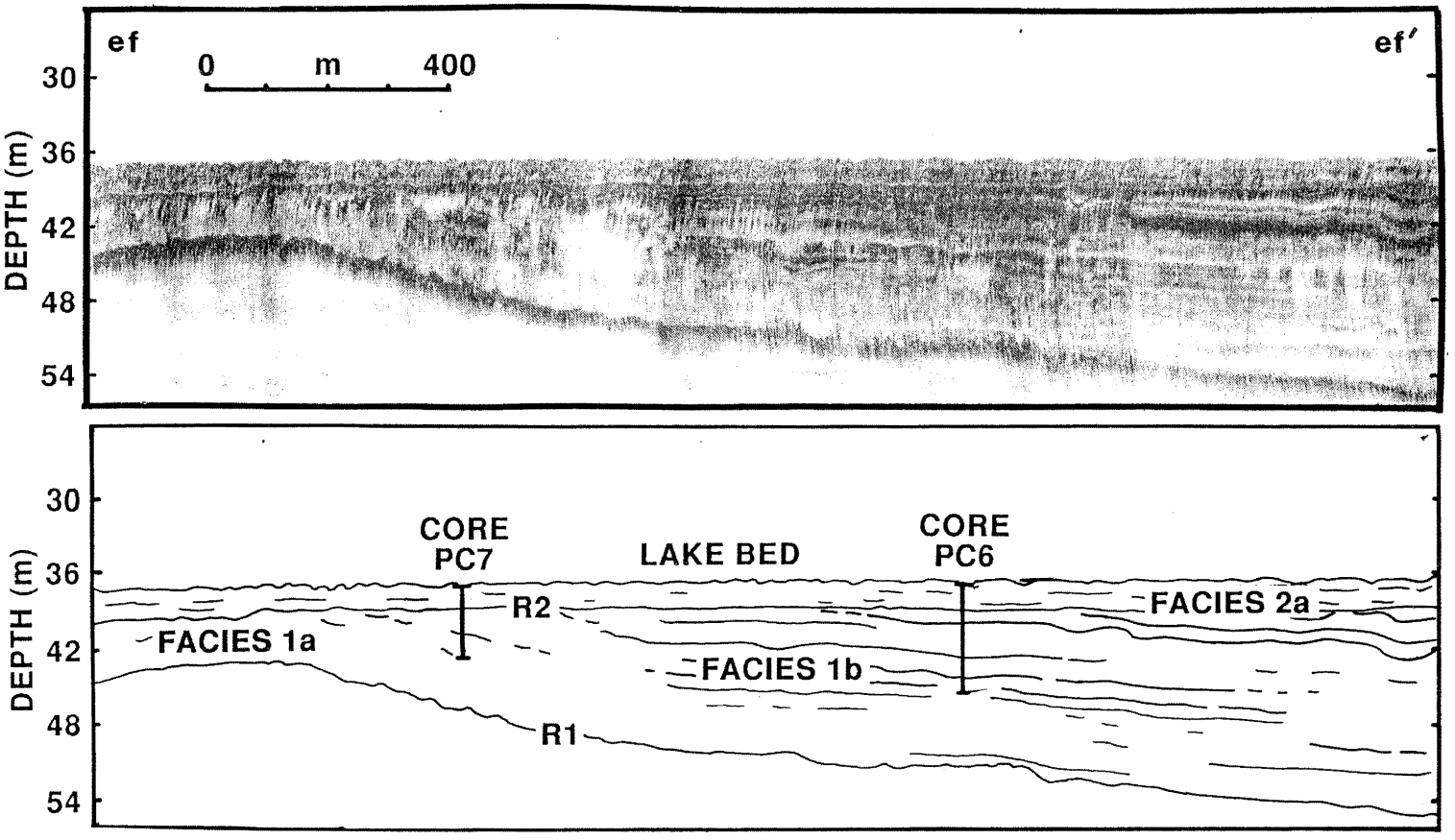

Fig 2.4 Echogram profile with line interpretation, showing facies 1a, on a bedrock high, interfingering with facies 1b at lower elevations.

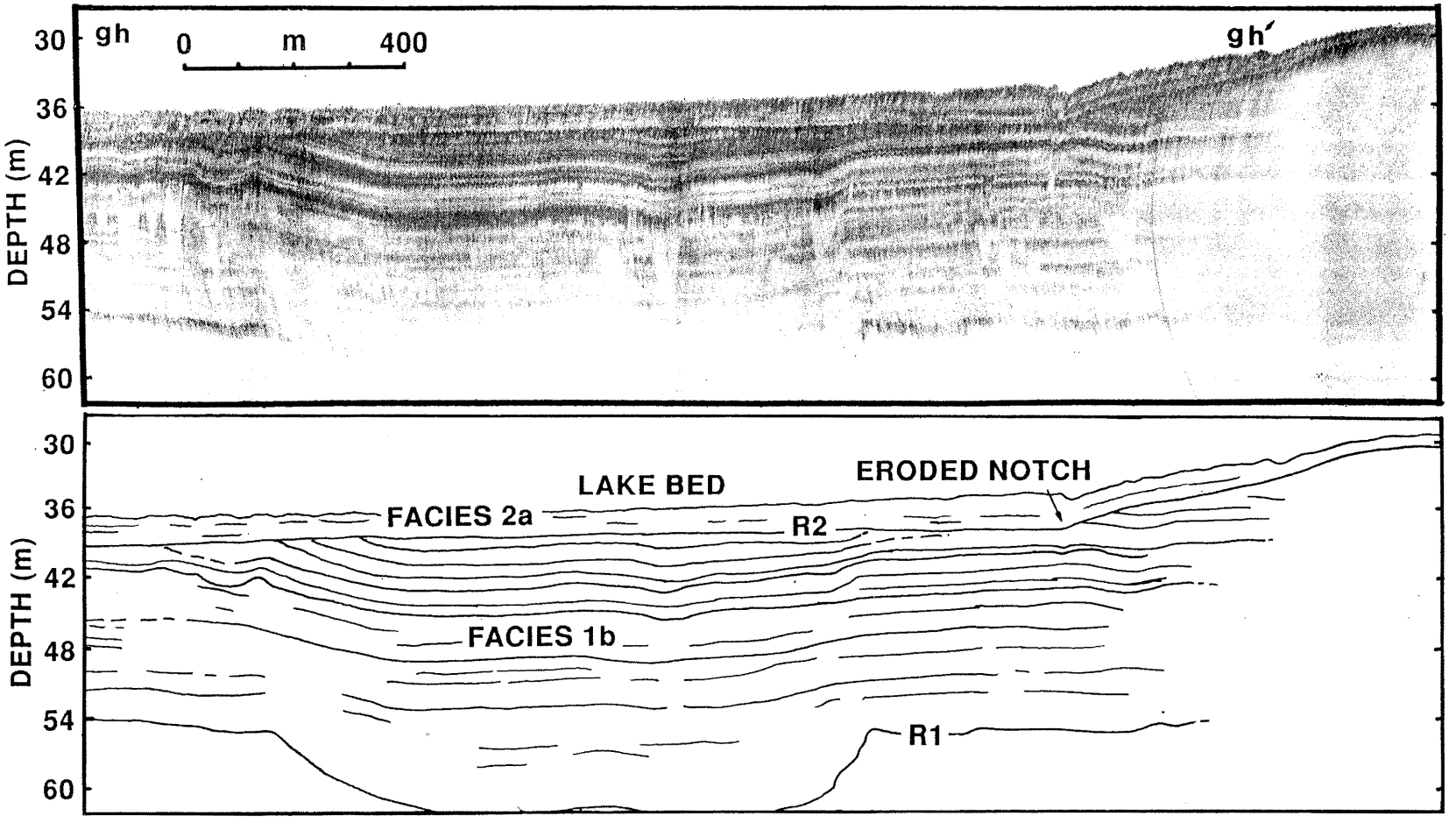

Fig 2.5 Echogram profile with line interpretation, showing an erosional notch (shoreface) at a water depth of ca 30 m truncating the well stratified facies 1b.

occur generally beyond the 40 m isobath, (figs. 2.3, 2.8, 2.8a and 2.10) and are characterized by many relatively weak, mostly continuous parallel coherent internal reflections. Thin accumulations of facies 2a occur in water depths less than 30 m.b.d. and northeast of Long Point Bay. These thinner accumulations are characterized by scattered, mostly discontinuous weak internal reflections in figures 2.2, 2.4 and 2.5, reflectors are stronger and more continuous in figures 2.7 and 2.11. Accumulations of facies 2a occur in Long Point Bay, with thicknesses commonly less than 6 m. This facies is characterized by many distinct, mostly continuous, parallel, coherent, internal reflections (figs. 2.7 and 2.7a). A series of breaks, which offset reflectors, occur in this facies in Long Point Bay (figs. 2.7 and 2.7a). Some reflectors appear truncated (at or just below the lakebed), implying a period of erosion limited to depths less than 20 m below lake level (figs. 2.7 and 2.7a). Facies 2d appears structureless in seismic section (figs 2.7 and 2.7a) and is found only in Long Point Bay, above facies 2a.

Facies 2b, an isolated body of sediment averaging 3-5 m thick at its center, is over 10 km long and approximately 1 km wide (figs. 2.6, 2.9, 2.10 and 2.13). This sediment body thins and pinches out near its extremities, with the eastern boundary undefined. This facies appears to interfinger with facies 2a (figs. 2.6 and

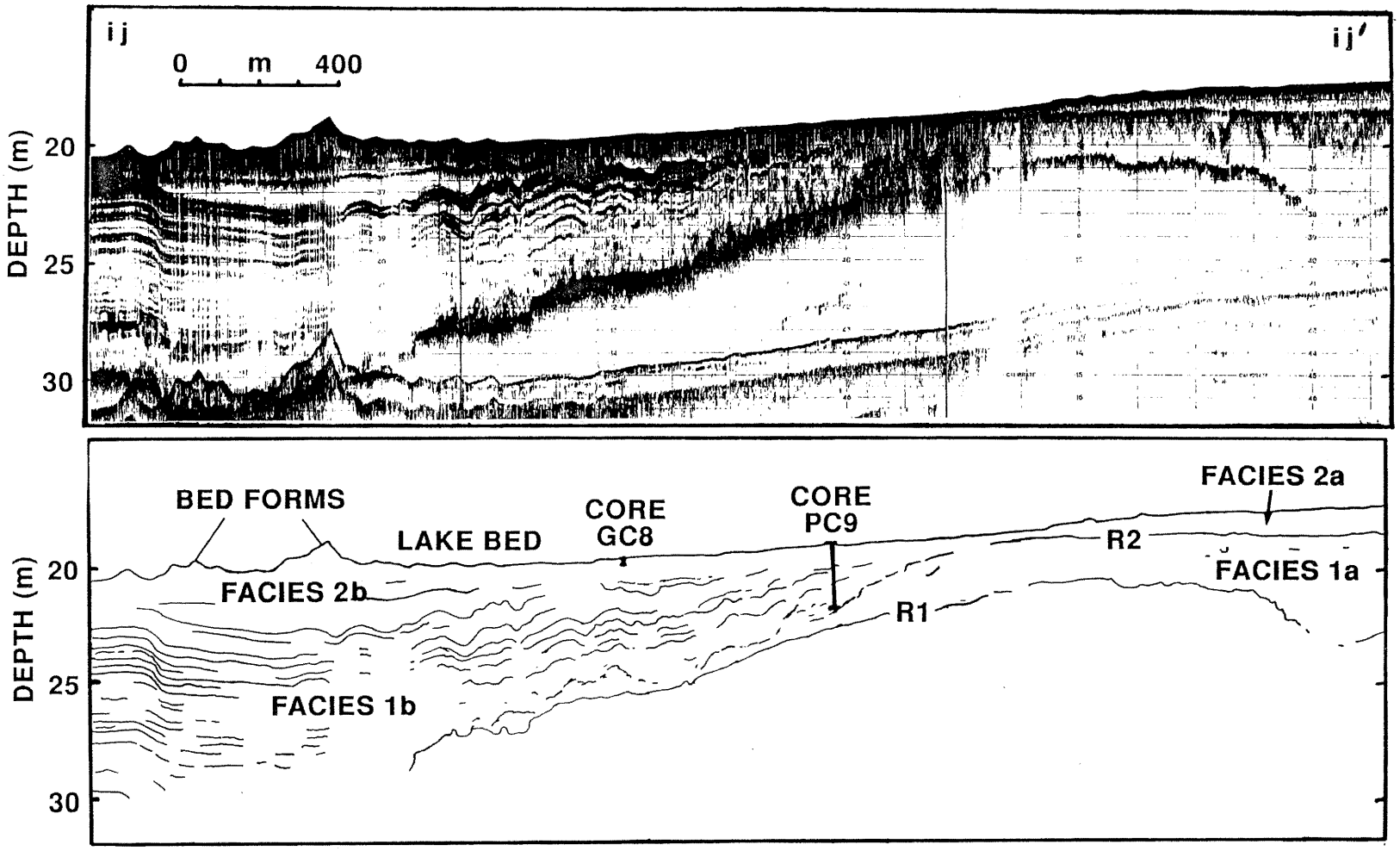

Fig 2.6 Raytheon 7kHz profile with line interpretation. Facies 2b (sand with bedforms) and 2a unconformably overlie facies 1a and 1b.

2.9). This facies is further characterized by surficial features which rise to over 1 m above the lake bottom with rounded or peaked crests. These features have symmetrical sides and internal foresets with apparent dips in a lakeward direction. However, much of facies 2b has massive or spotty internal reflectors.

A lakebed depression, which cuts into the lake sediment, is found in water depth less than about 20 m (2.7 and 2.7a). The feature in fig. 2.7 and 2.7a has a depression (ca.1 m in depth) with berms (soil piles) on either side (ca.30 m wide), and may be due to ice scour. Ice scours and the ice scouring process has been documented in Lake Erie by Grass (1984). Grass (1984) determined that scours occurred in the eastern Lake Erie basin in 13 to 25 meters of water and were caused by ice ridge keels. The scours observed were approximately 4.5 to 6 km long, 10 to 100 m wide and up to 2m deep. The lakebed feature observed in this study (figs. 2.7 and 2.7a) is similar in nature to those described by Grass (1984) and therefore likely has an ice scour genesis. The lakebed features observed in fig 2.2 occur below the range of water depths for ice scour occurrences found by Grass, (1984) and therefore are more likely bedforms.

Interpretation:

The surficial sediments of the eastern basin of Lake Erie have been subdivided into two distinct seismic

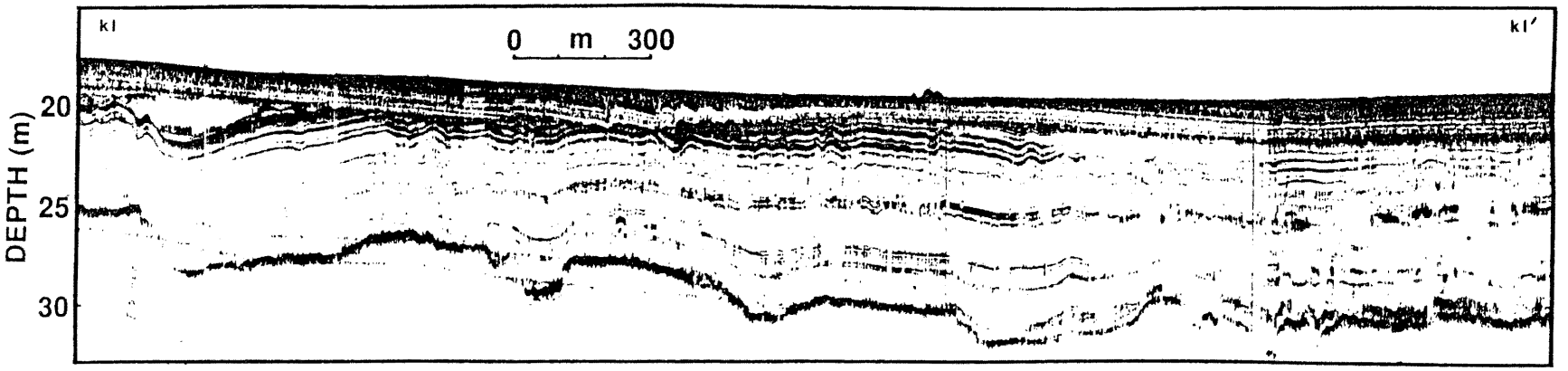

Fig 2.7 Raytheon 7kHz profile kl-kl' from Long Point Bay.
(see Fig 2.7a for line interpretation).

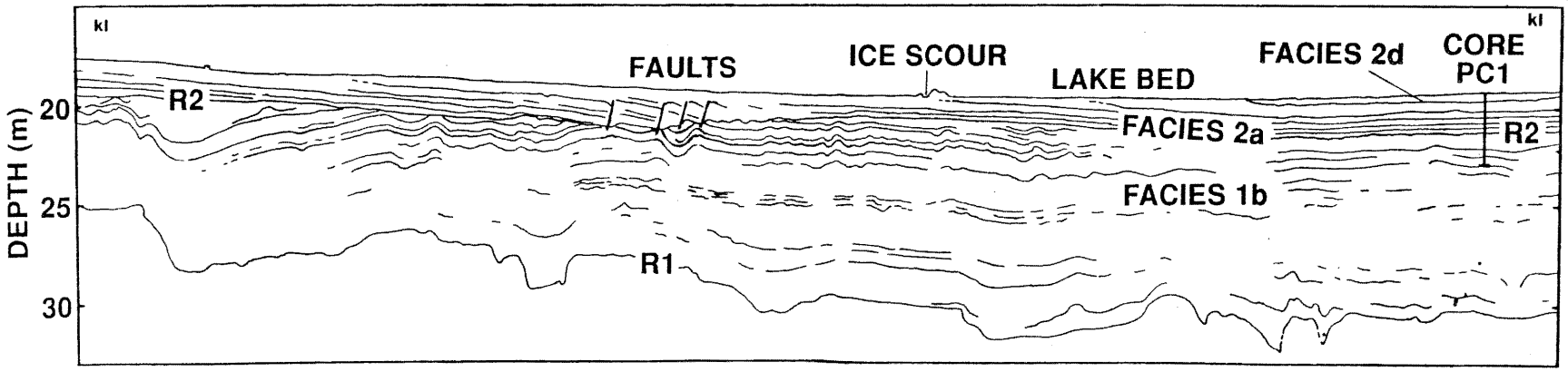

Fig 2.7a A Late Holocene unconformity separates facies 2d from facies 2a (Long Point Bay), best seen in core PC-1.

sequences based on acoustic properties. Seismic sequence 1 underlies sequence 2 and therefore is older. Two major reflectors, R1 and R2, have been identified and appear as distinct boundaries to the sequences. The R1 reflector is lowest and is interpreted as an eroded Paleozoic bedrock surface. It is generally accepted that the lake basin has been formed by erosional processes (Wall, 1968). However, Sanford et al. (1985) have interpreted long term fracturing with rotational displacement within the Paleozoic bedrock; this hypothesis suggests a structural element in the lake basin history. A possible fault controlled bedrock feature (figs. 2.8 and 2.8a), with vertical movement expressed in the recent sediments (note flexure in reflections), suggests recent fault movement but could also be due to differential sediment compaction.

The R2 reflector separates seismic sequences 1 and 2 (figs. 2.2-2.11). This reflector is an erosional unconformity in part, truncating underlying seismic reflectors along the flanks of the basin but appears to be non-erosional deeper in the basin where it is marked by a grouping of relatively strong coherent parallel reflections. A shoreface notch and erosional platform have been carved into seismic facies 1b above 39 m depth (figs. 2.5 and 2.9). These features are sharply defined; they occur beneath modern sediments (sequence 2) and are definitive indicators of a prior history of erosion. The shoreface notch may be a

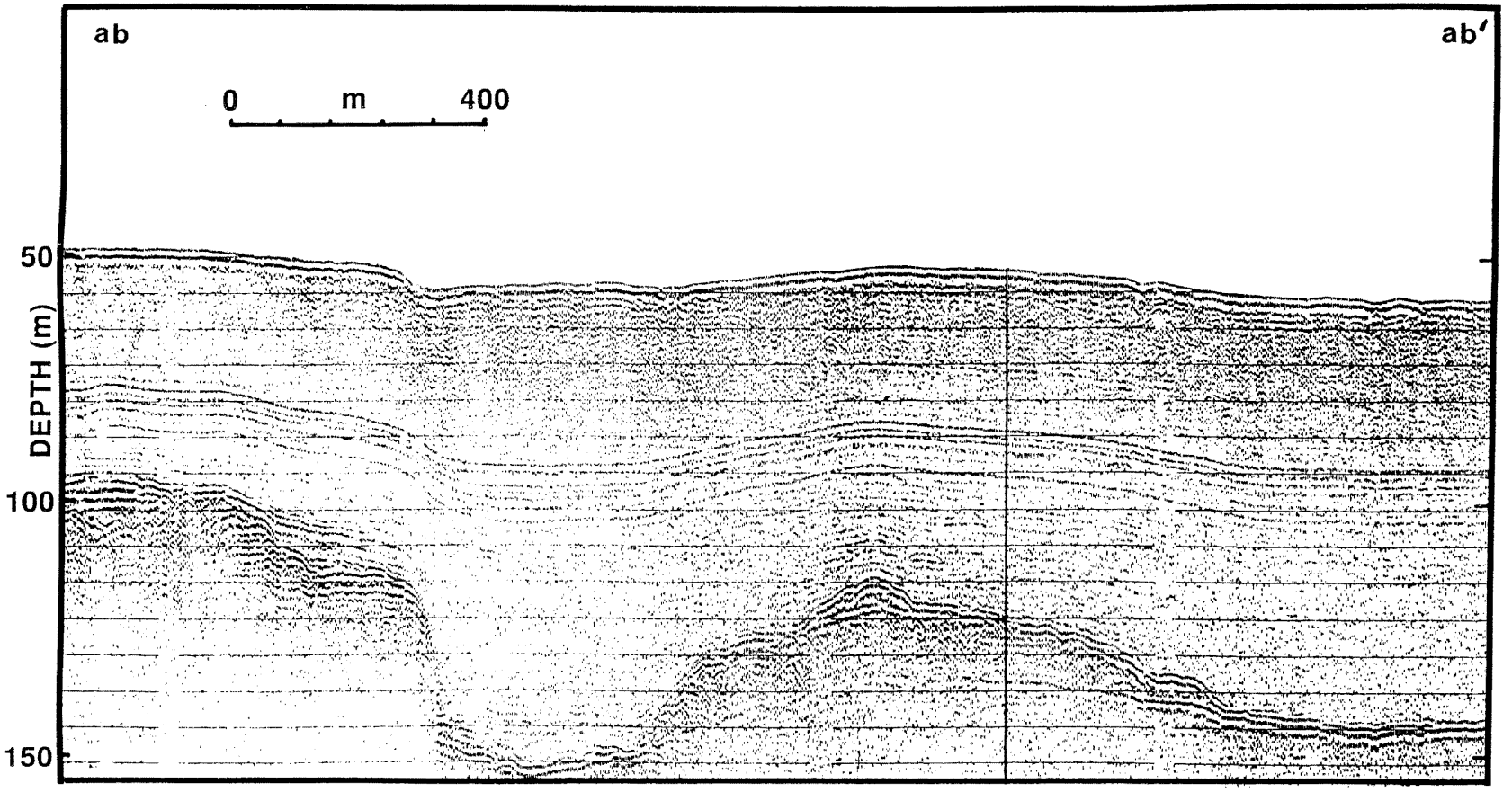

Fig 2.8 Seismic boomer profile ab-ab' (see Fig 2.8a for line interpretation).

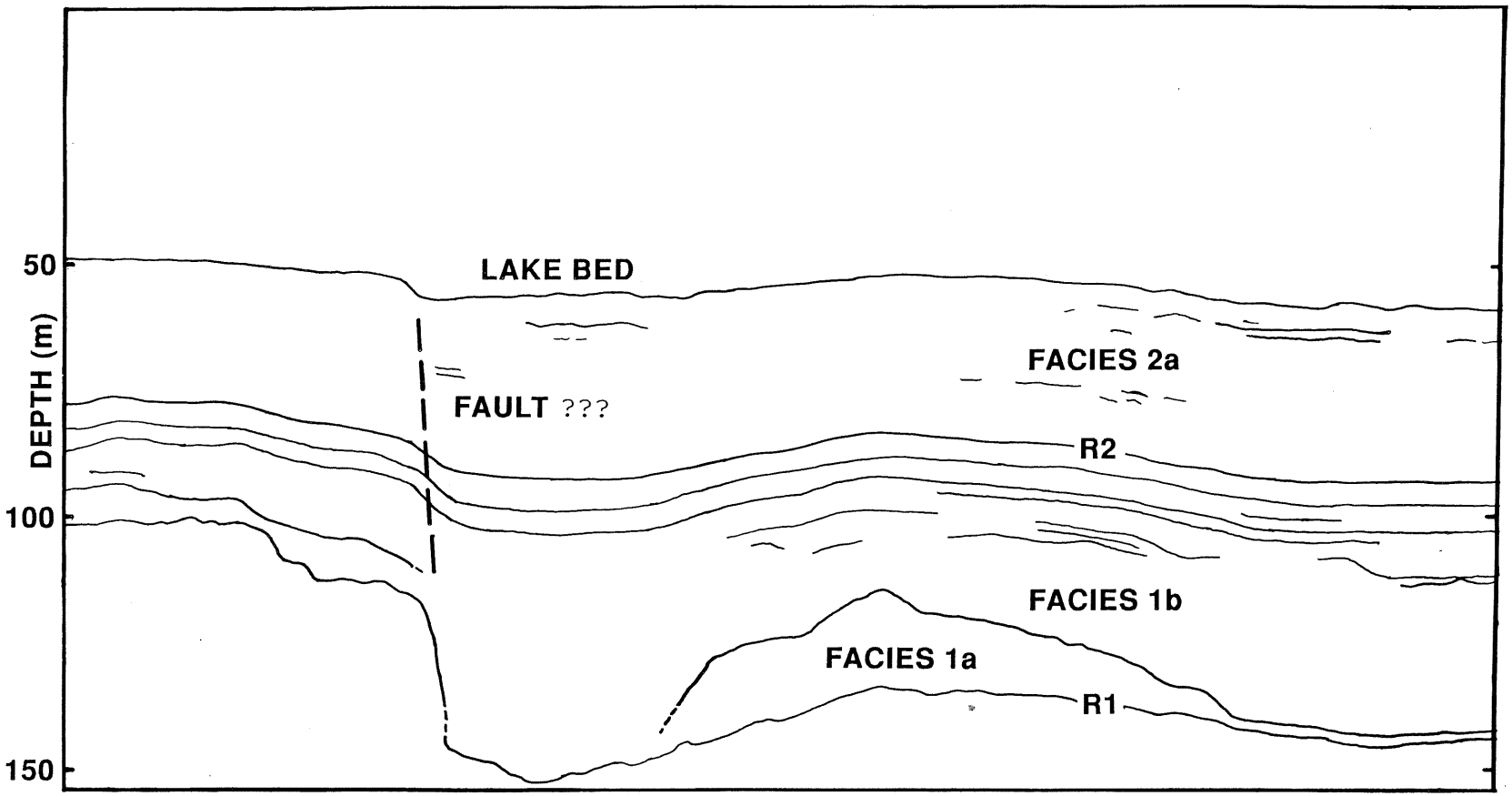

Fig 2.8a Bedrock scarp and associated lake bed step and subsurface reflector flexure found in the deeper areas of the eastern basin. These features may also be due to differential sediment compaction, with greatest settlement occurring where facies 2a and 1b are thickest.

remnant of an early shoreline, now found 30 m below present lake level. Erosion limits rise in an easterly direction, from 39 m.b.d. to 25 m.b.d. (see fig. 2.12; Coakley and Lewis, 1985). Much of the erosion of sequence 1 was likely due to wave induced bottom currents in nearshore areas of this low level lake. Raised shoreline features rimming Lake Erie have been differentially upwarped in an easterly direction by glacial isostatic adjustment (Calkin and Feenstra, 1985). The easterly rise (upwarping) of the erosion limit found below the present lake level may also be due to glacial isostatic adjustment. St.Jacques and Rukavina (1973) suggest a present nearshore erosion limit of less than 10 m.b.d. in the Long Point Bay area. This evidence would therefore suggest that a much lower lake level and smaller lake existed sometime between the deposition of facies 1b and 2a and 2b.

Two seismic facies, 1a and 1b, have been recognized within sequence 1. Facies 1a is limited in extent within the basin and is the lowermost (stratigraphically oldest) facies in the section. Chaotic internal structures and a strong surface reflection give this facies a massive appearance. Similar characteristics have been recognized in marine sequences and interpreted by many workers (e.g. King and Fader, 1986 and 1991) as glacially derived drift, where the former presence of a grounded glacier is probable; a similar interpretation can be applied to facies 1a.

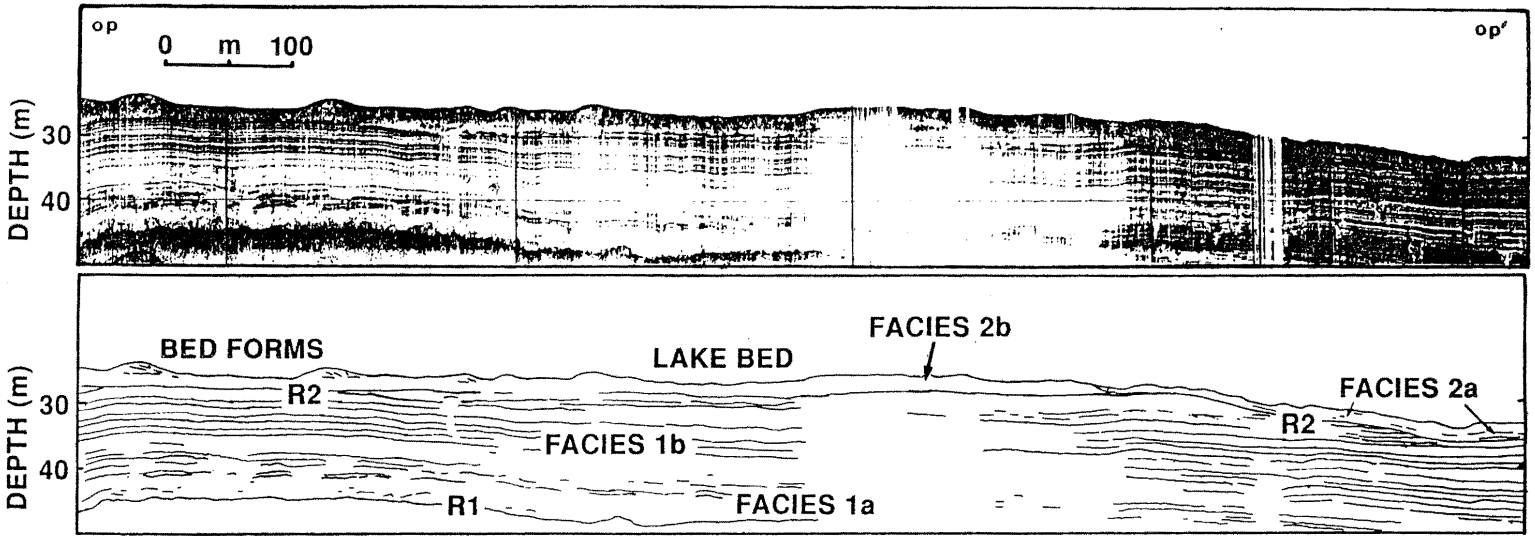

Fig 2.9 Broad-band seismic profile and line interpretation illustrating the internal structures of the bedforms of facies 2b and erosional notch (shoreface) found on the extreme right of the diagram.

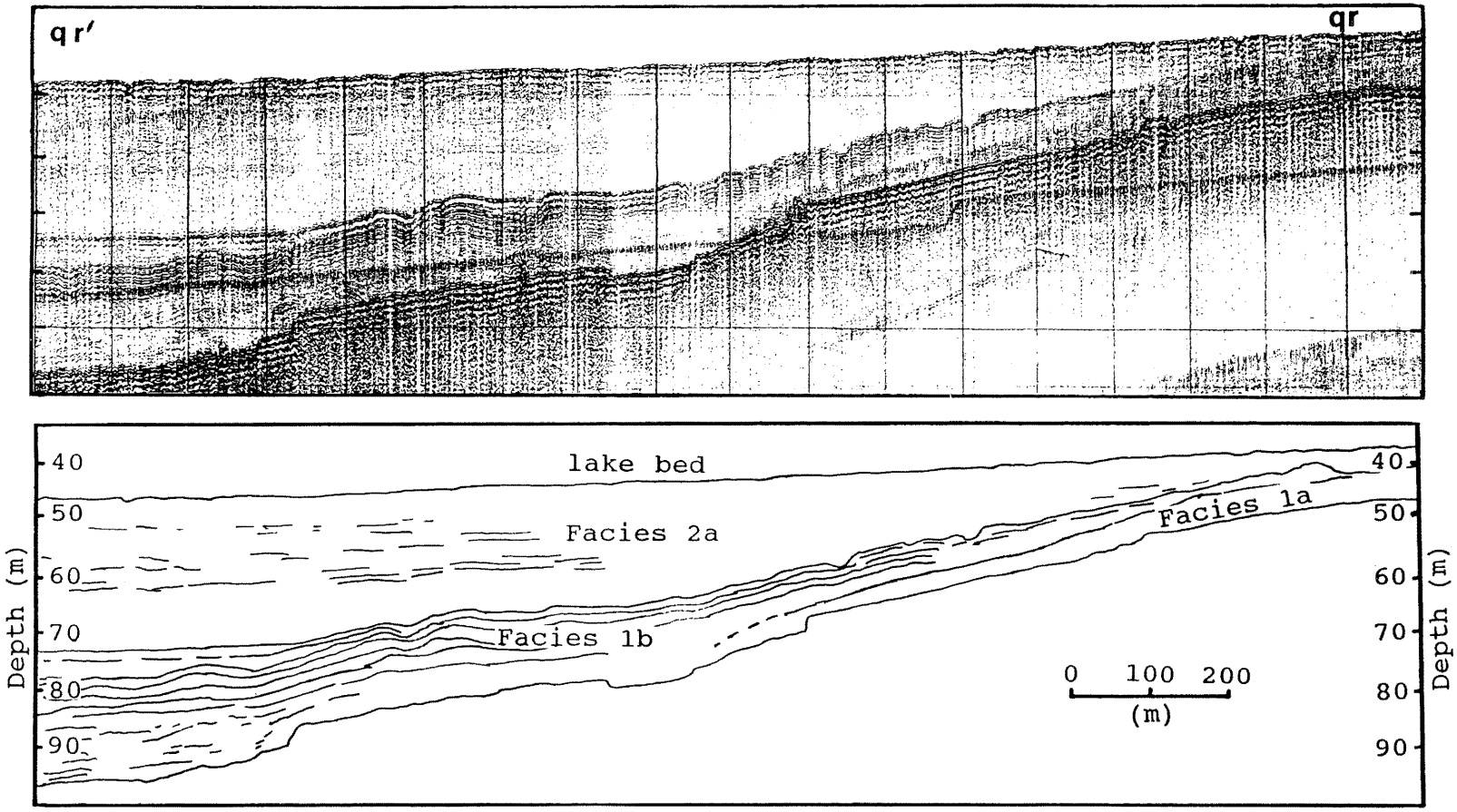

Fig 2.10 Broad-band seismic profile and line interpretation, illustrating the rough nature of the R2 reflector and the lakeward limit of facies 1a.

The interfingering relationship of the lower portion of facies 1b with the lower portion of facies 1a, along the flanks of the basin, suggests that their deposition at these sites was coeval.

Facies 1b dominates seismic sequence 1 with its high amplitude parallel coherent internal reflections and wedge shape geometry. This facies is mostly conformable throughout the basin, reflecting the stability of the basin. Where facies 1b overlies bedrock slopes, with apparent dips as great as 15^0, deformation of acoustic reflectors occurs (figs. 2.3, 2.6 and 2.10). Downslope processes may be responsible for generating soft sediment folds in facies 1b. Hill et al. (1982) recognized (in the Beaufort Sea) the importance of downslope creep deformation, which can appear as folded beds and are similar in nature to those found in facies 1b (figs. 2.3, 2.6 and 2.10). Only facies 1b is deformed in this manner, suggesting that the process is not ongoing but occurred prior to deposition of facies 2a. Dewatering of the sediments during this process could have enhanced the deformation.

The overall seismic character suggests a low energy environment where deposition of well stratified sediments could occur. Relatively thick sections of facies 1b occur shoreward of the 40 m isobath where thin, recent sediments are accumulating (sequence 2, figs. 2.4, 2.5, 2.7, 2.7a and 2.9-2.11). Thicker accumulations of facies 1b occur in

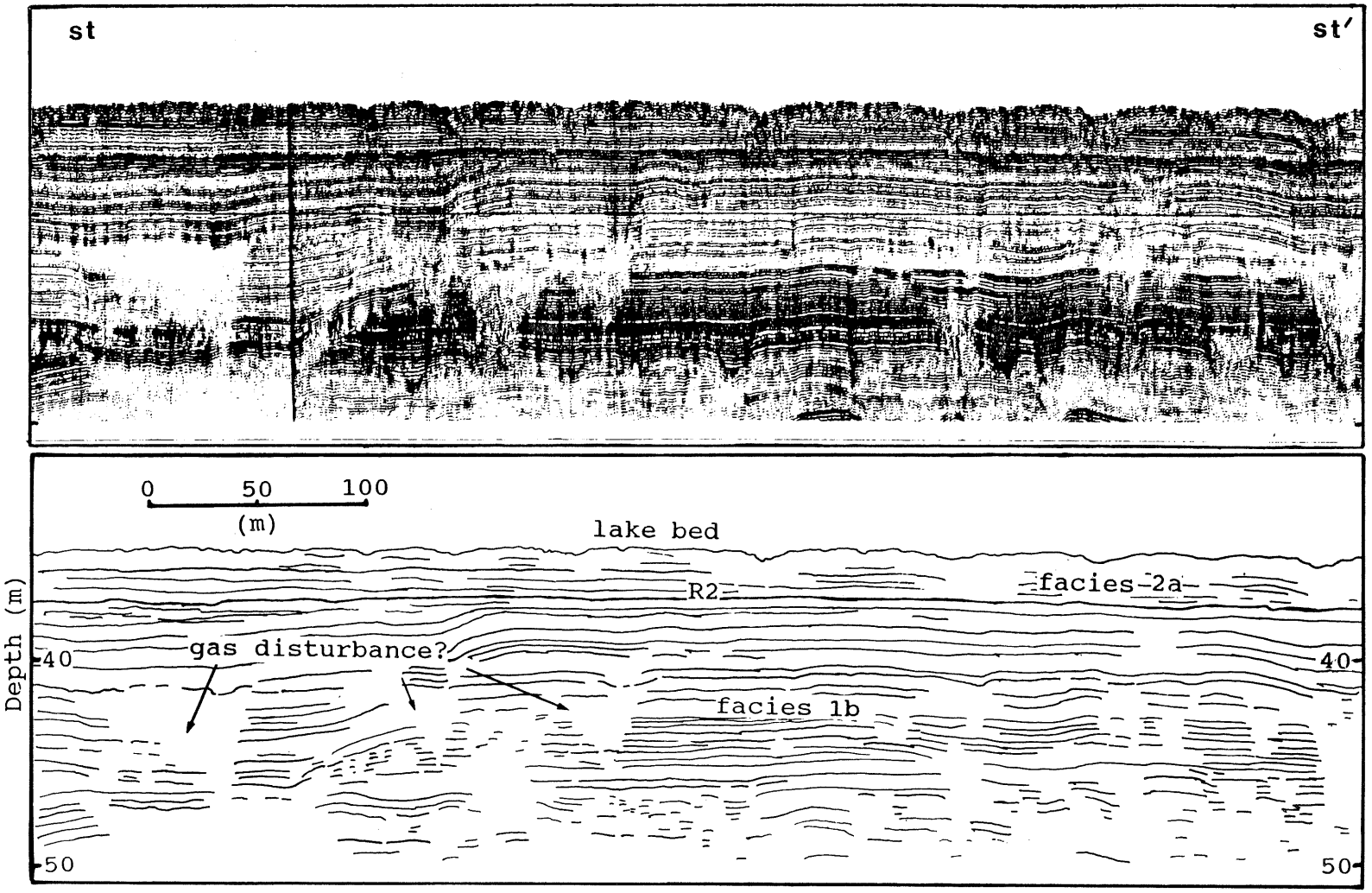

Fig 2.11 Broad-band seismic profile and line interpretation, illustrating reflection free areas which maybe due to gas disturbance.

deeper parts of the basin, generally below 40 metres water depth. The presence of facies 1b in shallow water where erosion now occurs and the well stratified nature of the sediments suggest that sedimentation occurred in water depths greater than present levels would allow. Reflection free areas, best seen in figs. 2.4 and 2.11, may be due to concentration of pore fluids, possibly brought, for example, by the venting of gas or dewatering of the sediments during seismic events. Masking of reflections due to gas charged sediments may also account for some of these reflection free areas.

Seismic sequence 2 is the uppermost sequence and consists of seismic facies 2a and 2b. Facies 2a dominates sequence 2; its relatively weak, mostly continuous parallel coherent internal reflections and body geometry suggests a ponded style of deposition throughout much of the basin, with onlap occurring in nearshore areas (figs. 2.2, 2.3 and 2.10). In shallower areas, generally < 30 m, the internal reflections are less continuous and coherent in nature. However, in Long Point Bay internal reflectors are more continous, parallel and coherent in nature.

In Long Point Bay, offset of internal reflectors in facies 2a suggests soft sediment faulting has occurred (figs. 2.7 and 2.7a). The faulting may be due to possible dewatering of the sediments. Many of these faults offset reflector R2; and internal reflectors in the upper part of

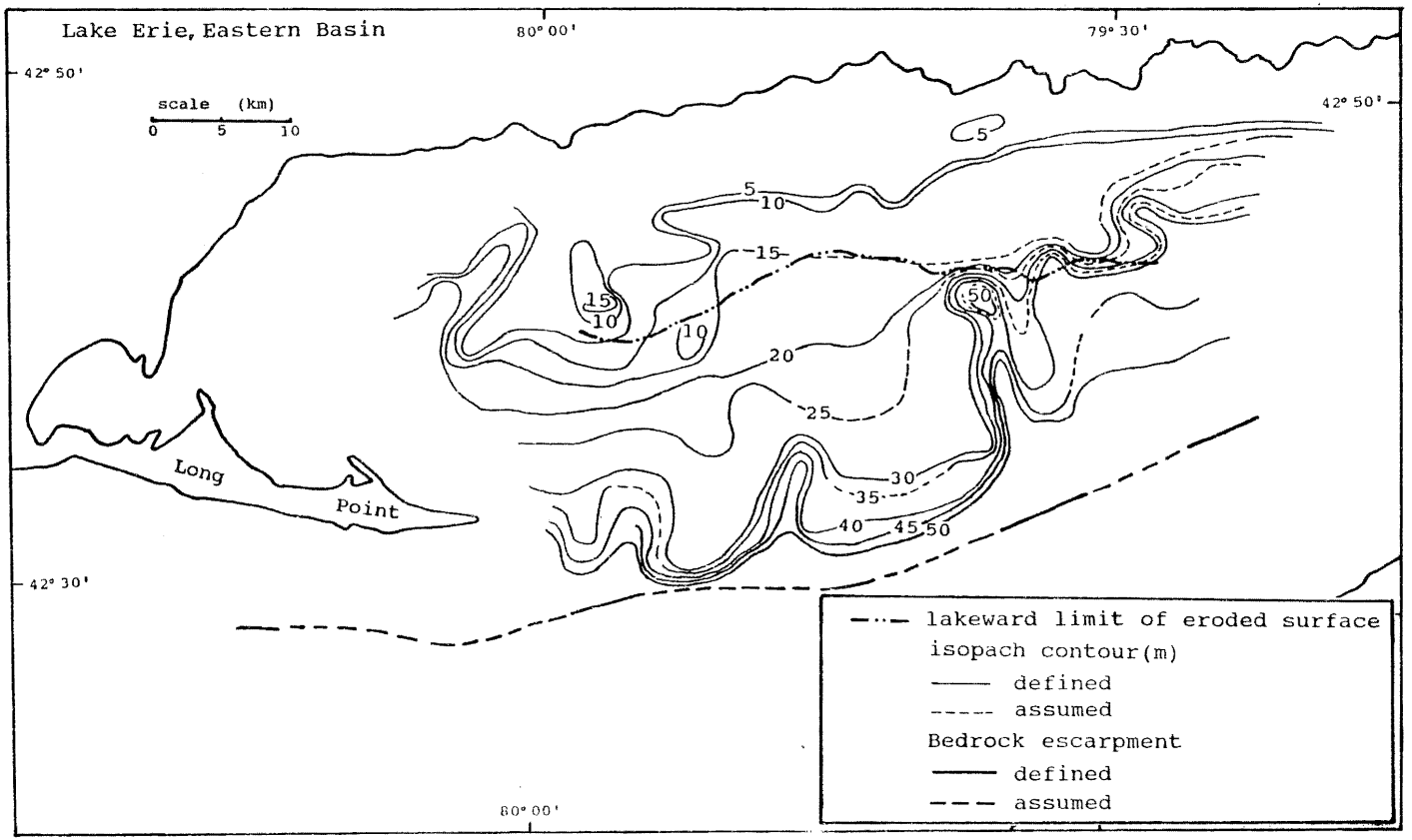

Fig 2.12 Isopach map: Sequence 1 (contours are in meters between regional reflectors R1 and R2).

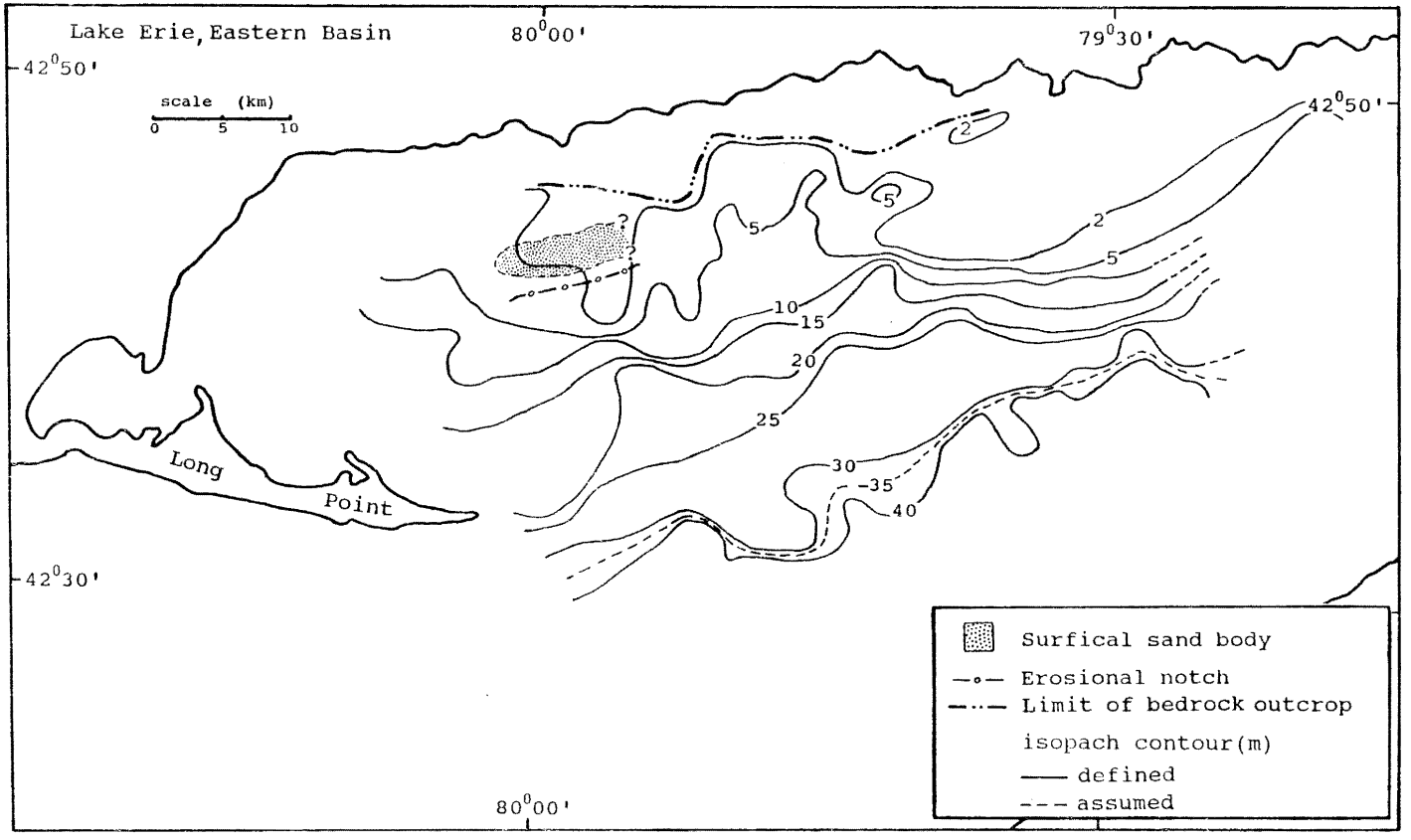

Fig 2.13 Isopach map: Sequence 2 (contours are in meters between regional reflector R2 and the lake bottom).

sequence 1 are folded (figs. 2.7 and 2.7a). Truncation of reflectors within facies 2a suggests an episode of erosion. This erosional surface appears at water depths < 20 m and is best seen in Long Point Bay (figs. 2.7 and 2.7a). This erosional surface does not coincide with the erosional reflector R2, but rather is found above it in the acoustic sequence and is therefore younger in age. This surface is mantled by a thin accumulation of more recent lake sediment (facies 2d). St.Jacques and Rukavina (1973) suggest that maximum water depth of present lake bottom erosion is limited to 10 m. A lower lake level stand may therefore explain this erosion surface.

Facies 2b is interpreted on the basis of geomorphic and acoustic character as a surface sand body which developed in nearshore or beach environment, now relict, but is still being reworked. Some of the bedforms associated with this facies have internal foresets, suggesting sediment transport and possible reworking. However, in situ reworking of the lake bottom cannot account for the 3-5 meter thick facies. This facies lies between 20 and 25 metres of water, well below the present erosion limit suggested by St.Jacques and Rukavina (1973). Although acoustic profile data suggest that facies 2b developed after the formation of the erosional unconformity surface (R2), it is associated with an erosional notch in facies 1b. Facies 2b is interpreted as a relict beach deposit, accumulated during a previous low

lake stage whose shoreface is likely represented by the erosional notch in facies 1b found just lakeward of facies 2b (figs. 2.5 and 2.9). The source of this sand may have been derived from subaqueous deltas or from the erosion of facies 1a (Fig 2.4) further offshore from the erosional notch (Fig 2.5).

Nearshore areas, along Long Point, show strong bottom returns with little or no penetration, suggesting highly reflective granular sediment. This area and the nearshore zone have been texturally mapped by St.Jacques and Rukavina (1973). They found that in the Long Point area the sediment is predominately sand and silt. The northern nearshore zone of eastern Lake Erie apart from Long Point, is dominated by bedrock and glacial sediment, veneered with lag deposits of sand and gravel.

Chapter 3

CORE STUDIES

Introduction:

Lithology

Findings from detailed lithologic descriptions and grain size analysis from 6 piston and 6 gravity cores from eastern Erie basin, are presented in this chapter. Additional ground truthing is provided from a 120 m borehole, drilled in 1963, near the tip of Long Point (Lewis, 1966; fig. 1.2), referred to hereafter as the Long Point Borehole (LPBH). The sediments are categorized into their lithological facies and possible mode(s) of deposition are discussed.

Lithofacies Descriptions:

The sediments have been divided into 6 lithofacies based on lithological properties. These lithofacies are:

1. Lithofacies 1a : Gravel-sand-mud
2. Lithofacies 1b : Laminated red-brown mud
3. Lithofacies 2a : Laminated gray mud
4. Lithofacies 2b : Brown or gray sand
5. Lithofacies 2c : Muddy sand
6. Lithofacies 2d : Massive gray mud

Sedimentary structures, colour, visual grain size estimates, sediment consistency and the nature of contacts are important criteria used in distinguishing the

lithofacies. Facies designations are based on split core and x-radiograph observations.

Lithofacies 1a: Gravel-sand-mud:

This facies appears to be the lowest encountered in the sediment section and was sampled only in piston core PC-7. This facies consists of a uniform, fine mud matrix in which many clasts can be found. It is dark gray to gray in colour (10YR 4.5/1) and moderately soft in consistency. No structural details exist giving this facies a massive appearance. Only 10 cm of this facies was sampled (fig. 3.16).

Facies 1a is extremely poorly sorted with a standard deviation of 4.02 phi and mean grain size of 8.10 phi. The clay and silt content accounts for over 80% of the sediment, with sand and gravel comprising the remainder at over 11 % and 4% respectively, (fig. 3.6 and appendix). The grain size distribution is extremely leptokurtic and negatively skewed. The contact between this facies and facies 1b is irregular and distinct.

Lithofacies 1b: Laminated red-brown mud:

Dark gray (10YR 4/1) and brown (2.5Y 5/2) laminations characterize this facies. Generally less than 1 cm thick, these laminations occasionally show rhythmic character; some laminations have a wavy appearance (fig. 3.4). Contorted sediment exists in core PC-7 between 210 and 260 cm. The sediment is firm in consistency, except in cores 9 and 1

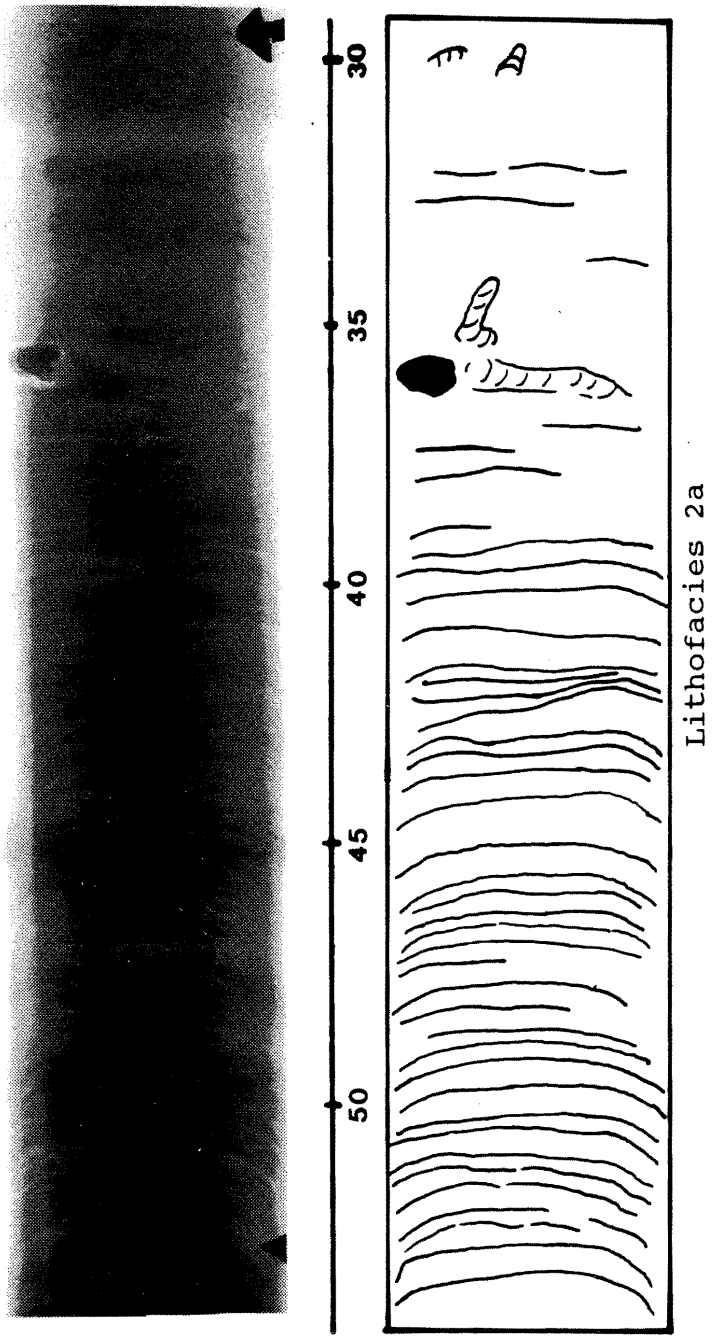

Fig 3.1 X-radiograph of lithofacies 2a (core PC1 30-54 cm) illustrating its well laminated structure.

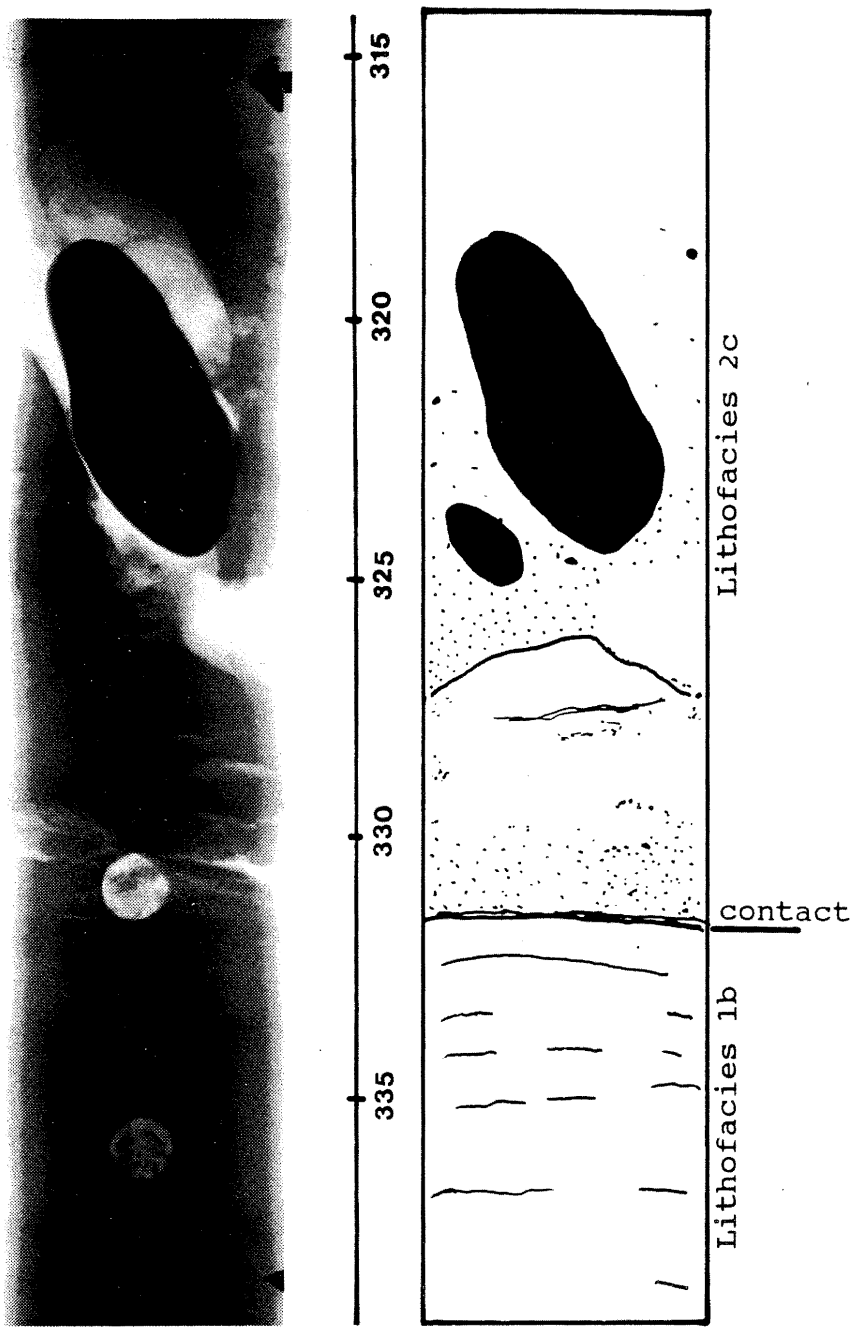

Fig 3.2 X-radiograph of lithofacies 1b and 2c (core PC1 315-339 cm) showing the rough nature of the contact and internal structures. Note the presence of large clasts in facies 2c.

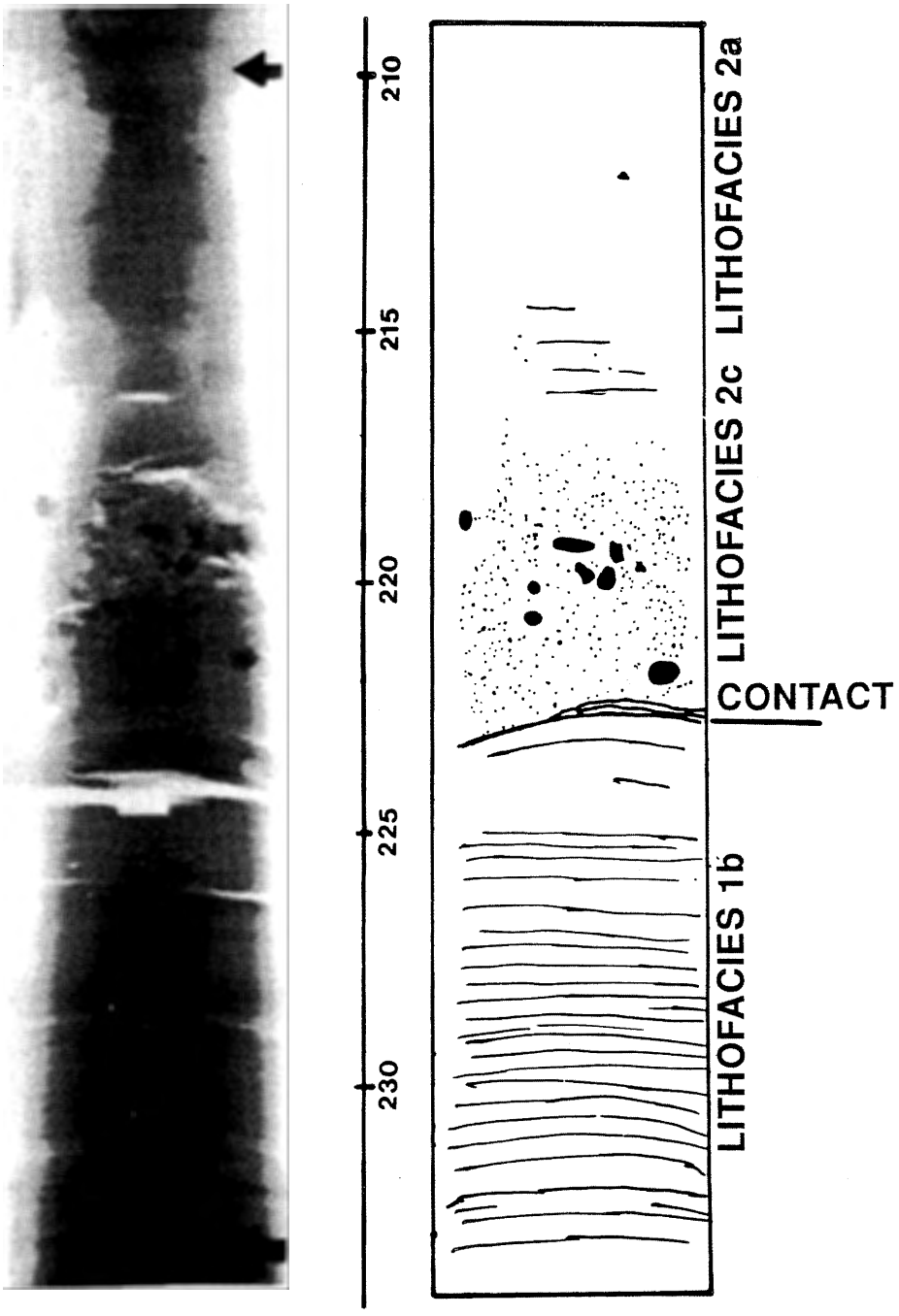

Fig 3.3 X-radiograph of lithofacies 1b, 2c and 2a (core PC-9 210-234 cm) showing the rough nature of the contact and internal structures of each facies.

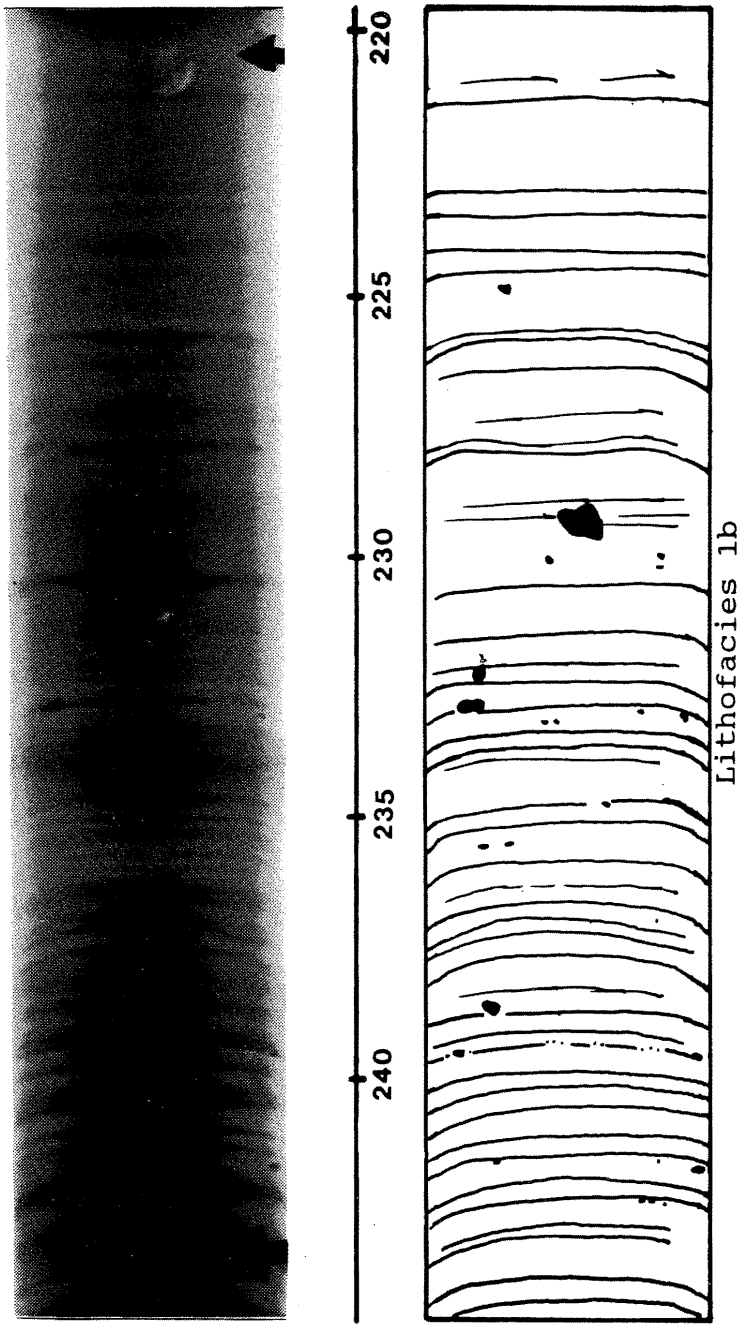

Fig 3.4 X-radiograph of lithofacies 1b (core PC-6 220-244 cm) showing its well laminated structure. Note the occasional dropstone.

where the sediment is extremely stiff and lower water content was observed. Reddish brown (5YR 3/3) and gray mud clasts are present. Thin silt/sand laminations and lenses exist singularly or in groups throughout this facies. Contact between silt/sand laminations and overlying and underlying mud is sharp. Climbing ripples were observed in a thin silt/sand lamination (ca 1 cm thick) in piston core PC-9. The occasional isolated pebble is present. The contact between facies 1b and the overlying facies 2a is sharp and irregular in nature (figs. 3.2 and 3.3), except in the deeper LPBH where the contact is gradational.

Grain size ranges from 7.99 phi to 10.68 phi, with most above 10 phi. Standard deviation is between 1.46 and 3.02 phi, making this sediment poor to very poorly sorted. The clay and silt content typically account for almost 100% of the sediment, with sand as low as 0.1 % and no gravel (fig. 3.7 and appendix). However, as mentioned above, pebbles were observed in lithological descriptions. One grain size analysis had an elevated sand content of over 11% (fig. 3.7). The grain size distribution is extremely leptokurtic and negatively skewed. This facies was sampled in all the piston cores, as well as the Long Point Borehole (LPBH) where it is described as a faintly laminated reddish gray clay with occasional limestone pebbles, silt lenses and silt seams (Lewis, 1966). In places this facies is massive in nature with alternating reddish gray clay and silt zones,

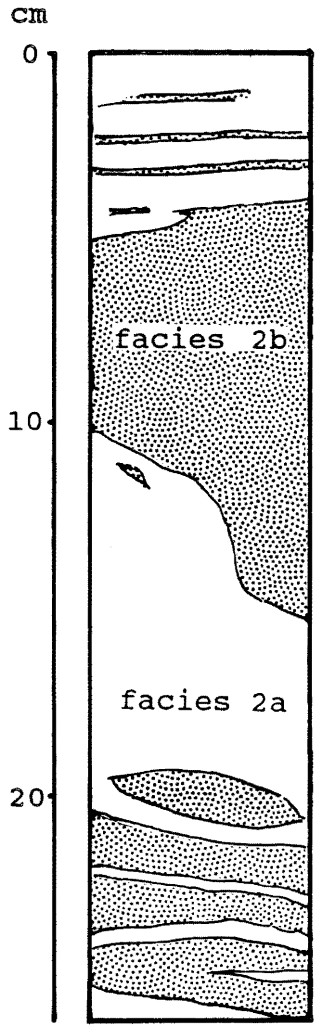

Fig 3.5 Lithology of gravity core G-8 illustrating the interfingering nature of facies 2b with facies 2a.

some sorted sand and basal gravel found in the lowest portions of LPBH, (between 105 and 118 meters, see fig. 3.11).

Lithofacies 2a: Laminated gray mud:

Facies 2a unconformably overlies facies 1b except in the LPBH, where a complete pollen sequence suggests that the contact is conformable. This facies consists of a very soft to soft dark gray (10YR 4/1) to dark grayish brown (2.5Y 42) mud. Weak laminations, generally less than 1 cm thick, typify this facies. However, bioturbation does occur, giving a less structured appearance in portions of this facies (fig. 3.1). Vertical mixing of the sediment due to bioturbation seems incomplete. Black reduction spots and streaks (sulphide) occur often. Gas escape features are present in core PC-3 , mostly destroying the primary sedimentary features. Fine continuous and discontinuous silt and fine sand laminations, some wavy in nature, occur singly or in groups throughout portions of this facies.

The mean grain size ranges between 8.84 and 10.08 phi, with most above 9.0 phi. Standard deviation ranges between 2.06 and 3.29 phi, making this sediment very poorly sorted. The grain size distribution is extremely leptokurtic and negatively skewed. This facies is dominated by fine grained sediment, with silt content ranging from 13.5 to 46.1% and clay content ranging from 52.4 to 85.3%. Sand content varies little in this facies and exists in small quantities,

ranging from 1.3 to 3.8%, gravel is absent (fig. 3.8 and appendix).

Lithofacies 2b: Brown or gray sand:

This facies was sampled only in gravity core GC-8 and piston core PC-9 and PC-10. This facies consists of a brown (10YR 5/3) to gray (10YR 5/1) coloured, medium to fine grained, clean sand. Internal structures are not evident, giving this facies a massive appearance. In gravity core GC-8 the sands interfinger with the recent muds of lithofacies 2a (fig. 3.5). However, interfingering of 2a with 2b does not occur at depth; piston core PC-10 showed that the facies 2b was at least 3m thick. The sands of facies 2b consist of 75 to 80% quartz and 20 to 25% lithic grains. The quartz grains are subangular to subrounded with a medium degree of sphericity. The lithics consist predominately of carbonates and are rounded to subrounded with a medium to high degree of sphericity. Some mud balls (clasts) are found with the sand.

Lithofacies 2c: Muddy sand:

Coarse sediment, consisting of sand, pebbles, cobbles and shell debris mixed with mud, is found between facies 1b and 2a (figs. 3.2 and 3.3). The sediment in this zone is approximately 25 cm thick, or less, and fines upwards into facies 2a. The mean grain size ranges between 3.34 and 4.73 phi and sorting is very poor, with standard deviation between 2.16 and 4.17 phi. Cumulative frequency curves show

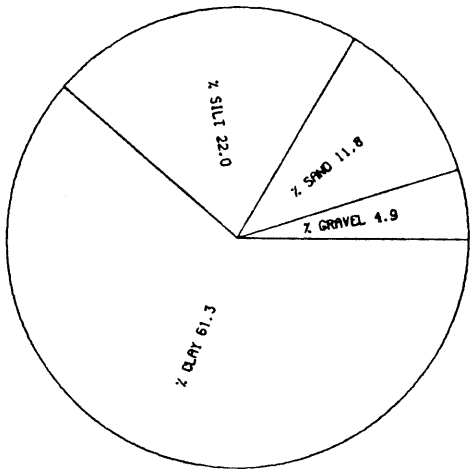

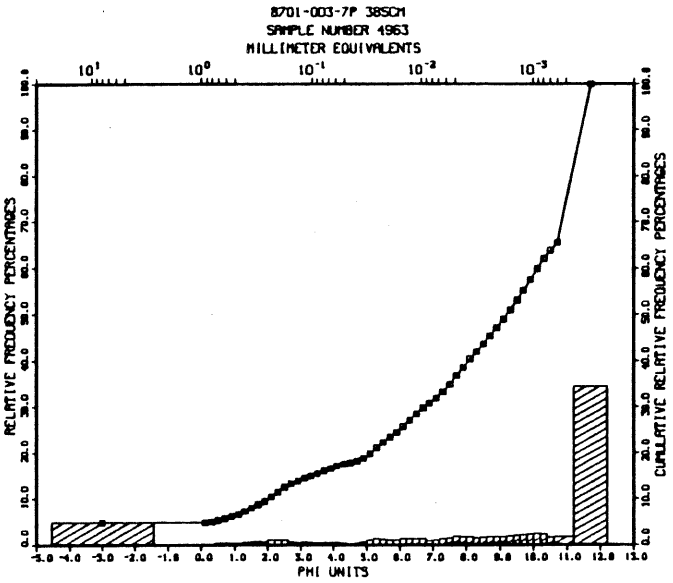

Fig 3.6 Grain size analysis: Facies 1a.

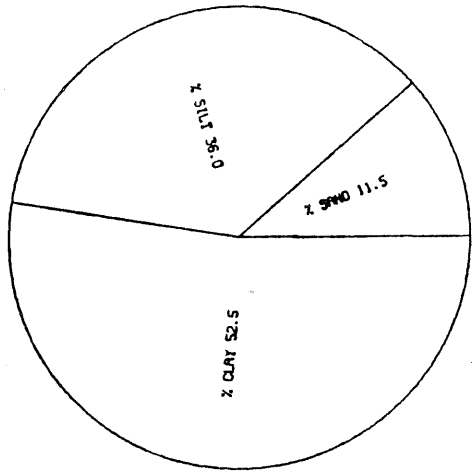

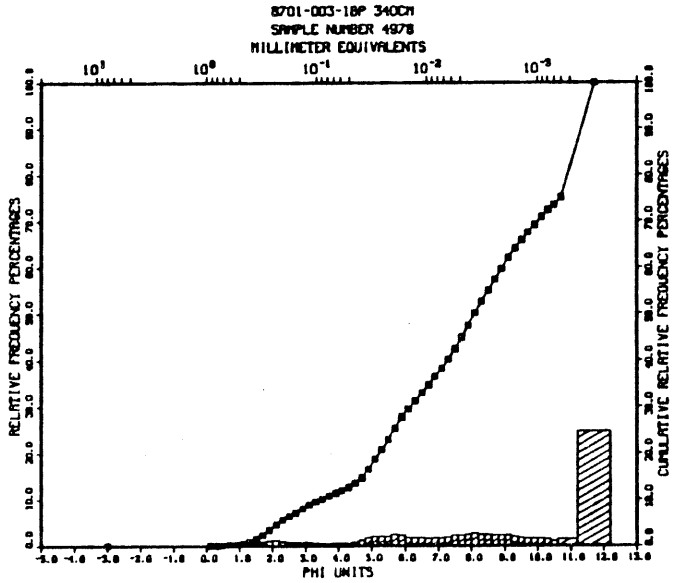

Fig 3.7 Grain size analysis: Facies 1b.

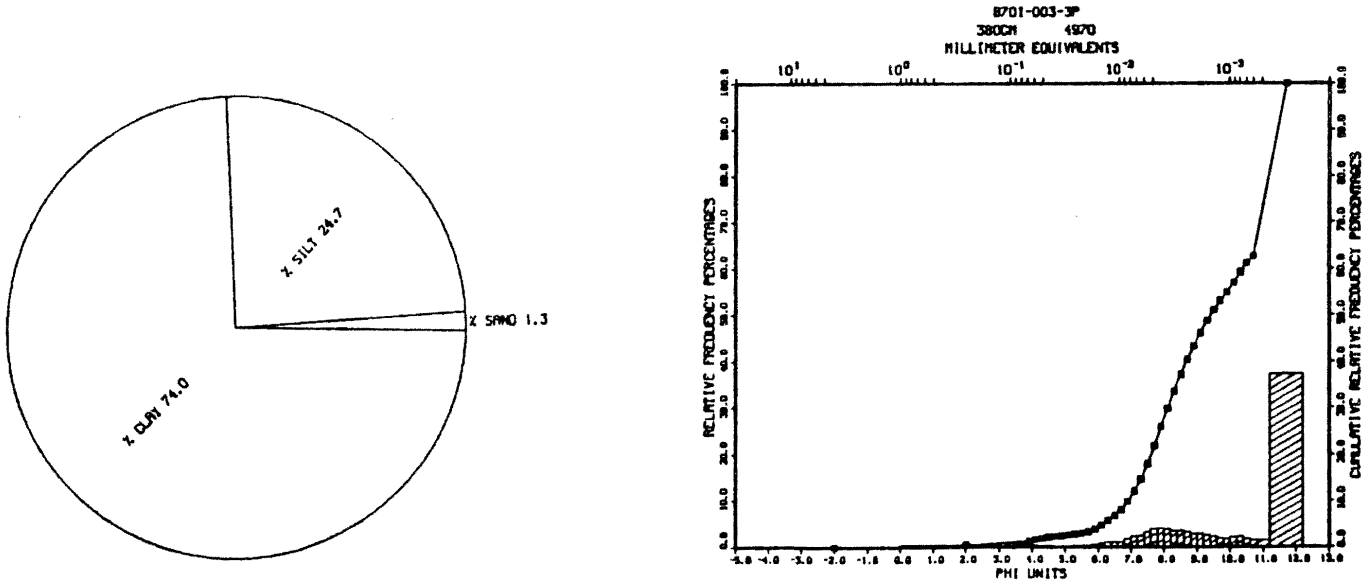

Fig 3.8 Grain size analysis: Facies 2a.

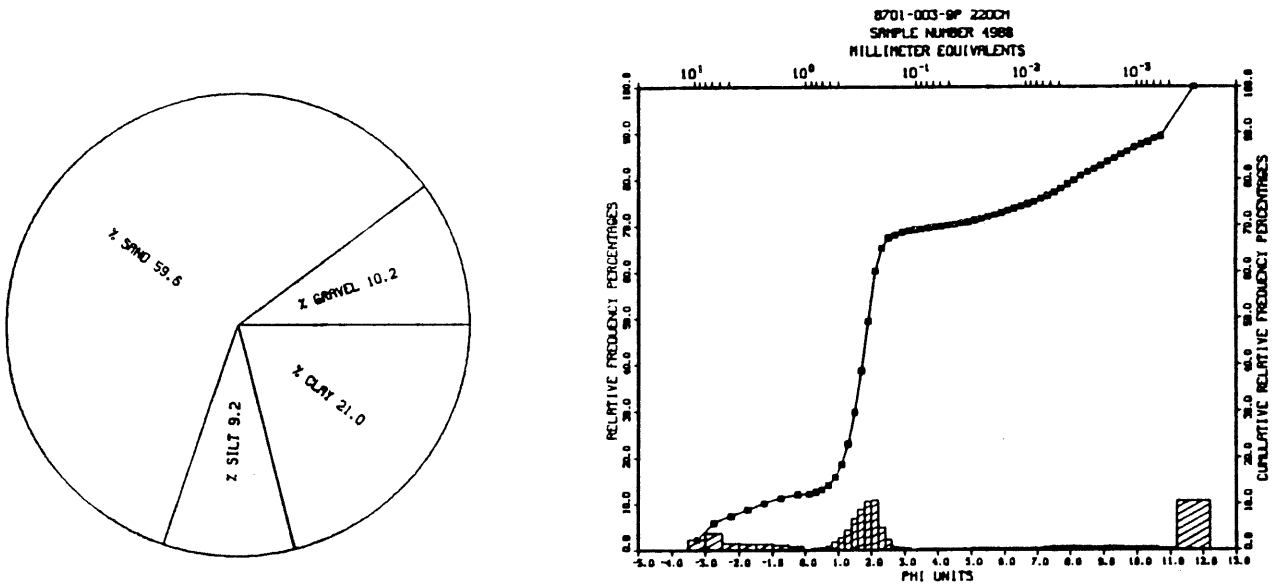

Fig 3.9 Grain size analysis: Facies 2c.

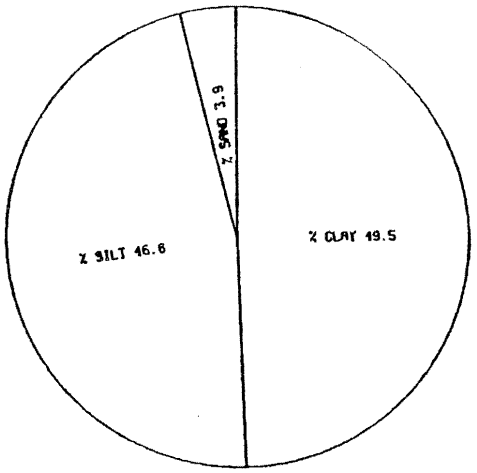

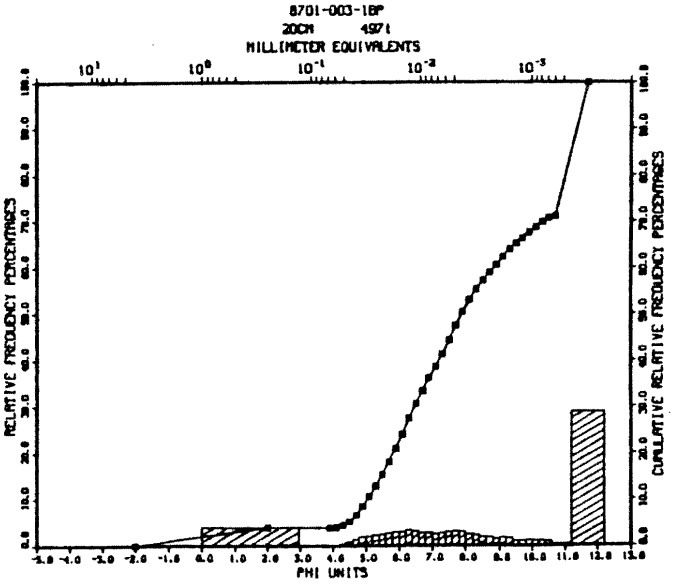

Fig 3.10 Grain size analysis: Facies 2d.

that samples from this zone are bimodal in nature and that the dominant sand mode is moderately well sorted, (fig. 3.9 and appendix). Gravel content ranges from 0.1 to 10.2%, with the silt and clay components together ranging between 30.2 to 43.7% of the sediment. Sand dominates this facies, ranging between 55.5 and 69.5%. This zone is thickest and best developed in cores PC-1 and 9, and to a lesser degree in core PC-7. A small amount of sand appears in core PC-3 mixed with the mud just above the contact between facies 1b and 2a; this zone does not exist in the LPBH. The boundary which separates lithofacies 1 and 2 in cores PC-3 and the LPBH is distinct but not wavy in nature as it appears in cores PC-1, 9, 6, and 7 (figs. 3.13-3.17). Lithofacies 2c rests above and in contact with this boundary.

Lithofacies 2d: Massive gray mud:

This facies consists of massive grayish brown to dark gray silty mud. This facies occurs in the top 37 cm of core PC-1 and the top 41 cm of core PC-9. A slight change in colour and a concentration of coarser material distinguishes this facies from facies 2a (figs. 3.13 and 3.17). This facies occurs above and in contact with a wavy, sharp contact surface.

A grain size analysis of facies 2d from core PC-1 shows clay and silt content to be almost evenly split at 49.5% and 46.6% respectively (fig. 3.10 and appendix). Sand constitutes only 3.9% of the sample. The sediment is very

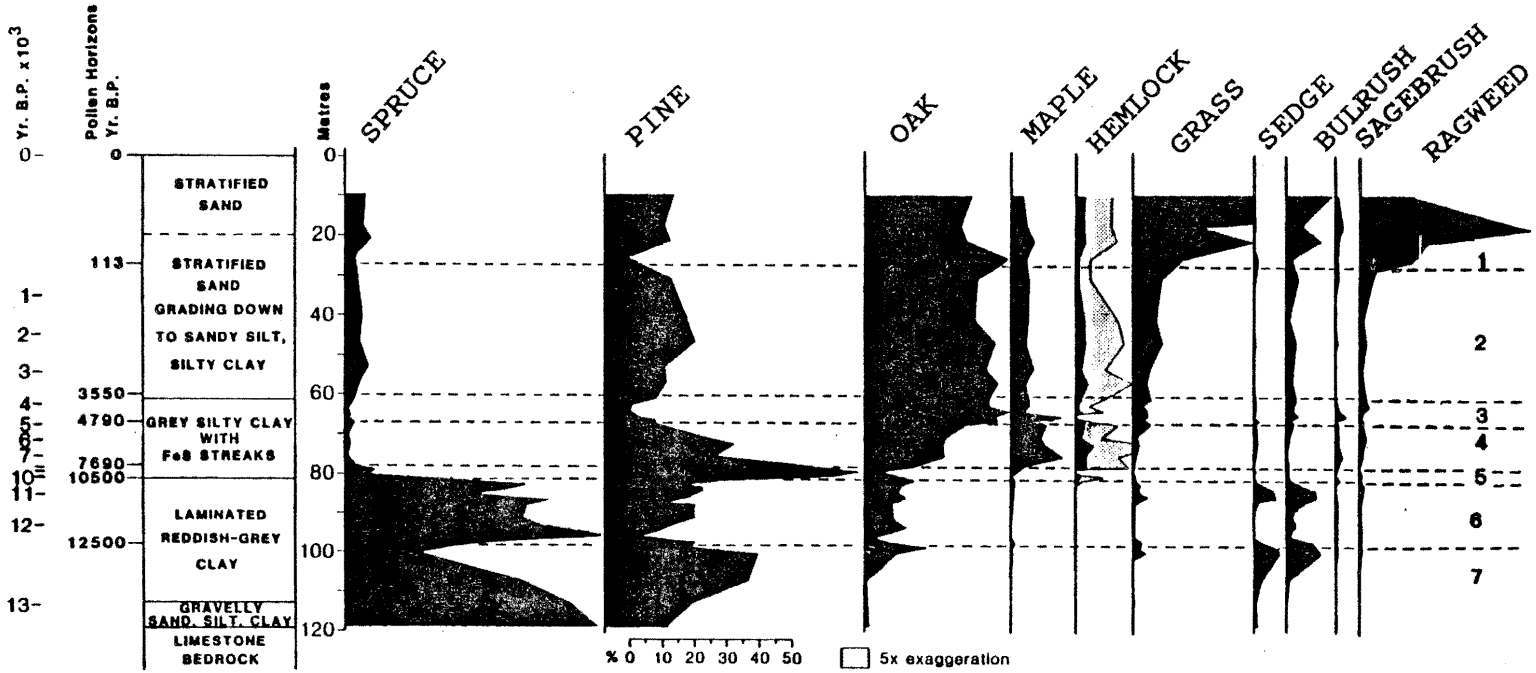

Fig 3.11 Pollen stratigraphy for Long Point borehole (LPBH), courtesy of T.W.Anderson.

poorly sorted with a standard deviation of 2.71 phi with a mean grain size of 8.30 phi. The sediment is coarsely skewed and very leptokurtic.

Pollen Chronology:

A radiocarbon dated pollen stratigraphy was established from sediment sequences in bogs and small inland lakes to the north (Karrow, 1963) and south (Kapp and Gooding, 1964) of Lake Erie. Lewis et al. (1966), established that the Lake Erie pollen record, dated by radiocarbon, can be useful in dating and correlating sediments within the Lake Erie basin. Pollen profiles from vertical sediment sequences in Lake Erie provide chronological control for this study.

Three cores, piston cores PC-3, PC-6 and PC-9 (see fig. 1.2 for location) were chosen for palynological studies. A detailed pollen analysis of core PC-3 and partial analysis of cores PC-6 and PC-9, were performed under contract by Francine McCarthy (Dalhousie University). Additional pollen analysis on core PC-3 was completed by Dr. T.W. Anderson of the Geological Survey of Canada. The Long Point Borehole (LPBH) pollen diagram was made available by Dr. T.W. Anderson and is included as figure 3.11. Frequency profiles of selected pollen types for core PC-3 are shown graphically in figure 3.12.

The lowest pollen assemblage in the LPBH pollen profile (Fig. 3.11), is dominated by sedge-sagebrush, giving these sediments an age older than 12,500 y.B.P. This pollen

assemblage commonly implies tundra or forest-tundra conditions which would have existed shortly after ice retreat (Anderson, 1982). The sedge-sagebrush/spruce boundary has been defined at 12,500 y.B.P., with spruce dominating the next pollen assemblage for 2,000 years until 10,500 y.B.P., as shown in figure 3.11.

Piston core PC-3 bottomed within the spruce zonation, giving a good pollen profile of a portion of the spruce maximum and decline (fig. 3.12). Therefore, these sediments are younger than 12,500 y.B.P. but older than 10,500 y.B.P. These sediments are referred to earlier in this chapter as lithofacies 1b, and are stratigraphically equivalent to those sediments found in LPBH. Low pollen counts in core PC-3 at the top of the spruce zone (780 cm down core) may be due to oxidation and /or loss of pollen from washout (Anderson, pers. comm. 1989).

The spruce dominated pollen zone gives way to a pine dominated zone at approximately 10,500 y.B.P. The lithologies of cores LPBH and PC-3 also change at this point, from a brown or reddish brown, laminated mud to a grey, silty mud. The spruce-pine transition indicates a major vegetation change from spruce to pine dominated mixed forest (Lewis et al., 1966; Anderson, 1984; Fritz et al., 1975). Pollen in general is very poorly preserved at level 770 cm in core PC-3, with high numbers of indeterminable pollen (34%). Low pine percentages, relative to the very

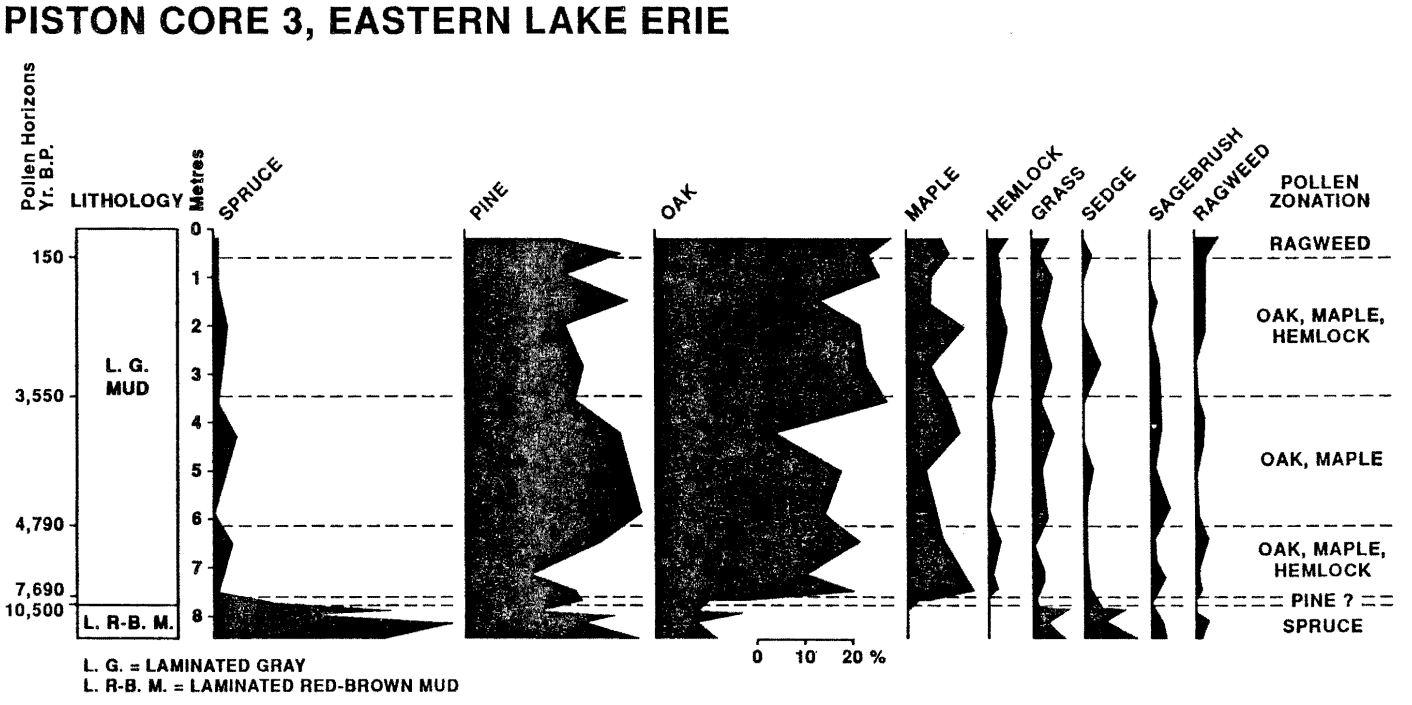

Fig 3.12 Pollen stratigraphy for core PC-3, analysed by F. McCarthy.

high values of the LPBH (approx. 75%), also at level 770 cm, may indicate that a portion of the pine zone is missing in core PC-3 (see figs. 3.11 and 3.12). The percentage of pine pollen declined sharply after 7690 y.B.P. with increasing percentages of oak, maple and hemlock occurring up core. The boundaries of the next three zonations are based mostly on the fluctuations of hemlock. The post-pine rise of hemlock increased to a peak and declined to a minimum value at 4790 y.B.P. (figs. 3.11 and 3.12). The decline in hemlock persisted until 3550 y.B.P. Pine percentages fluctuated during this time in cores PC-3 and LPBH with occasional increases greater than 30%. However, oak and maple dominated this mixed forest environment. High percentages in hemlock pollen further up core signify a hemlock recovery and are dated at 3550 y.B.P. A very recent horizon marker, associated with forest clearance and the establishment of European-type agriculture, is the ragweed pollen rise dated at ca 300 to 110 y.B.P.; this is present in both cores PC-3 and LPBH. This shows that complete sediment sections were sampled by both cores. To determine the age of several unconformities, found in cores PC-6 and PC-9, several pollen samples were taken. Pollen analysis has confirmed the existence of an unconformity between 225 and 212 cm and between 50 and 30 cm in core PC-9 (see fig. 3.17 and table 3.1). The sample at 225cm is rich in spruce as well as pine, placing it in the late spruce zone (ca

Table 3.1 Pollen Results

Core PC-9

	30 cm	50 cm	212 cm	225 cm
Picea	x	10.6	x	16.7
Pinus	22.9	28.7	40.9	42.2
Quercus	31.2	13.6	21.8	6.9
Acer	1.8	1.5	5.5	0
Tsuga	9.2	0	6.4	0
Gramineae	8.3	10.6	6.4	11.1
Cyperaceae	5.7	6.1	x	3.3
Artemisia	2.7	0	x	2.2
Ambrosia	3.7	x	x	1.1

x= <1% All values are in %.

Core PC-6

	95 cm	115 cm
Picea	x	17.3
Pinus	19.8	26.9
Quercus	28.8	11.5
Acer	5.4	0
Tsuga	9.9	0
Grominiae	4.5	3.8
Cyperaceae	1.8	1.9
Artemisia	1.8	1.9
Ambrosia	x	0

x = < 1% All values are in %.

10,500 y.B.P.). The sample at 212 cm is rich in oak, maple and hemlock, therefore dating younger than 7690 y.B.P. The sample at 50 cm is rich in pine and spruce but low in hemlock, placing it in the oak, maple zone (after 4790 y.B.P. and before 3550 y.B.P.). The relatively high percentages of ragweed and grass, found in the overlying sample 30 cm, would place these sediments in the very base of the ragweed zone (ca 300 to 110 y.B.P.). Similar pollen control from core PC-6 (see fig. 3.15 and table 3.1) also confirms the presence of an unconformity similar in age to the oldest found in core PC-9. The sample from 115 cm, just below the unconformity, shows the age of the muds, from facies 1b, to be early postglacial (ca. 10,500 y.B.P., from the dominance of spruce and pine pollen), placing these sediments in the spruce zonation. The sample from 95 cm, (dominated by maple, oak and hemlock) shows that the sediments overlying the unconformity are younger than 7690 y.B.P. (see table 3.1).

The oldest uncomformity, dated both in cores PC-6 and PC-9, would have to be ca 10,500 y.B.P. and may well have occurred during the early pine zonation. The younger unconformity, dated only in core PC-9, could not have occurred before 4790 y.B.P. Implications of these findings will be discussed further in Chapter 4.

Geotechnical Properties:

Five piston cores (PC-1, 3, 6, 7, and 9) and four

gravity cores (G-1, 3, 6, and 7) were extensively tested and subsampled for their geotechnical properties. Shear strength, bulk density, water content, porosity and sonic velocity measurements were plotted against down-core lithology, (see figs. 3.13 - 3.21). The testing and analysis of these data has produced an additional means of characterizing the sediments. This characterization has helped to differentiate between lithofacies and aid in stratigraphic correlation. Geotechnical properties are largely dependent upon sediment type and grain size which are controlled by source area, depositional environment and burial history. The geotechnical investigation has yielded insight into geological processes which affected the sediments.

Water Content:

Elevated water content values, in excess of 70%, appear at the top of core PC-1 (fig. 3.13), near the sediment water interface. Values quickly decrease to near 40%, (below 30 cm) and are maintained near this level throughout facies 2a. An abrupt decrease in the water content occurs below the boundary between facies 1b and 2a. Water content values fall below 20% near the contact, with values increasing somewhat (to about 30%) near the core bottom (see fig. 3.13). The highest rate of decrease in facies 2a occurs within the upper portion of the sediment column. Core PC-9 has a similar water content curve, with the exception that

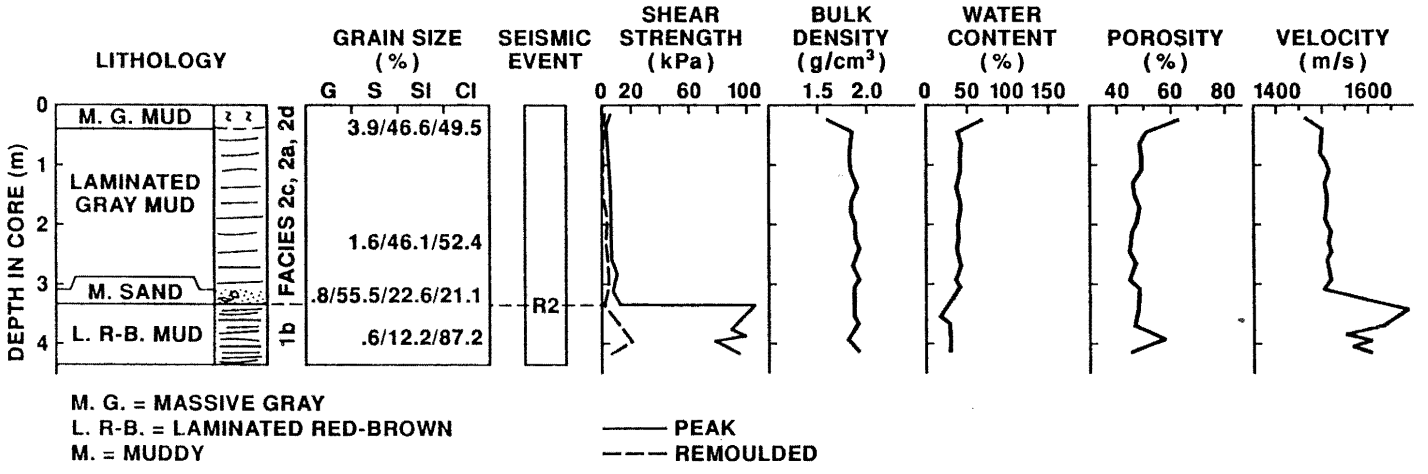

Fig 3.13 The down-core shift to higher shear strength and lower water content at ca 330 cm depth clearly mark the R2 unconformity between facies 2a and 1b.

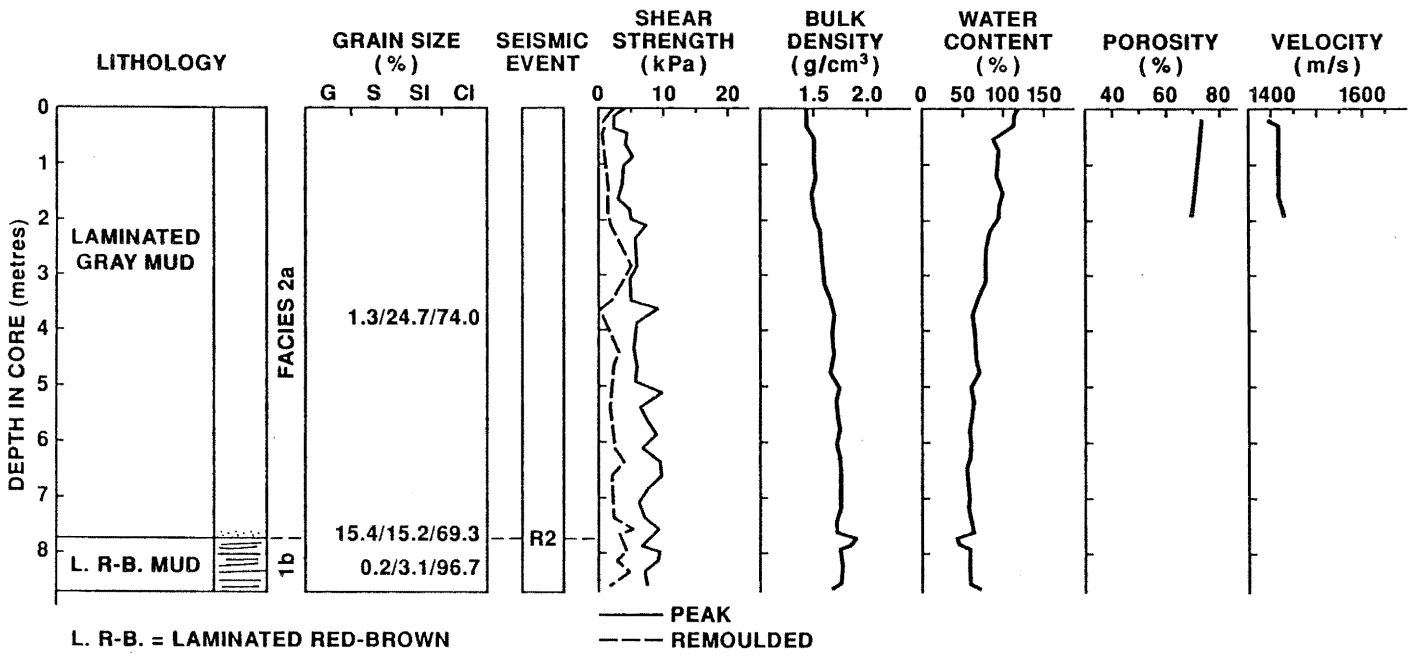

Fig 3.14 Physical property profiles show normal consolidation with depth, even across R2 between facies 2a and 1b at ca 780 cm depth.

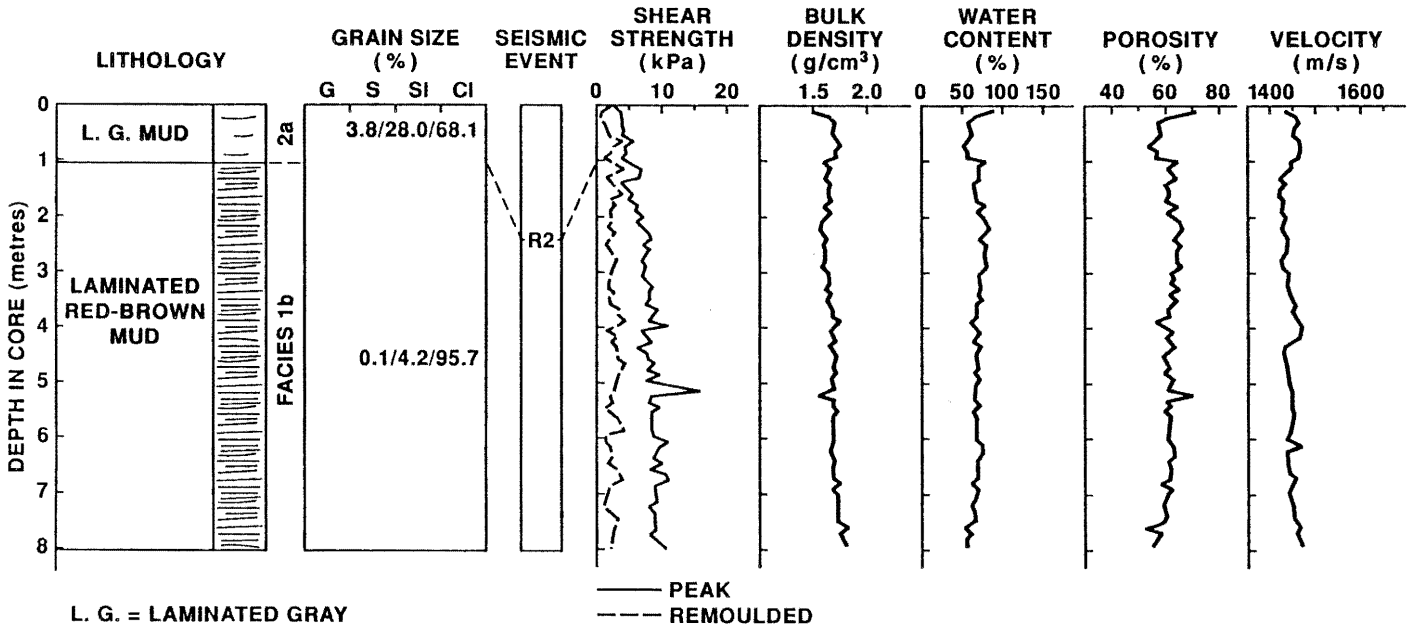

Fig 3.15 Changes in lithology and physical properties distinguish facies 1b from 2a and clarifies the R2 boundary, at ca 105 cm depth.

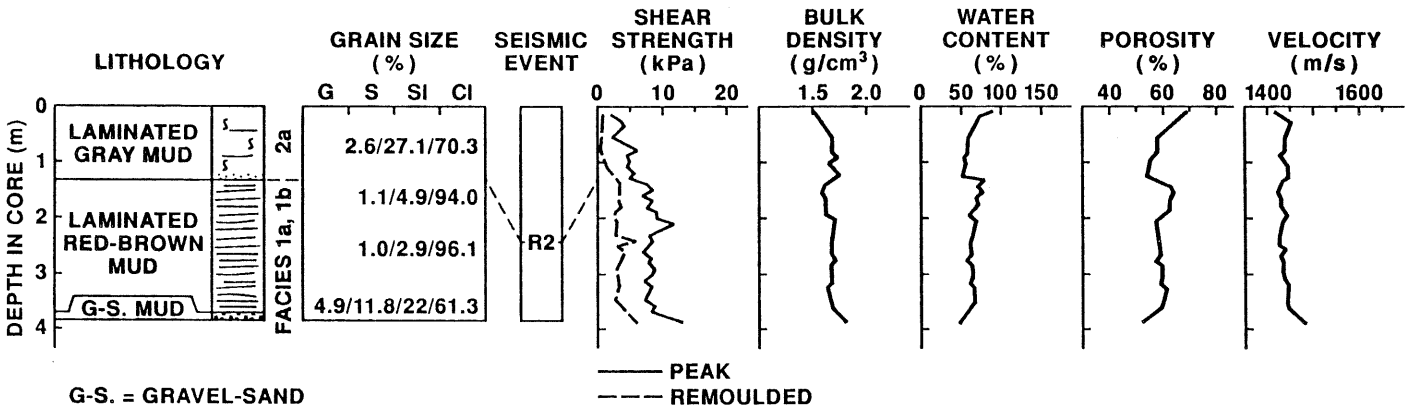

Fig 3.16 Changes in lithology and physical properties distinguish facies 1a from 1b and 2a at ca 370 cm and ca 140 cm depth, respectively.

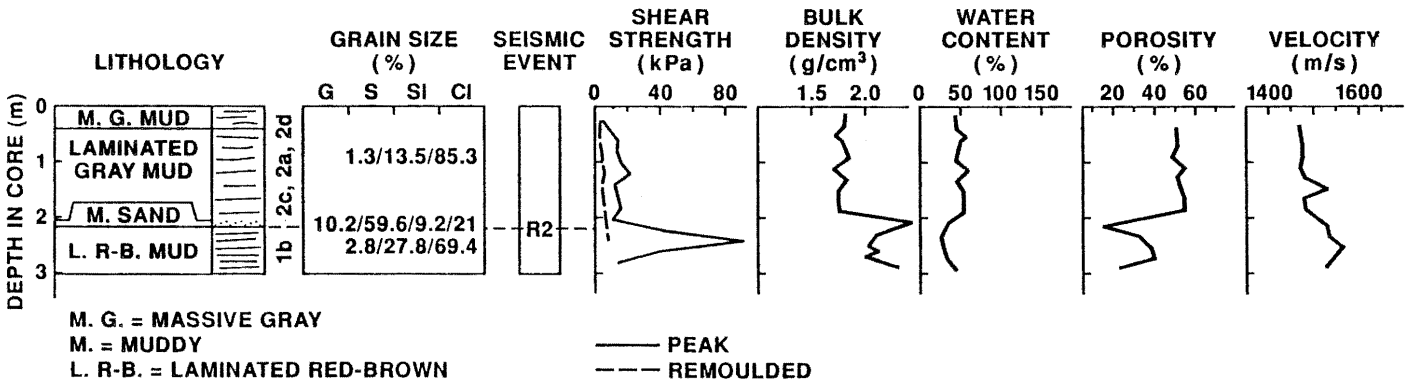

Fig 3.17 The down-core shift to higher shear strength and bulk density, and lower water content at ca 220 cm depth clearly mark the R2 unconformity.

high water content values for facies 2a are not observed in the upper portion of the sediment column (see fig. 3.17). Also, slightly higher water content values for facies 1b are observed near the core's end (within 40%). The abrupt decrease in water content values observed across the erosional boundary between facies 1b and 2a, and the low values found within facies 1b, suggest that the sediments of facies 1b are desiccated. Zeman (1976), observed low water content values in sediments below an erosional unconformity in a suite of boreholes from the central basin of Lake Erie. He interpreted these findings as indicators of a previously desiccated and subaerially exposed sediment. The erosion and desiccation observed in these cores are also considered to be a result of subaerial exposure.

Water content values for cores PC-3, 6 and 7 are very high near the core tops (near the sediment water interface), with values between 90 and 120% (figs. 3.14 -3.16). Water content values are very high, (between 120 and 190%), at the sediment water interface, in gravity cores G-3, 6 and 7 (figs. 3.19-3.21). Water content values in excess of 100% indicate that there is more water present in the sample than sediment. These levels, when compared with those in piston cores PC-3, 6, and 7, suggest that the very top portion of sediment may be missing from each piston core. Unlike what is observed in PC-1 and 9 (figs. 3.13 and 3.17) overall water content values decrease steadily down core within

facies 2a. However, water content minima are similar (near 40%). Water content values, within facies 1b, increase below the erosional boundaries in cores PC-6 and PC-7 (jump to approx. 80%) and then continue to decrease down core (to values less than 50%, figs. 3.15 and 3.16), evidence that the surface, not the subsurface, of facies 1b was affected by the desiccation process. Water content values in facies 1b from core PC-3 (fig. 3.14) largely remain constant down core. Water content values for facies 1a, found only in core PC-7, drop sharply to levels just above 40% (fig. 3.16). Sediments of facies 1b, found in cores PC-3, 6 and 7, are not dessicated and therefore were not subaerially exposed. These cores are found further offshore in water depths greater than 30 m (see table 1.1). Both cores PC-1 and 9 are found at water depths less than 20 m and nearer shore.

Undrained Shear Strength:

Muds of facies 2a are very soft in consistency, with most undrained shear strength values below 10 kPa, (figs. 3.13-3.21) and a maximum value less than 25 kPa. Near the sediment water interface, values are extremely low, with most values below 5 kPa. Below the sediment water interface the shear strength shows a tendency to increase slightly with depth, which reflects the underconsolidated state of the sediment. Peak values above the trend of the curve are best observed in figures 3.14 and 3.16 and may be due to

natural partial cementation. Higher shear strength values are observed in facies 2a, near the contact with the underlying facies 1b, than at the sediment water interface.

The consistency of facies 1b is soft to very stiff with shear strength values ranging from <5 kPa to values approaching 110 kPa. The softer sediment of facies 1b is found in deeper water, further offshore, in cores PC-3, 6 and 7 (figs. 3.14, 3.15 and 3.16). These sediments have undergone erosion but low shear strength values suggest that these sediments are not overconsolidated.

Very high shear strength values are observed in cores PC-1 and PC-9, within facies 1b (figs. 3.13 and 3.17). High shear strength values, in core PC-9, decline rapidly down core from a high of near 80 kPa to a low of approximately 16 kPa. High values are maintained in core PC-1, with values greater than 80 kPa. These measurements were from sediments which have undergone erosion and possible dessication due to subaerial exposure.

Facies 1a, in core PC-7, has a shear strength value of approximately 15 kPa, giving the sediment a rather soft consistency. In general the data indicate an inverse correlation between shear strength and water content.

Bulk Density:

The bulk density curve appears to be inversely related to the water content curve (figs. 3.13 - 3.21). Low bulk density values (less than 1.5 g/cm^3) appear at core top,

near the sediment water interface. Bulk density values increase with depth, ranging mostly between 1.5 and 2.0 g/cm^3. In core PC-9 high bulk density values, near or in excess of 2.0 g/cm^3, are found in facies 1b. A peak value approaching 2.9 g/cm^3 is found in the coarse layer just above the erosional contact between facies 1b and 2a, in core PC-9. This peak value is considered anomalous and is presented with caution. These elevated values are not found in any other cores which have sampled facies 1b.

A drop in bulk density from approximately 1.7 g/cm^3 to near 1.5 g/cm^3 in cores PC-6 and 7 occurs across the contact between the overlying facies 2a and facies 1b. From this point, within facies 1b, bulk density values continue to increase down core (figs. 3.15 and 3.16). A small positive jump in bulk density occurs at the 2 metre mark in core PC-7 (fig. 3.16). A positive peak in bulk density (an increase from approx. 1.5 g/cm^3 to near 1.7 g/cm^3 down core) occurs at the contact between facies 1b and 2a (see fig. 3.14).

Porosity:

The porosity curve closely follows, in a positive sense, the shape of the water content profile. Porosity generally decreases with depth in core, with the greatest fluctuations occurring between facies 1b and 2a (figs. 3.13 - 3.17). Porosity percentages are highest near the sediment water interface, reaching values of 80% or more. Porosity lows generally exceed 40% except in core PC-9 where a value

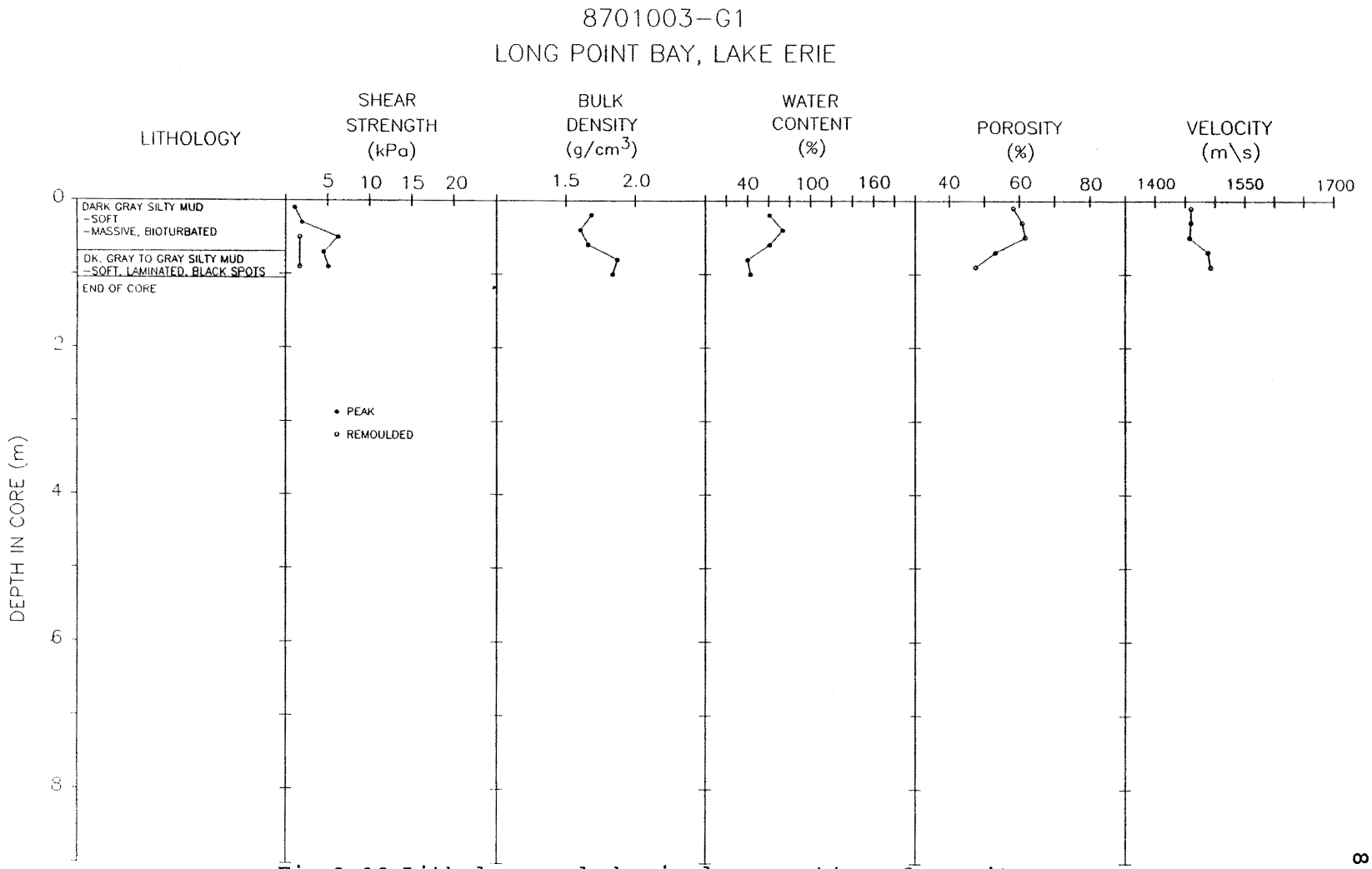

Fig 3.18 Lithology and physical properties of gravity core G1.

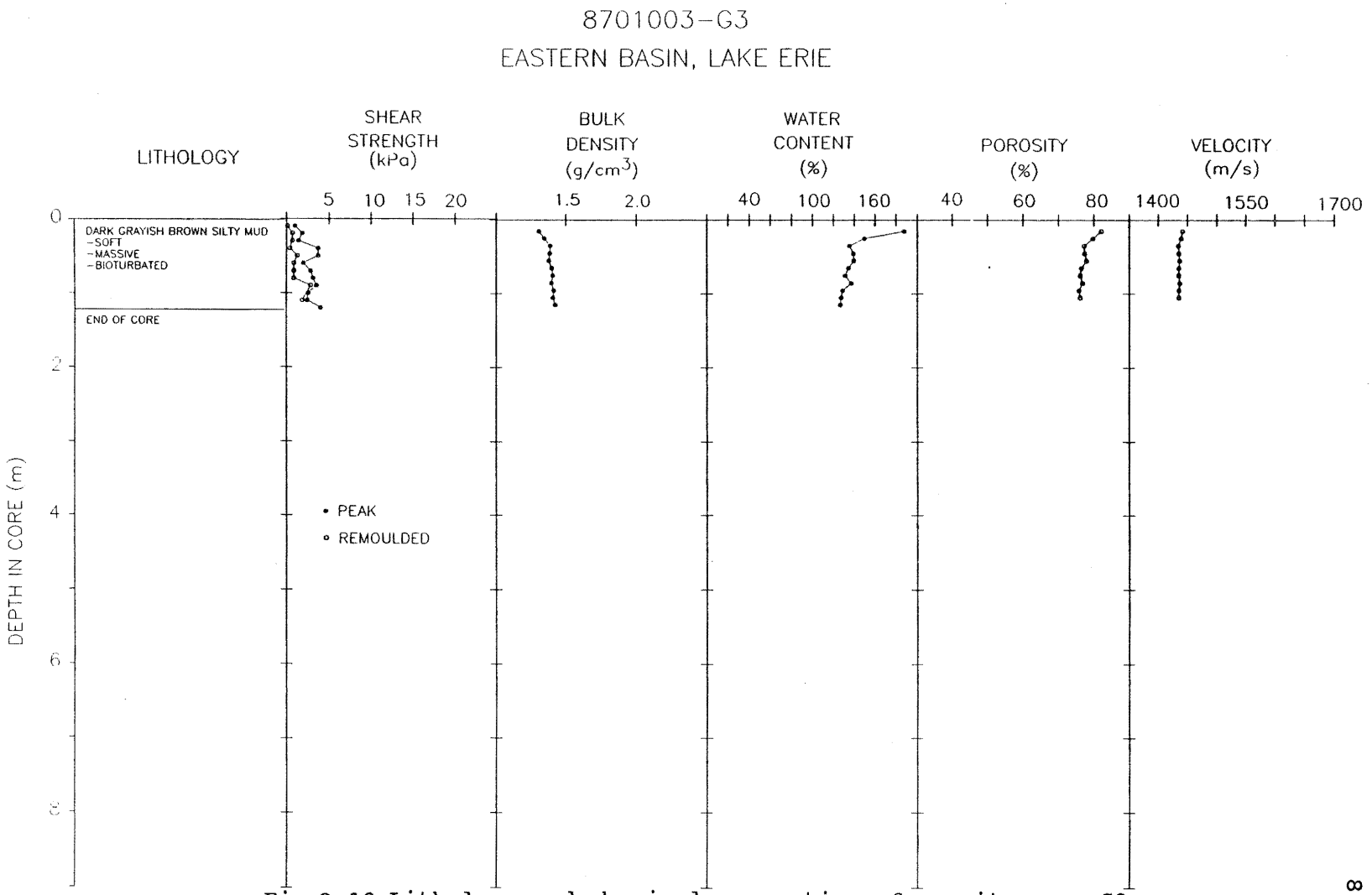

Fig 3.19 Lithology and physical properties of gravity core G3.

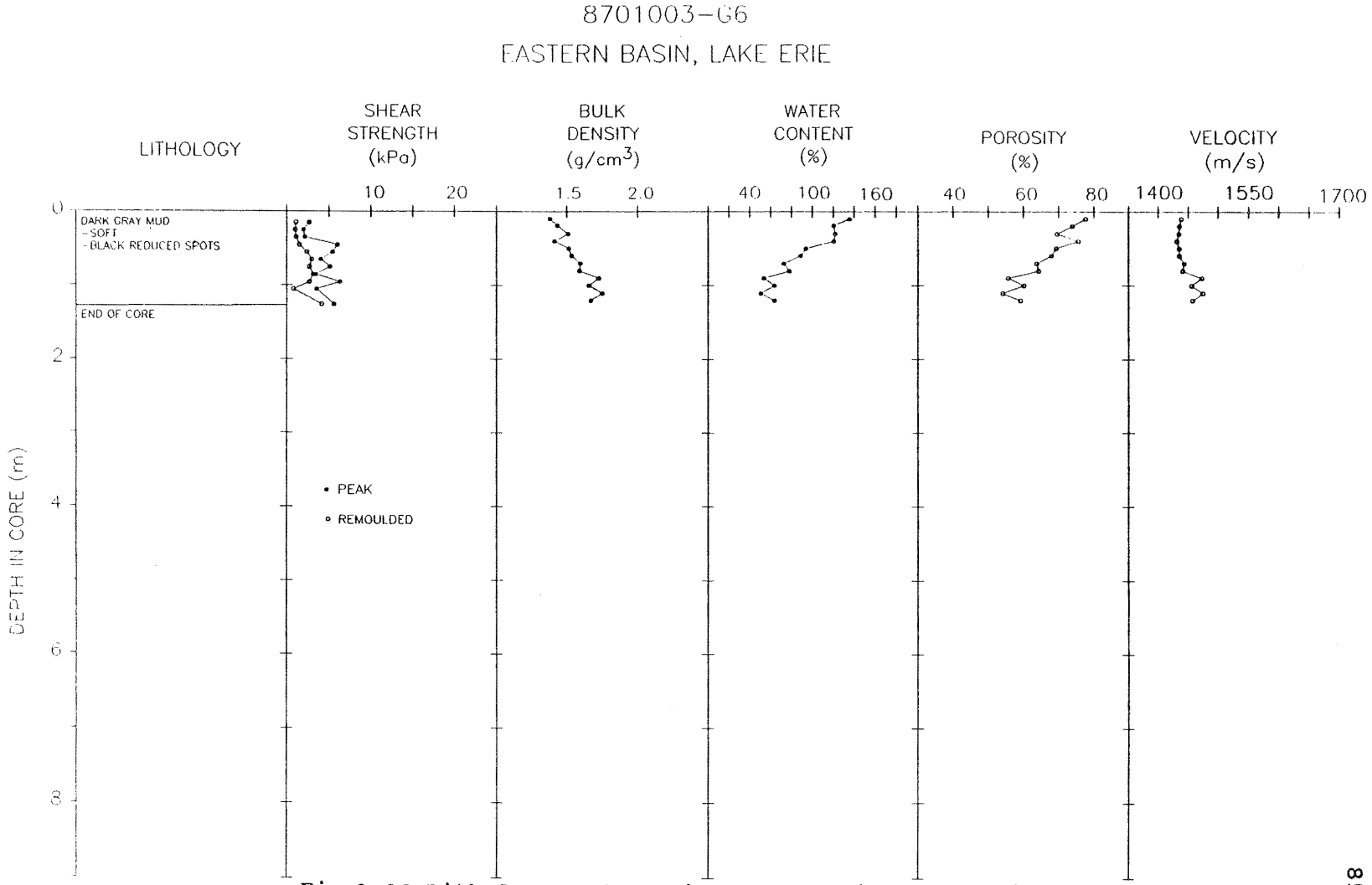

Fig 3.20 Lithology and physical properties of gravity core G6.

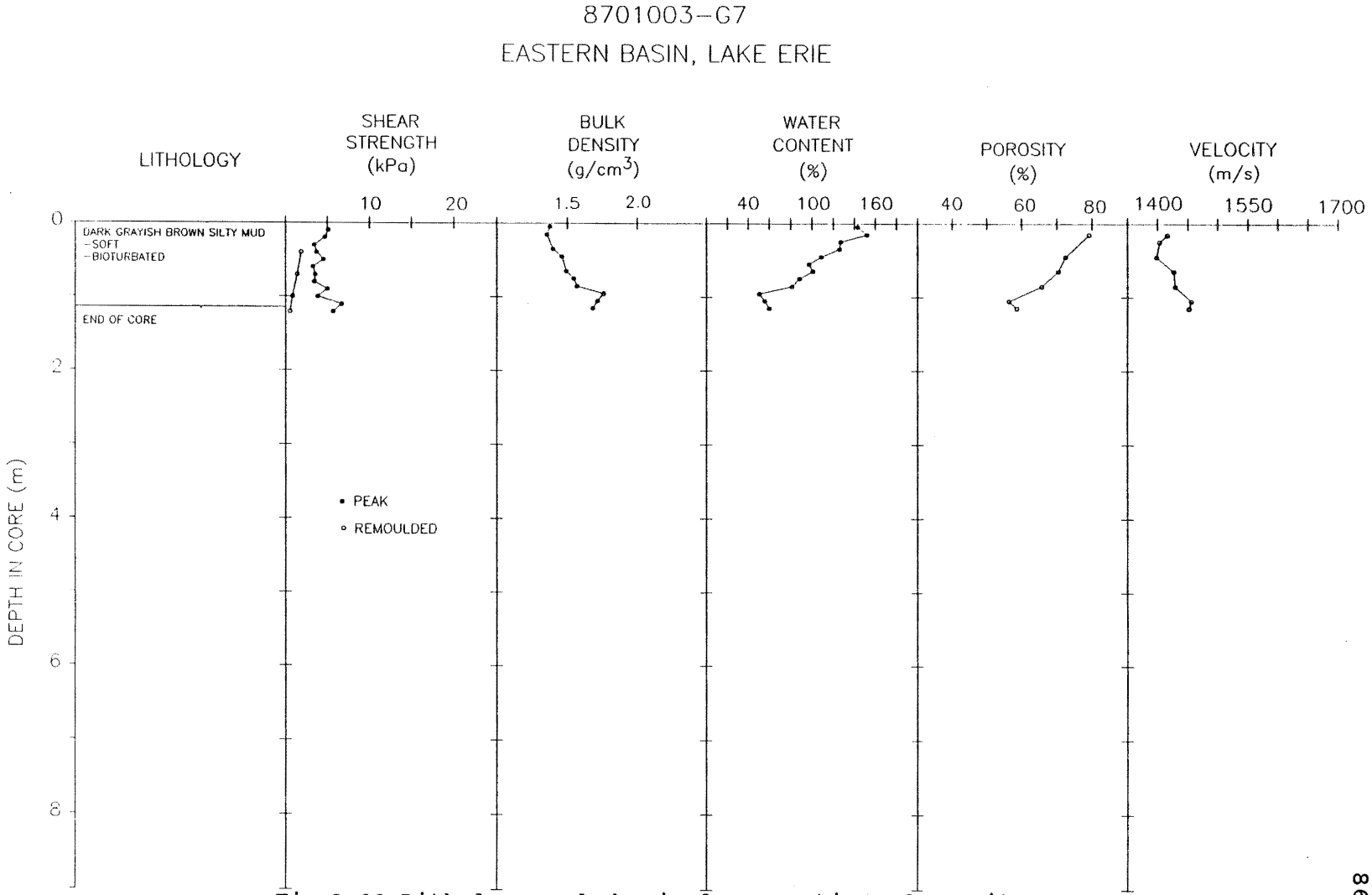

Fig 3.21 Lithology and physical properties of gravity core G7.

of less than 20% occurs in coarse material at the contact between facies 1b and facies 2a (fig. 3.17). Porosity values, for facies 1b, range from less than 20% to 70%, with most values between 50 and 60%. Porosity percentages, for facies 2a range between 35% and 85%, with most values situated between 50% and 60%.

Velocity:

The velocity profiles in figures 3.13 and 3.21 show an inverse relationship to water content and porosity percentages down core. As porosity and water content values decrease overall with depth the velocities increase. The velocity curve is similar, in shape and fluctuation, to the bulk density profiles; this is best seen in figures 3.13 and 3.15 - 3.17. Generally, as bulk density increases or decrease in core, so too do the velocities. Similar relationships were documented by Nafe and Drake (1957), Morgan, (1969) and Hamilton (1970).

Velocities near the sediment water interface range between 1400 m/s and 1450 m/s. Velocities generally rise down core, broadly maintaining values between 1450 m/s and 1500 m/s. A velocity decrease across the contact between facies 2a and 1b, (from 1450 m/s in facies 2a to 1425 m/s in facies 1b), occurs in cores PC-6 and PC-7. At this point in the cores, the velocity decreases correspond to decreases in bulk density and increases in porosity and water content values. However in cores PC-1 and PC-9 increases in

velocity occur across this boundary. Velocities jump, in core PC-1, from a steady state of approx. 1500 m/s in the overlying facies 2a to a peak of nearly 1700 m/s in facies 1b. Velocities fall again but remain elevated between 1500 m/s and 1600 m/s for the remainder of facies 1b. Velocities, in core PC-9, jump from values between 1450 m/s and 1550 m/s in facies 2a to between 1500 m/s and 1550 m/s in facies 1b. An overall increase in porosity and decrease in water content accompany these velocity changes in cores PC-1 and PC9. Bulk density increases in core PC-9 where velocities increase in facies 1b, but remain unchanged in core PC-1 (see figs. 3.13 and 3.17). A velocity decrease, in core PC-6, at approximately 4.30 meters down core, occurs in facies 1b. Other physical property profiles, from this core, do not show any corresponding variations (fig. 3.15).

Stable Isotopes:

Stable isotope ratios in ostracode shells ($\delta^{18}O$ and $\delta^{13}C$) and pollen trends from the LPBH, reveal the influence of cold melt waters from the Upper Great Lakes on the eastern basin of Lake Erie (fig. 3.22; Lewis and Anderson, in press; Fritz et al., 1975). Lewis and Anderson (1990) suggest that these melt waters suppressed summer warming and contributed to the 11-10.5 ka climatic reversal of the southern Great Lakes, suggested by palynological evidence (Shane, 1987; Lewis and Anderson, 1989). The isotope data also show that cold melt water inflow influenced Lake Erie

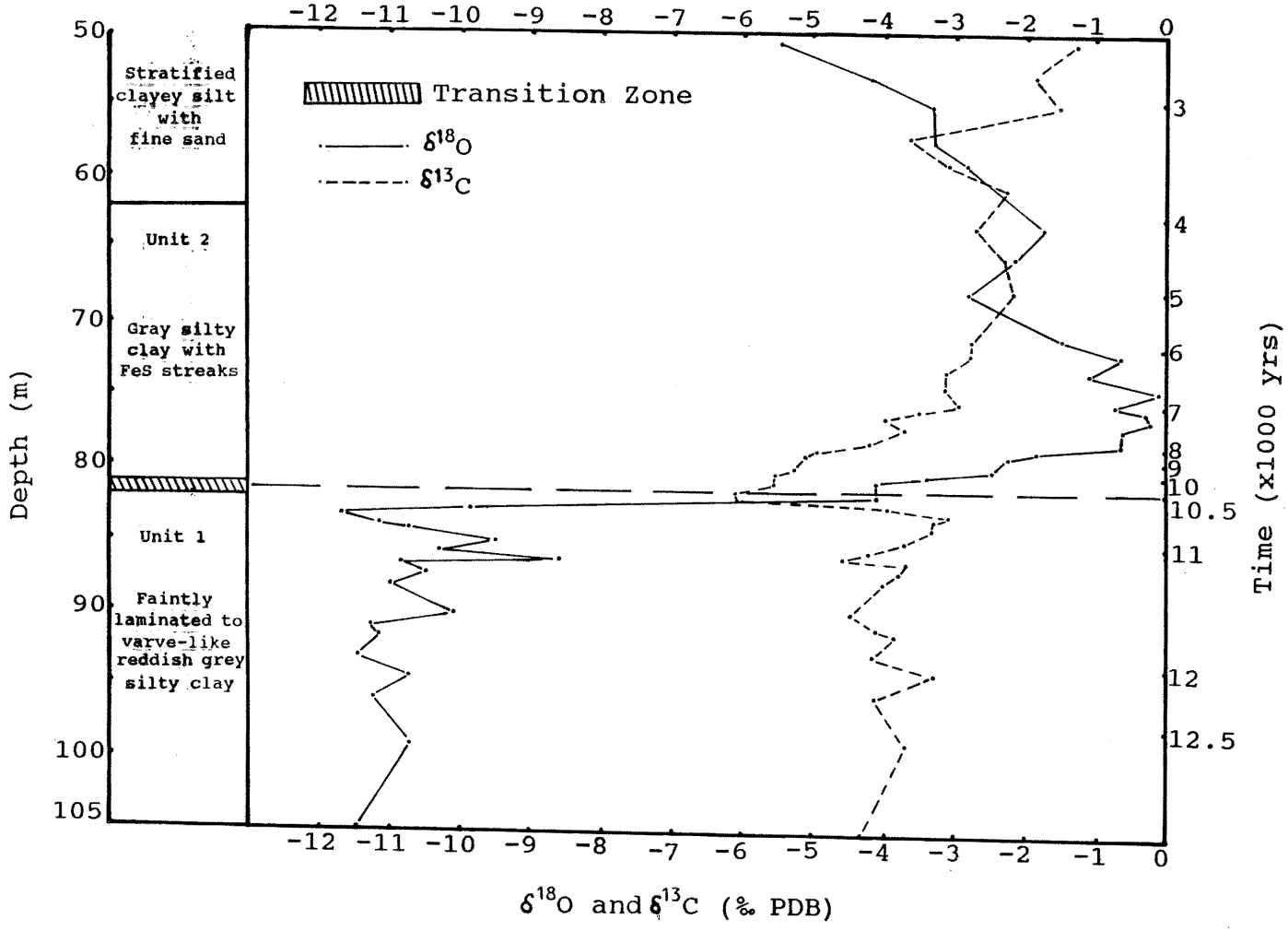

Fig 3.22 Stable isotope curve for the Long Point Borehole.

after retreat of local glacial ice (ca 12,400 y.B.P.) and persisted until ca 10,500 y.B.P. when Upper Great Lakes glacial waters began to bypass the Erie basin. These interpretations by Lewis and Anderson (1990) further support the lithostratigraphic, physical property and acoustic stratigraphy, which suggest an elevated lake level for this time in the eastern basin. Stable isotope data (low $\delta^{18}O$ signifying meltwater presence) further demonstrate that seismic sequence 1 is a cold water sediment deposited during late glacial and postglacial times (ca 13,000 y.B.P. to 10,500 y.B.P.). Stable isotope data (high $\delta^{18}O$) suggest that Sequence 2 was deposited under warmer water conditions between ca 10,500 y.B.P. and the present. Earlier work by Fritz, et al. 1975, from a borehole in central Lake Erie, has also recorded the enrichment of $\delta^{18}O$ at ca 10.5 ka but, because of discontinuous sampling in that borehole, the onset of the enrichment of $\delta^{18}O$ has not been documented.

Facies Interpretation:

Facies 1a:

This facies underlies facies 1b and occurs only in core PC-7. The textural and massive nature of this diamicton suggests a possible ice-influenced genesis. Similar units from boreholes in the Central Erie basin are described by Zeman (1976) as till deposits. Eyles and Miall (1984) suggest that diamicts may owe their origins to ice rafting and suspension deposition in ice proximal

environments. The possible origins for this facies are unclear from the textural data alone, so further discussion will occur in chapter 4.

Facies 1b:

Structural, textural and geotechnical evidence suggests that this fine grained, well laminated sediment was deposited at depth in quiet water by turbidity currents and/or rainout sedimentation. Pollen data from cores PC-3 and the LPBH would make this facies late glacial to early postglacial in age, suggesting that these sediments were influenced by large proglacial lakes and postglacial lake levels with a similar sediment source. The basal portion of LPBH (ca 105 to 118 meters) may have been influenced by melt water currents from glacial ice, delivering a larger volume of coarse sediment to the basin. Rhythmically laminated mud, with dropstones, silt laminations, lenses and mud clasts are features found in this facies. Similar structural features were described by Eyles, et al. (1983), from the Scarborough Bluffs and interpreted by them to be of turbidite orgin. No evidence of bioturbation exists, suggesting rapid sedimentation and further supporting a turbidite orgin. Contorted sediments found in core PC-7 may be due to dewatering, sediment creep or grounded ice.

The upper surface of facies 1b, in all cores except LPBH, has undergone a period of non-deposition or erosion. Facies 1b, in cores PC-1 and PC-9, has high shear strength

values, depressed water content and higher velocities than normal. It is interpreted that these sediments may have been desiccated due to subaerial exposure. This is clear evidence that lake waters receded from this area and indicates a previous low lake level stand. Further treatment of previous lake levels and their possible timing will be discussed in Chapter 4.

Facies 2a:

This facies occurs directly above facies 1b and above 2c over the erosional unconformity. The soft fine grained nature of these sediments suggests a low energy environment in protected or deeper portions of the lake. This interpretation suggests that lake levels rose again crossing the erosional surface and the desiccated sediments of facies 1b; allowing more recent lake muds to be deposited. Bioturbation is evident, a process which has mixed the sediment and eliminated evidence of laminations in portions of this facies. With sedimentation rates as high as 0.5 cm/y (Coakley, 1985), biological mixing of the sediments in these areas may not have been able to keep pace; this may explain why only portions of this facies have been biologically mixed. Facies 2a has a greater tendency towards higher silt content than facies 1b. Thick accumulations of facies 2a occur, ca. 8 m in core PC-3, and ca. 70m in LPBH, with much thinner amounts in the other cores, ca. 3m or less. The variations appear to be

controlled mostly by water depth, with the larger accumulations occurring in deeper water.

Pollen evidence suggests that this facies was deposited continuously after 10,500 y.B.P. in some areas (in the LPBH area) to the present day.

Geotechnical evidence shows a normally consolidated sediment with depth. These data prove to be an excellent tool in differentiating this facies from facies 1b below and others in the sediment section. These data will prove to be useful in establishing stratigraphic correlations in the upcoming Chapter 4.

Facies 2b:

Textural and lithologic descriptions, of cores PC-8, GC-8 and PC-10, suggest that facies 2b is a sand body at least 3 meters thick whose near surface sediments interfinger with muds from facies 2a (fig. 3.5). The interdigiting relationship with facies 2a reveals that dynamic forces presently rework or recently reworked the surface of the sand. A veneer of mud does not mantle these sands suggesting that bottom currents are sweeping the lake bottom, affecting the sands minimally while preventing sedimentation of mud. The rounded nature of the carbonate component and the angular to subrounded surfaces of the more resistant quartz grains and the clean uniform size of the sand suggests that they were affected by a high energy surf environment, like that at the present shoreface of the lake.

The mud balls (clasts) found in this facies are similar to those found on present day beaches (C.F.M. Lewis pers. com.); their presence is consistent with an interpretation of this facies being a beach deposit in a mud rich environment. The present erosion limit of ca. 10 m, suggested by St.Jacques and Rukavina (1973) is well above the water depth of the core site (ca. 20 m). Bottom currents having only a minimal effect on the sand and could not necessarily explain its presence and maturity. The energy regime necessary to winnow, concentrate and round these sands likely occurred during a previous low lake stand.

Facies 2c:

Facies 2c, the muddy sand, lies above and on the erosional contact between facies 1b and 2a and is an interface between these two deposits. This facies appears to be associated with the erosional unconformity found in all cores in water depths less than 35 m. Core 3 is interpreted to have experienced a period of non-deposition, at the contact, rather than one of erosion. The LPBH has a conformable contact which lies in depths (ca 80 m) beyond the influence of the erosion. Lithological, geotechnical and pollen data all suggest a complex major depositional change occurred during formation of facies 2c.

The close association of facies 2c with the erosional surface, its thin nature, textural character and physical

properties suggest that this facies is a shallow water lag deposit. This lag deposit would have developed during transgression or regression of lake waters where high energy bottom currents could winnow out the fines and transport or sort coarser sediment.

Facies 2d:

This facies was found only in cores PC-1 and 9 in water depths less than 18 m. The contact between this facies and the underlying facies 2a appears to be erosional in nature. This erosional surface occurs locally and could represent either lower water levels than present day (10 m.b.d.) with an erosional limit not exceeding 20 m, or an increased sheltering from waves. Facies 2d is very similar to facies 2a and represents a recent soft lake sediment deposit. This facies, however, is local in nature and represents redistributed material mostly from facies 2a within Long Point Bay.

CHAPTER 4

Discussion and Conclusions

Stratigraphy:

The stratigraphy of sedimentary fill of the eastern Lake Erie basin, as presented in this study, is based on seismic data together with data derived from analyses of piston and gravity cores. Stratigraphic correlations and sedimentary interpretations were achieved using acoustic profile data, supported by lithologic, palynological, physical property and stable isotopic data from cores. Descriptions of sediments encountered in a 120m borehole to bedrock at the tip of Long Point (LPBH) were also used in establishing the eastern lake basin stratigraphy.

Core to core correlations of sediment lithofacies and seismic sequences are presented in figs. 4.1 and 4.3. The lake basin sediment stratigraphy is summarized in Table 4.1 and 4.2. Down core profiles of physical properties for each core are shown in figs. 3.13 to figs. 3.21, inclusive. The stratigraphic position of each core with respect to an acoustic profile, through the core location, is shown in figs. 2.3, 2.4, 2.6 and 2.7.

Seismic sequence 1 consists of seismofacies 1a and 1b which are equivalent to lithofacies 1a and 1b respectively (they are referred together as facies 1a and 1b in the following discussion). Seismic sequence 2 consists of seismofacies 2a and 2b; seismofacies 2a is equivalent to

Table 4.1 Stratigraphy of the unconsolidated sediments of the eastern basin of Lake Erie.

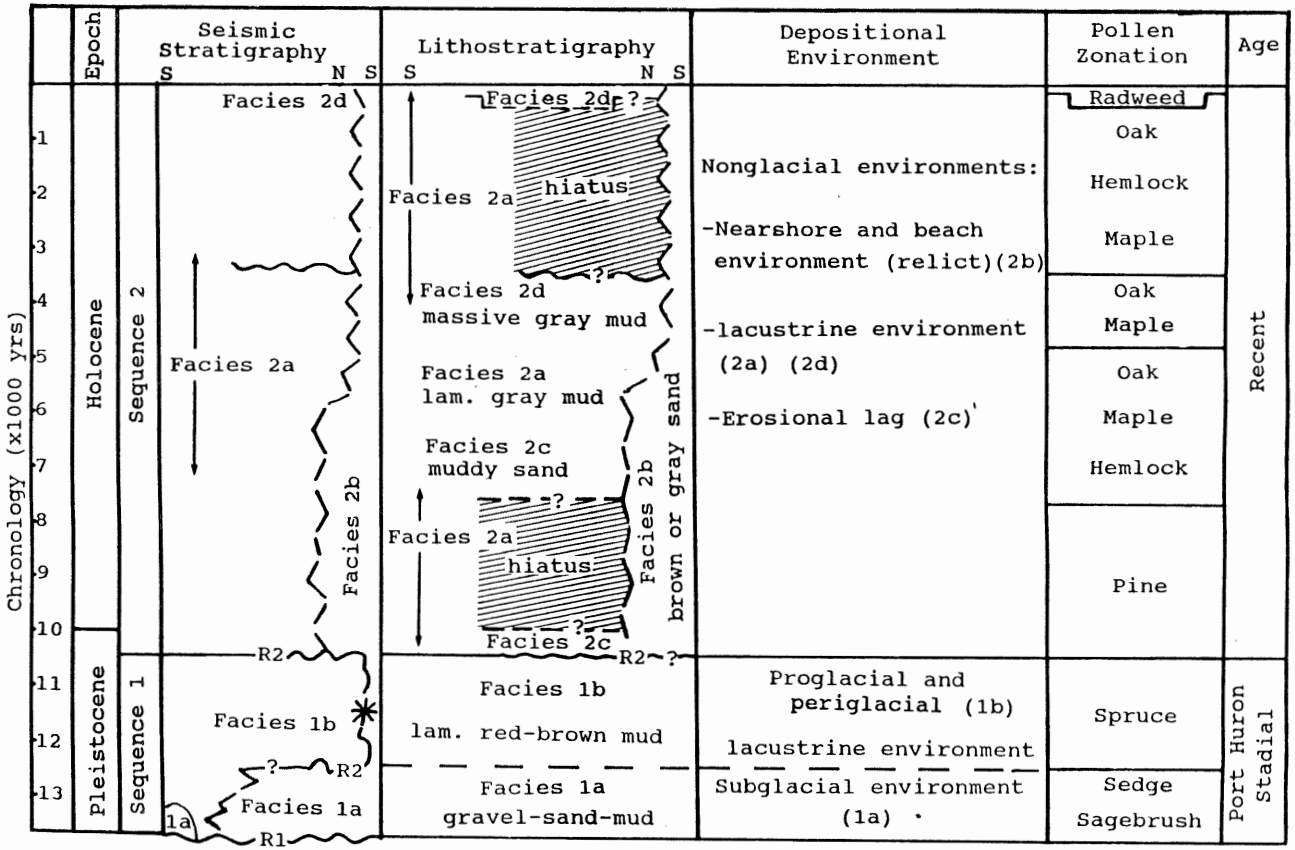

*The R2 erosional event occurred ca 10,500 y.b.p., eroding both facies 1a and 1b (due to basin and facies geometry) and is not time transgressive (between ca 12,500 and 10,500 y.b.p.) as the diagram may imply.

TABLE OF FACIES

BOUNDARIES	SEQUENCE	FACIES	SEISMIC CHARACTER	LITHOLOGY	COMMENT
	2	2d	few internal reflections	massive gray mud	lacustrine (modern)
	2	2b	scattered, mostly discontinuous, weak reflections	brown or gray sand	lacustrine shore sand (relict)
	2	2a	weak continuous parallel coherent reflections	laminated gray mud	lacustrine (post 10.5 ka)
	2	2c		muddy sand	lag
R2					
	1	1b	high-amplitude parallel coherent reflections	laminated red-brown mud	lacustrine (>10.5 ka)
	1	1a	spotty and chaotic reflections	gravel-sand-mud	glacial diamict (>12.5 ka)
R1					

Table 4.2 Simplified stratigraphy and table of facies for the unconsolidated sediments of the eastern basin of Lake Erie.

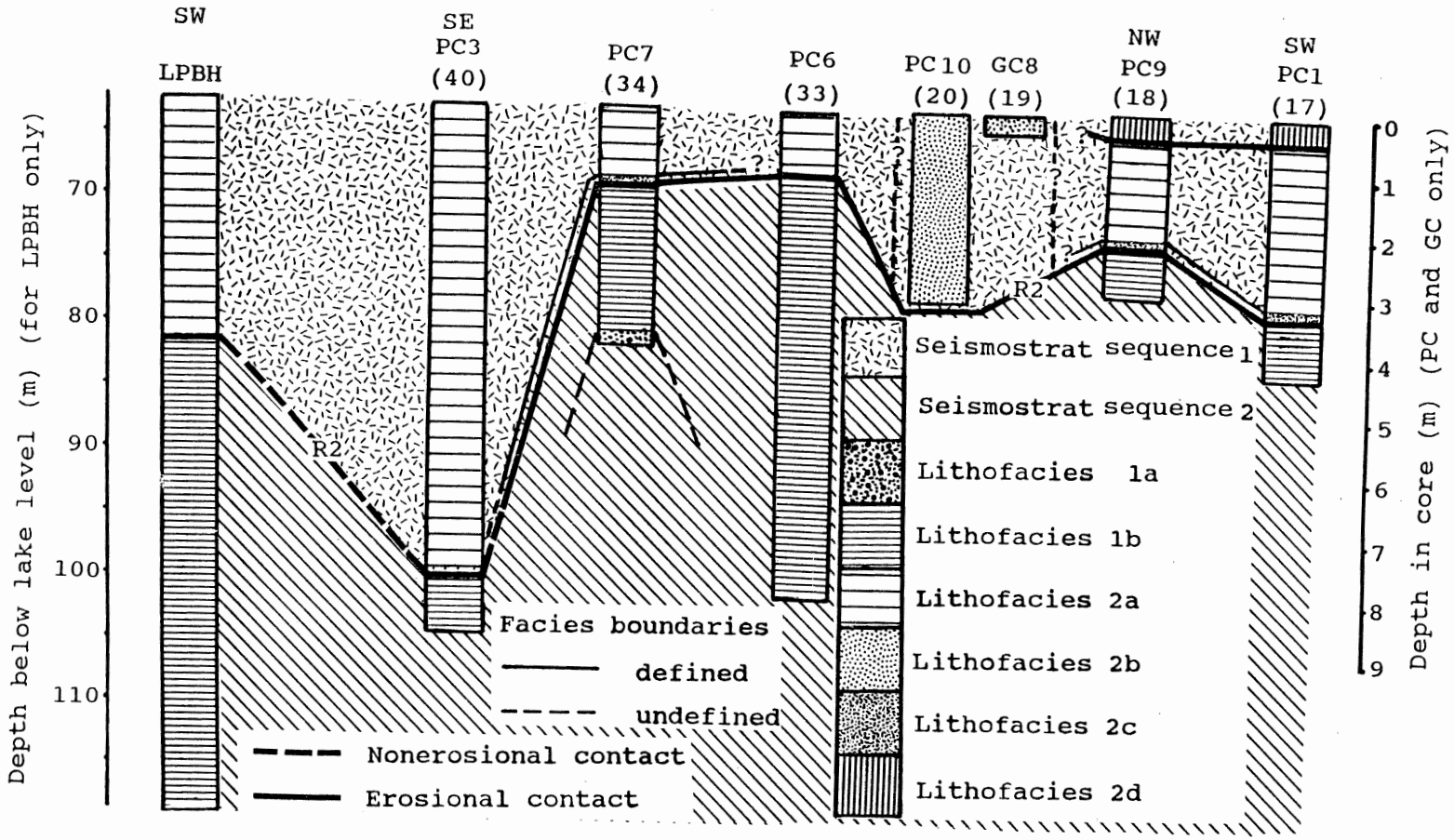

Fig 4.1 Correlation diagram for eastern Lake Erie cores (See Fig 1.2 and Table 1.1 for core locatons). Water depths shown in brackets ( ) are in meters.

lithofacies 2a, 2c and 2d, (together referred to as facies 2a in the ensuing dicussion) and seismofacies 2b is equivalent to lithofacies 2b, (referred to below as facies 2b, see Table 4.1 and 4.2). Figure 4.3 summarizes the relationship of the various facies and geomorphological features in the Late Quaternary deposits of the northern margin of the eastern basin of Lake Erie (see fig 4.2).

Facies 1a:

Textural and seismic data outlined in chapters 2 and 3 suggest that facies 1a is a glacially derived till. The interfingering relationship of facies 1a with the lower portion of facies 1b suggests that they would have a similar age. Pollen data from the bottom of the LPBH (fig. 3.11) dates the lower portion of facies 1b at ca 13,000 y.B.P. This facies represents sub-glacial ice contact deposition. The thin glacial ice was near its southern limit in the eastern Erie basin at this time and was likely mostly buoyed by lake water, thereby limiting the gravitational stress delivered to underlying sediment. Peak shear strength values increase in this facies to ca. 15 kPa. The aerial extent of this facies is limited to the flanks and bedrock highs of the basin.

Facies 1a is not found in the LPBH, but striated bedrock would suggest ice erosion in the past, however the timing is uncertain (Lewis, pers. com.). All occurrences of facies 1a are considered to be seismostratigraphically

equivalent but may not be exactly time equivalent; isolated showings of facies 1a found deeper in the basin may have been deposited during a different ice event (glacial phase) or they may be ice rafted material.

Facies 1b:

Facies 1b is a dark gray and brown laminated mud, which dominates sequence 1 due to its extent and thickness in the basin; it is found interfingering with or lying stratigraphically above facies 1a (fig. 4.1). This facies has been correlated successfully between cores (fig. 4.1), and pollen dating limits its age to between ca 13,000 y.B.P. and ca 10,500 y.B.P. (See Table 4.1 and 4.2). Core analysis and seismic data suggest these sediments were deposited in a periglacial and postglacial lake, where turbidity currents and rainout sedimentation delivered fine grain sediments in a relatively quiet lake environment. The summary diagram of fig. 4.3 clearly shows facies 1b's stratigraphic relationship within sequence 1 and with other lake basin features. Sequence 1 has been mapped into near shore areas (see fig. 2.12) and demonstrates that relatively high (near or above present datum) initial Early Lake Erie levels must have existed in eastern Lake Erie during the deposition of sequence 1 (until ca 10,500 y.B.P.). Compact, eroded and desiccated quiet water sediments of sequence 1 occur at 10 to 15 metres below datum. Allowing for original sediment thickness, with at least a 10 m assumed water depth, former

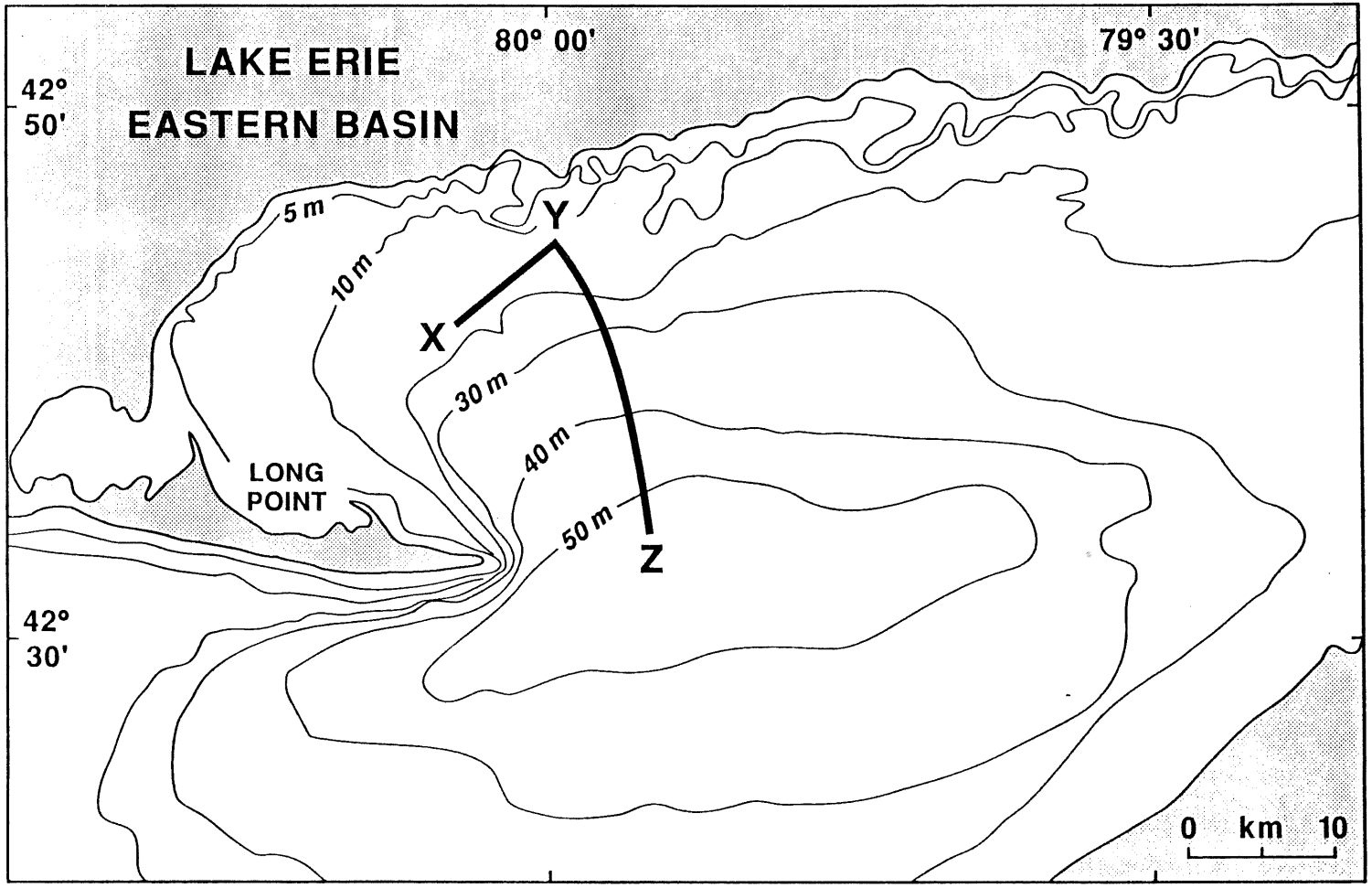

Fig 4.2 Location of generalized cross-section XYZ.

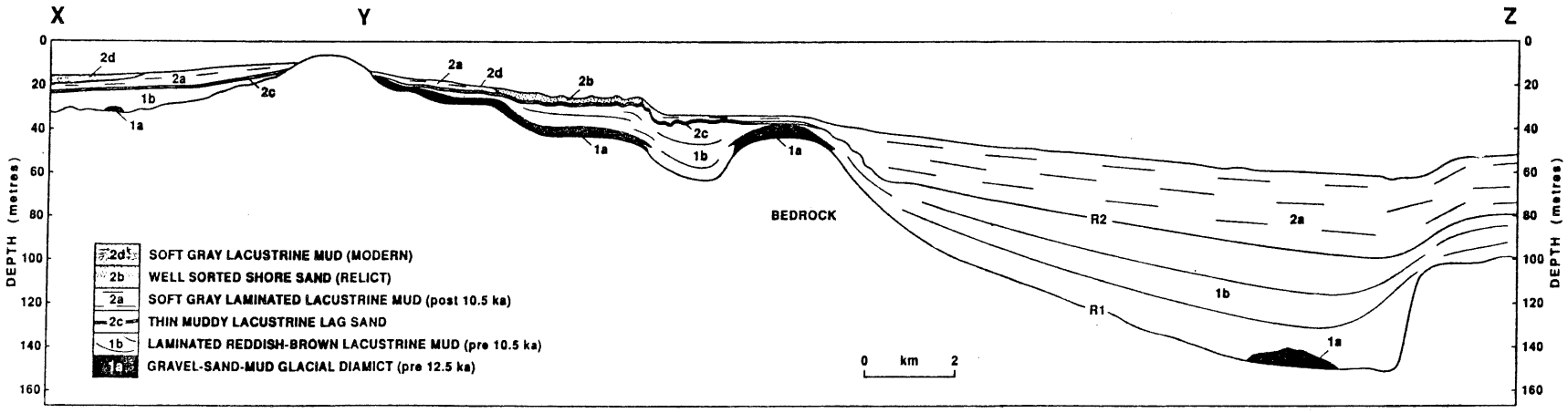

Fig 4.3 Generalized cross-section of unconsolidated lake sediments.

lake levels would have been at or above the present datum ca 12,000 to 10,500 y.B.P.

Seismic and lithologic data suggest that the regional reflector R2, which separates sequence 1 from sequence 2, is in part an erosional unconformity. These data show that facies 1a and 1b were both eroded above the level of the present 40 m isobath (Table 4.1 and 4.2). Pollen data suggest that the eroded sediment (facies 1b) is older than ca 10,500 y.B.P. The sediment overlying the eroded R2 surface is younger than ca 7700 y.B.P. but older than ca 5000 y.B.P., implying a depositional hiatus of at least 3000 years or more (see Table 4.1, 4.2 and 3.1).

Facies 2a:

Lithologic studies (Chapter 3) show that seismic facies 2a consists of lithofacies 2c, 2a and 2d. Lithofacies 2c is not resolved in seismic profiles but exists as a thin muddy sand above and on the erosional contact, recognized in seismic profiles as reflector R2. This facies likely developed as a residual lag, resulting from wave erosion of pre-existing sediments, as water levels fell and rose within the basin, between ca 10,500 and ca 7700 y.B.P.

Facies 2a consists of laminated gray mud resulting from offshore lake sedimentation. Palynologic and lithologic studies suggest that continuous deposition of facies 2a occurred in deeper portions of the eastern basin, from ca 10,500 y.B.P. to the present. Accumulations of facies 2a

commenced much later in the near shore areas above the erosional portion of the R2 unconformity (above 40 m.b.d.; between ca 7700 and ca 5000 y.B.P.). An erosional event limited to Long Point Bay occurred between ca 4800 and ca 3600 Y.B.P., with deposition above this unconformity occurring ca 300-150 y.B.P., creating as much as a ca 4500 year depositional hiatus. Lithofacies 2d, a massive brown to gray mud, lies above this restricted erosional surface in Long Point Bay. Lithofacies 2d in seismic profiles becomes one with lithofacies 2a further offshore as the limiting erosional boundary disappears. This suggests that lithofacies 2d is a continuation of lithofacies 2a with deposition occurring after the erosional hiatus in shallow water areas such as Long Point Bay.

Facies 2b:

This massive sand body (ca 3 to 5 m thick) rests above the erosional unconformity (R2) and appears to have been deposited due to a drop in water levels. The sand body accumulated as a beach deposit emplaced above the erosional shore face (notch) seen in figs. 2.5 and 2.6. Lithological and acoustic studies show that near surface facies 2b interfingers with facies 2a and that the sand body is not mantled by a veneer of lake mud. This suggests that bottom currents are keeping the sand body swept clean of fines, while limiting the movement of the sand at present. Recent sedimentation rates are low in this area and may also

account for the lack of mud mantling this facies.

Geological History: Depositional model and lake levels.

Stratigraphic evidence has allowed the reconstruction of the geological evolution of the eastern basin of Lake Erie over the past ca 13,000 y.B.P. (see Table 4.1 and 4.2). This geological evidence (based on seismostratigraphy, lithostratigraphy, biostratigraphy pollen zonations, physical properties analysis and stable isotopic evidence), has furnished an eight stage depositional lake model which is depicted in figs. 4.4-4.11 Lake levels and mean sedimentation rates for eastern Lake Erie are reconstructed in fig. 4.12.

The Port Huron ice advance, of the Erie lobe of the Laurentide Ice Sheet, occurred ca 13,000 y.B.P. ago, forming Lake Whittlesey at ca 50 m above present lake level (Calkin and Feenstra, 1985). This advance is marked on land (in the Erie basin), by the maximum extent of the Halton Till (Barnett, 1985). Pollen data from the LPBH show that early sedimentation within the present eastern Lake Erie basin began around this time (ca 13,000 y.B.P.). Sediment studies from the LPBH and other cores detailed in Coakley and Lewis (1985) show a lack of till under Long Point. However seismic and lithological analysis from this study suggests the presence of glacial till elsewhere in the basin, and demonstrates that grounded ice advanced southwestward down the basin as far as Long Point Bay during the Port Huron ice

advance (fig. 4.4). This assumes that much of facies 1a was deposited by the last (Port Huron) ice advance into the eastern Erie basin.

The glacial ice deposited facies 1a and the lower portion of facies 1b at the same time, but under somewhat different conditions. Seismic and lithological studies suggest that facies 1a is an ice contact till, found mostly on the flanks and bedrock highs of the basin. The till interdigitates with fine grained, well stratified sediments of the lower portions of facies 1b. Feenstra (1981) found a similar intercalated relationship between Halton Till and glaciolacustrine sequences at the recessional ice-margin and proglacial lake position on the Niagara Escarpment, between eastern Lake Erie and western Lake Ontario. It is interpreted that facies 1a was derived from subglacial meltout debris while the lower portion of facies 1b was derived from proglacial meltout sedimentation (fig 4.4). The well stratified nature of facies 1b suggests that sediment rainout and turbidity currents were important mechanisms during deposition.

Lake Whittlesey gave way to a series of lower proglacial lakes as the ice margin retreated from eastern Michigan, allowing westward drainage through the Huron and Michigan basins (Calkin and Feenstra, 1985; figs. 4.4 and 4.12). These westward draining, proglacial and postglacial lakes, consisting of Lakes Warren (204-209 m.a.s.l.), Wayne

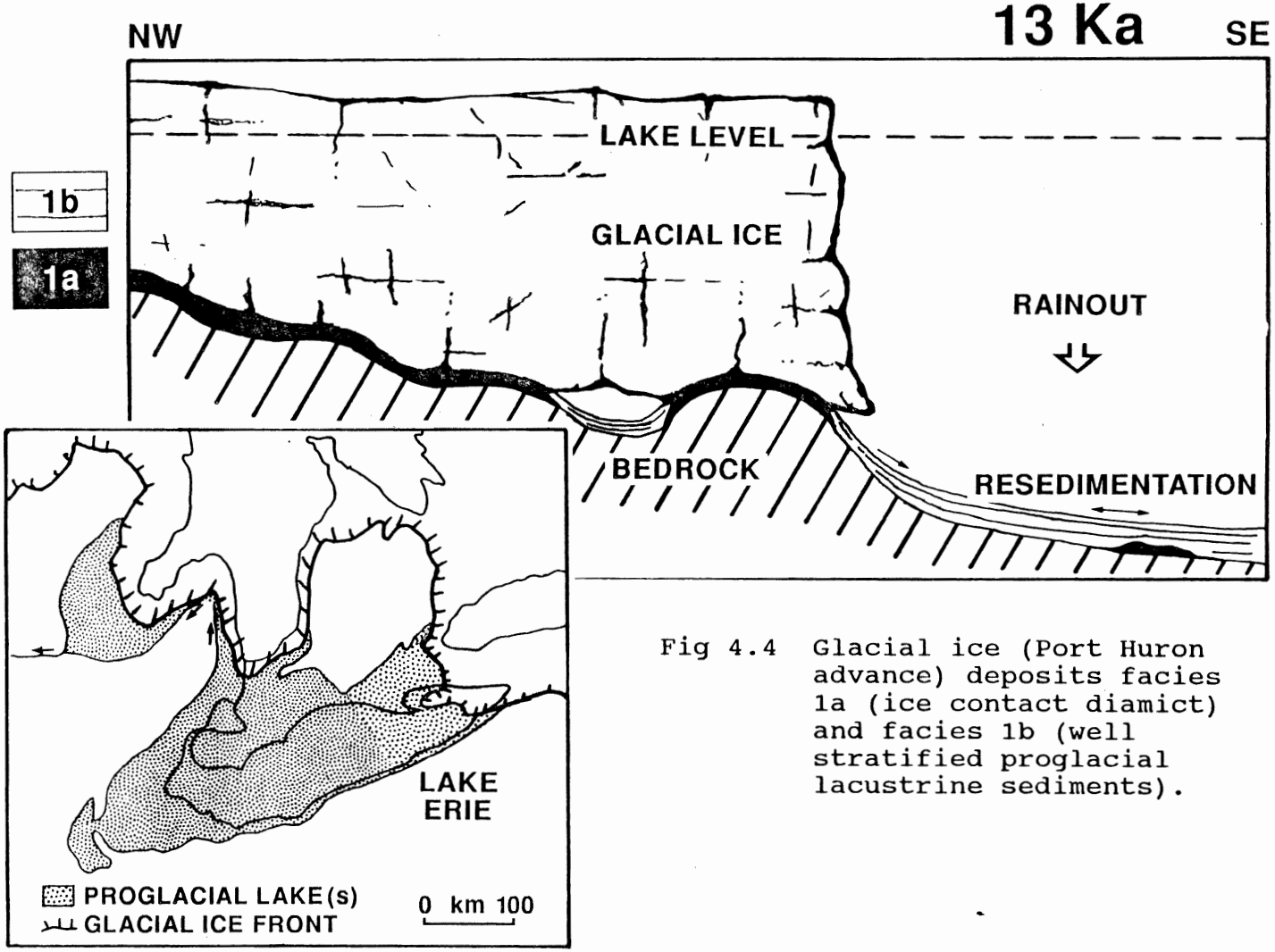

Fig 4.4 Glacial ice (Port Huron advance) deposits facies 1a (ice contact diamict) and facies 1b (well stratified proglacial lacustrine sediments).

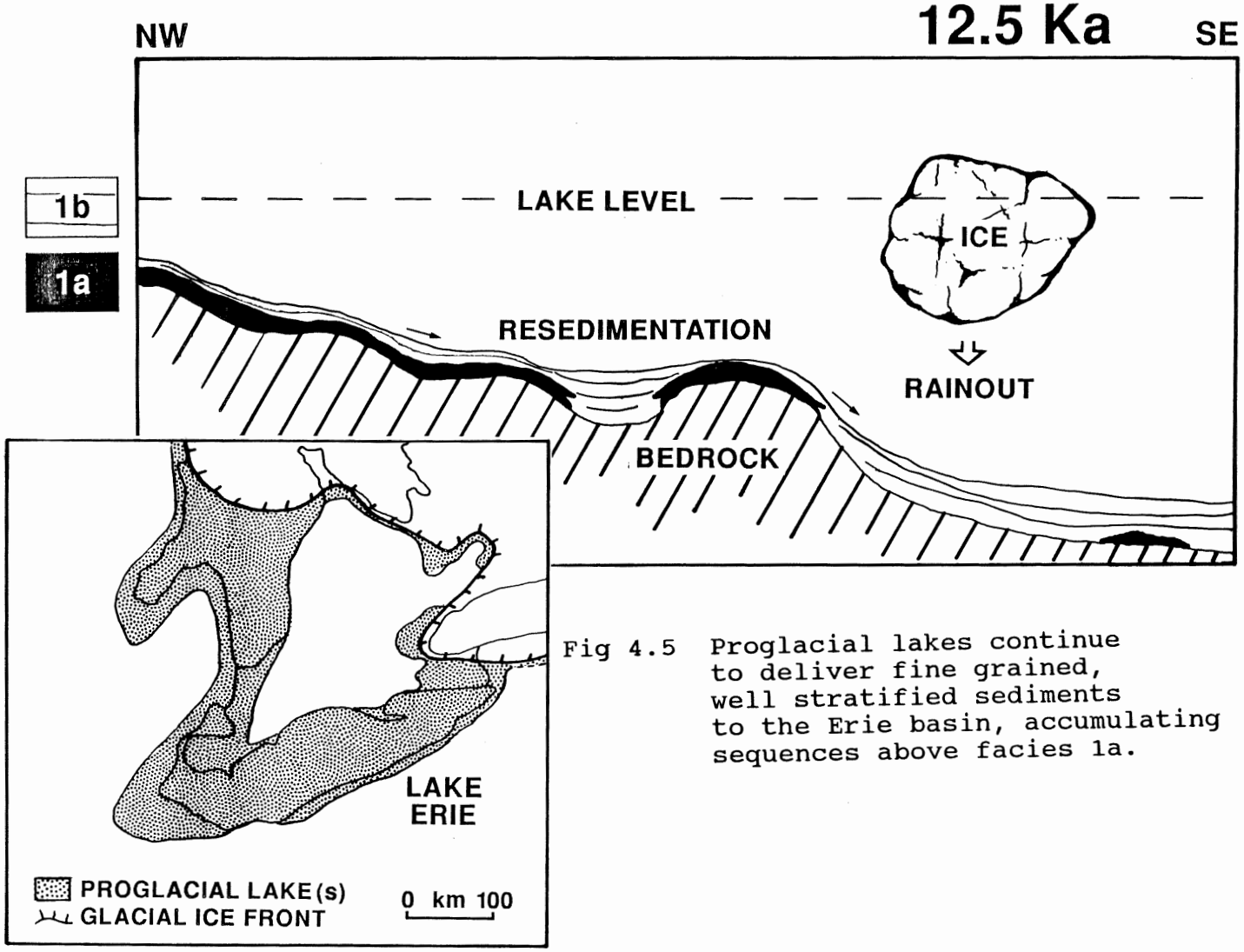

Fig 4.5 Proglacial lakes continue to deliver fine grained, well stratified sediments to the Erie basin, accumulating sequences above facies 1a.

(201 m.a.s.l.), Grassmere (195 m.a.s.l.), Lundy (189 m.a.s.l.), Dana (180 m.a.s.l.) and Early Algonquin (Dunnville; 184 m.a.s.l.), occupied the Erie basin from ca 13,000 y.B.P. to ca 12,500 y.B.P. (figs. 4.5 and 4.12).

These lakes continued to deliver the fine grained, well stratified sediments of facies 1b to the Erie basin, accumulating sequences above facies 1a. Similar lake sediments have been described by Feenstra (1981, Niagara Escarpment) and Barnett (1978a and 1978b,) on nearshore areas around Lake Erie. The well stratified and varve-like laminations of Facies 1b are likely due to both seasonal sedimentation resulting from rainout and sedimentation by turbidity currents. Eyles and Miall (1984) suggest that turbidity currents are important mechanisms in proglacial lake environments. Brodzikowski and Van Loon (1987) maintain that it is usually impossible to determine whether the "varved" sediments are seasonal deposits or formed by turbidity currents; they suggest that often both can be present.

The retreating Laurentide Ice exposed the Niagara outlet, allowed eastward drainage of the last proglacial lake and ended direct glacial influence in the Erie basin (ca 12,500 y.B.P.); this event marked the beginning of the Early Lake Erie phase in the Erie basin (Calkin and Feenstra, 1985).

Early Lake Erie received discharge from an early phase

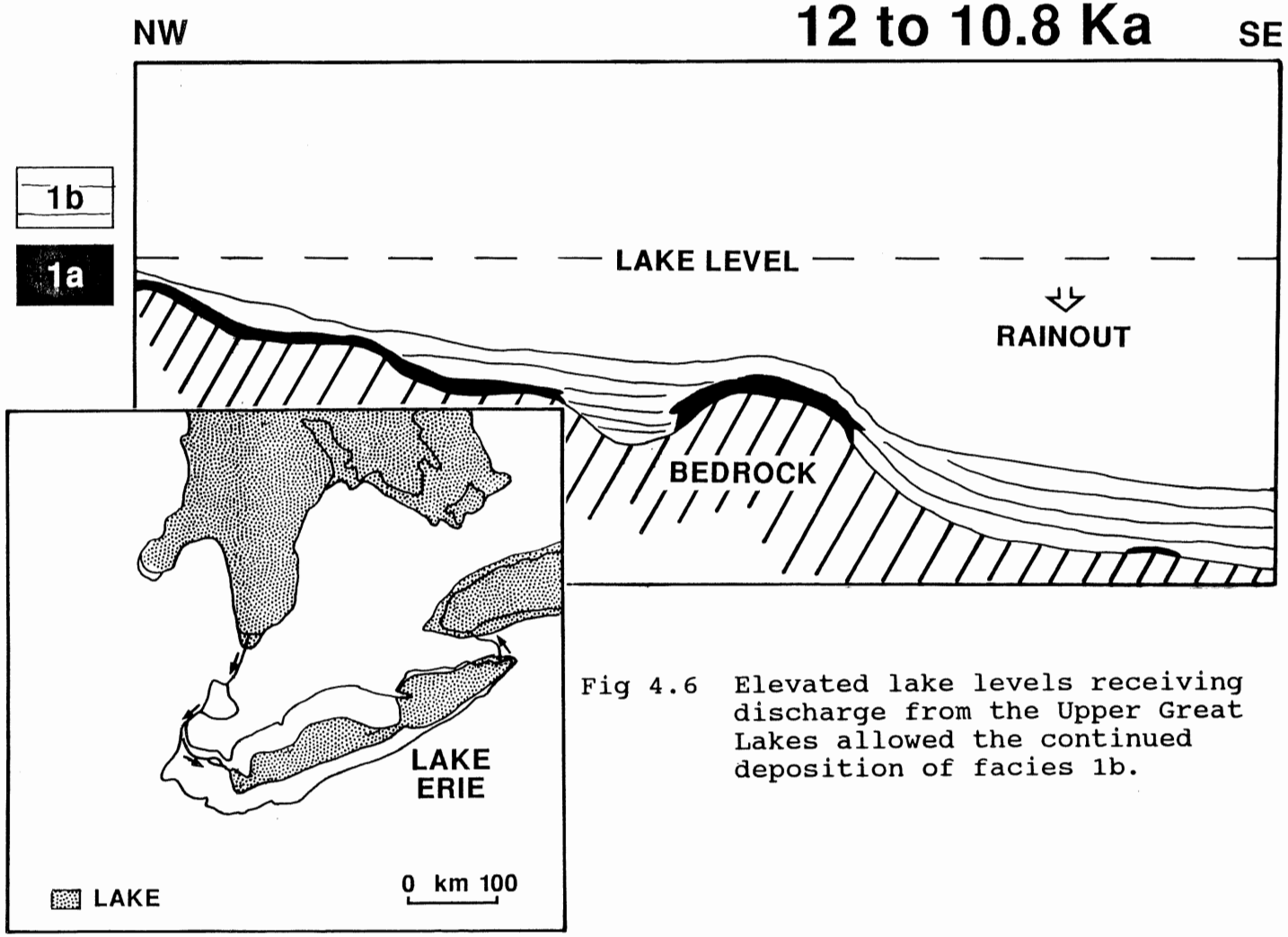

Fig 4.6 Elevated lake levels receiving discharge from the Upper Great Lakes allowed the continued deposition of facies 1b.

of Lake Algonquin from the Upper Great Lakes basin via the St. Clair River (Calkin and Feenstra, 1985). Lewis and Anderson (1989) have suggested that Upper Great Lakes waters had bypassed the Erie basin during the Kirkfield-Algonquin Lake phase (ca 11,200 y.B.P.) until the Main Algonquin phase (ca 10,800 y.B.P.). However, stable isotopic data from LPBH now suggest that cold glacial melt waters passed through the Erie basin, continuously from the last proglacial lake (ca 12,500 y.B.P.), until ca 10,500 y.B.P. (Lewis and Anderson, in press). Sufficient flow existed from the Upper Great Lakes, to maintain elevated lake levels in the eastern basin (fig 4.6). Sediment and seismic studies suggest that high water levels and similar sedimentation were maintained between ca 12,500 y.B.P. and ca 10,500 y.B.P. Feenstra (1981) suggests that elevated shorelines (ca 177 and 181 m.a.s.l.) found on the Niagara Peninsula were created by Early Lake Erie; this further supports elevated lake levels during this time. Early Lake Erie elevations are referred to here as Phase I levels (fig. 4.12), and were likely sustained by lake outflow over moraine crests on the Niagara Escarpment, as suggested by Coakley and Lewis (1985). The stable isotopic fluctuations (fig. 3.22) between ca 11,000 y.B.P. ka and ca 10,500 y.B.P. could represent variations in meltwater flow into the Erie basin and may explain the fluctuations in the Early Lake Erie levels seen by Feenstra (1981) on the Niagara Escarpment. Tinkler et al. (in

prep."A" and "B") have suggested that high water levels in excess of 183 m.a.s.l. on the Niagara Escarpment were controlled by the Niagara Falls Moraine (as well as by isostatic rebound, discharge from the Upper Great Lakes and climatic conditions) between ca 11,000 and 10,000 y.B.P. The Lyell/Johnson sill near the present Niagara Falls maintained lake levels from ca 8000 y.B.P. until it fell below the level of the Fort Erie sill (due to erosion); lake levels were then maintained by the Fort Erie sill.

Analyses by Lewis (1969) and Coakley and Lewis (1985) suggest that the initial water levels of the western and central basins of Lake Erie had been 15 m and 30 m, respectively, below present lake datum. The topographically higher western basin allowed Upper Great Lakes water to pass into the central and eastern basins but was elevated enough to prevent back flooding, between ca 12,000 and 10,500 y.B.P. Levels in the western basin were thought to be controlled by local sills and water levels in the central basin were thought to be confluent with the eastern basin after a short period of back flooding. However, radiocarbon dates are unavailable from the central basin, so the timing of the low water-level (ca 30 m.b.d.) indicators (wave-eroded glacial surface and buried channel) within this basin is uncertain. These low-water indicators may well correlate with similar indicators in the eastern basin which have a pollen chronology of ca 10,500 y.B.P. This would allow the

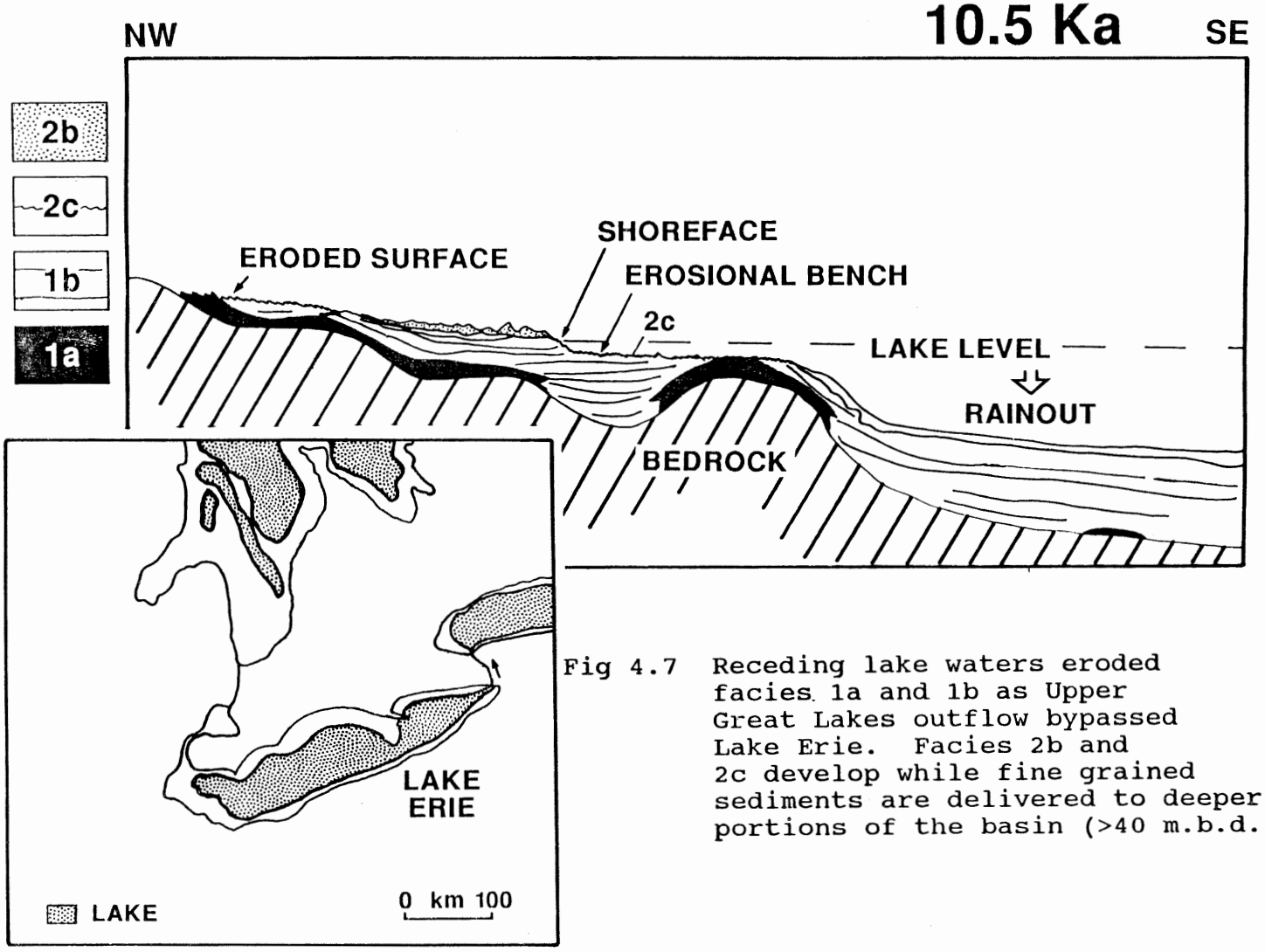

Fig 4.7 Receding lake waters eroded facies 1a and 1b as Upper Great Lakes outflow bypassed Lake Erie. Facies 2b and 2c develop while fine grained sediments are delivered to deeper portions of the basin (>40 m.b.d.).

waters of the central basin to be much higher than previously thought during the initial stages of Early Lake Erie; clearly more work is needed in this area.

By ca 10,500 y.B.P. lake levels in the eastern basin were quickly lowered as ice retreat opened eastward drainage to the Ottawa Valley through the Mattawa Valley, allowing Upper Great Lakes outflow to bypass Lake Erie (Lewis and Anderson, 1989). Lake levels in the eastern basin dropped to ca 30 m.b.d., pushing the shoreline far out into the basin (fig. 4.7 and fig. 4.12). This marked the beginning of Early Lake Erie Phase II.

Lewis (1969) and Coakley and Lewis (1985) have suggested increasing water levels in the western basin during this time. Isostatic readjustment may have allowed backflooding of the western basin which would have assisted in lowering water levels in the eastern basin.

This low level stand has been recognized in the eastern basin through sub-bottom geomorphic features (some pollen dated) such as an erosion platform on proglacial and postglacial sediment (Sequence 1), an erosional shoreface notch and associated sand body (beach deposit), plus abrupt down core changes in sedimentology, stable isotopic trends and physical properties which indicate a change in water conditions (see fig. 3.22 and Chapters 2 and 3). Other dated (ca 11,070 - ca 9,000 y.B.P.) low water level indicators have been recognized onshore (around the eastern

basin) by Barnett (1985). He suggests that lake levels in the Erie basin had to be lower than 189 m.a.s.l (or <15 meters above datum) and that the shoreline must have been farther out in the basin; this further supports the interpreted low water levels for Early Lake Erie Phase II. Coakley and Lewis (1985) suggest a period of minimum outflow between ca 10,500 and 8,000 y.B.P. through lower outlets to the west of the Niagara outlet. Tinkler et al.(in prep."A" and "B") imply that water continued to drain over the Niagara Escarpment after 10,500 y.B.P. through an old Niagara channel. These suggestions imply that low level early Lake Erie II could have drained over the Niagara Escarpment.

The glacial and postglacial sediments were eroded as the lake waters receded and the shoreline moved farther out into the basin. Sediment data from piston cores PC-9 and PC-1 and seismic data show that these sediments were also subaerially exposed and desiccated due to this fall in lake waters (after ca 10,500 ka). Coakley (1985) and Coakley and Lewis (1985) have described a similar erosional platform under Long Point and suggested that the sediments had also been subaerially exposed and desiccated. An erosional lag was developed (lithofacies 2C) as the waters fell during the lake shore recession. As the low lake level stabilized at ca 30 m.b.d. shore deposits accumulated, (lithofacies 2b, beach sands), above and along the shoreface (erosional

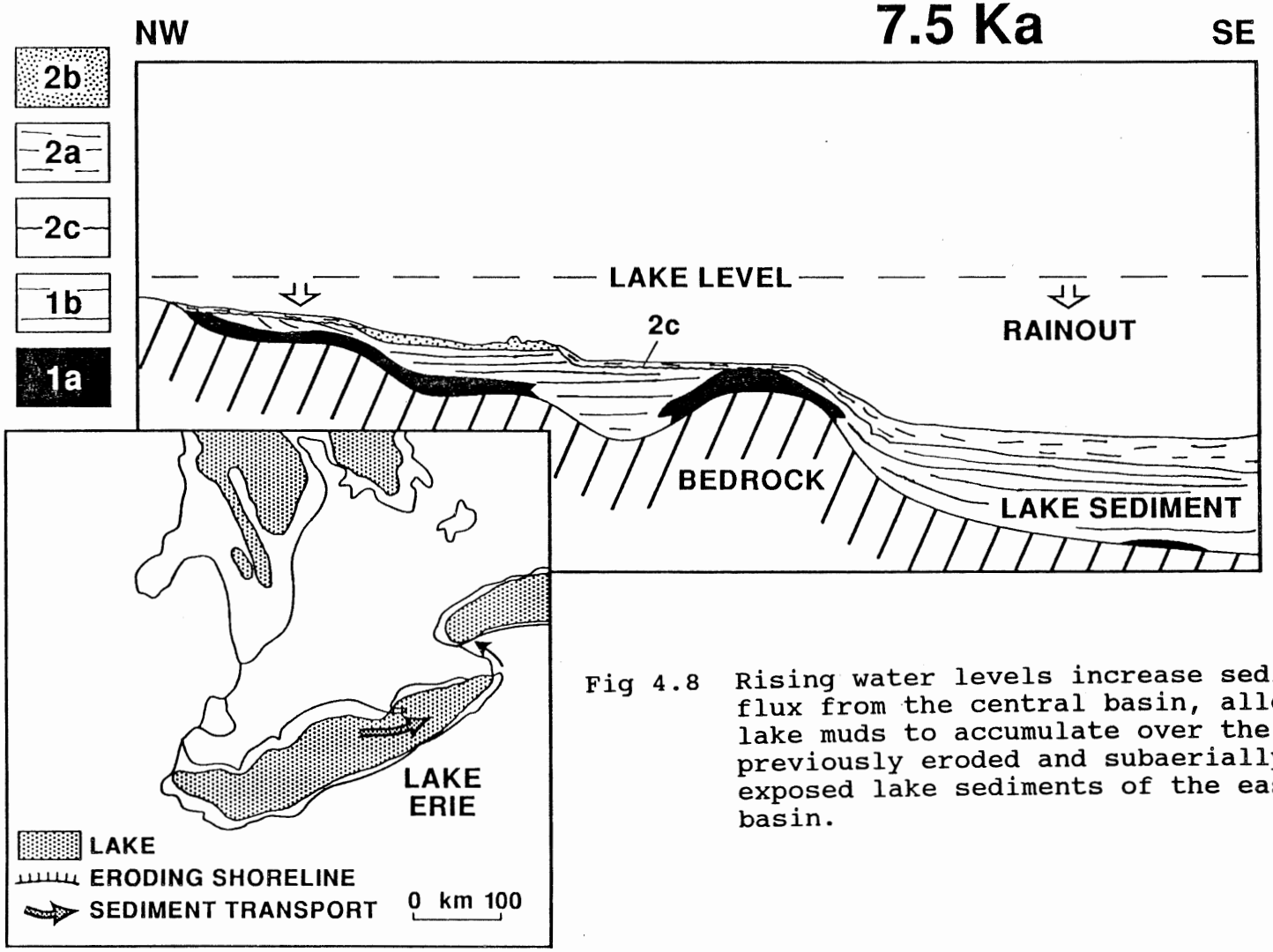

Fig 4.8 Rising water levels increase sediment flux from the central basin, allowing lake muds to accumulate over the previously eroded and subaerially exposed lake sediments of the eastern basin.

notch), while fine grained sediments were delivered to deeper portions of the basin (below 40 m.b.d., figs. 4.6 and 2.12 and 2.13).

From just before ca 10,000 y.B.P. to just after ca 8000 y.B.P. lake level increased from ca 30 m.b.d. to ca 10 m.b.d. (see figs. 4.8 and 4.12). Erosion likely occurred due to rising lake waters but may have been limited in areas where erosional lag deposits or beach sands protected the underlying soft sediments. This estimate of lake rise is based on the first appearance of recent lake sediments (facies 2a; pollen dated ca 7700 y.B.P.) to accumulate above the erosional unconformity (R2), at sites of cores PC-9 and PC-6. The erosional unconformity (R2) at these sites, is ca 20 m.b.d., so lake levels would have to rise at least by 20 m to 10 m.b.d. by ca 7700 y.B.P. to allow soft muds to accumulate. Coakley (1985) made similar observations from borehole studies on Long Point and Point Pelee; suggesting a lake level within 10 m (ca 10,000 y.B.P.) and 5 m (ca 7000 y.B.P.), respectively, of the present datum. Lewis (1969) proposed that lake levels were maintained between 15 m and 10 m below datum, between ca 10,000 y.B.P. and 6000 y.B.P. The increase in lake levels during this time was likely brought on by uplift at the Buffalo outlet. This scenario assumed that Lake Erie's water supply (precipitation and runoff) exceeded evaporative losses and that lake level was controlled by outflow at the outlet. All sub-basins of Lake

Erie would have been brought to one common level due to this rise.

The trend of the lake level curve for the eastern basin of Lake Erie (fig. 4.8), between ca 8000 y.B.P. and ca 5000 y.B.P. is almost flat, constrained by dated terrestrial evidence from the Clear Creek sequence and by dated lacustrine marsh material at Point-aux-Pins and pollen data from deep-water sediments (Coakley and Lewis, 1985). Other suggested levels for this time period are ca 5 m.b.d. (by Coakley, 1985) or 15 m.b.d. (Lewis, 1969). This study has chosen an intermediate level of 10 m as explained above. It is suggested by Coakley (1985) that the stability in lake levels was maintained by a climatic optimum, perhaps the mid-Holocene hypsithermal interval. A correlation may exist between offshore eastern Canada Late Quaternary climate fluctuations, as documented by Scott et al. (1984) and Late Quaternary lake level fluctuations as documented in this study (see Fig 4.12). Scott et al. (1984) interpreted cooling events between ca 10,000-7000 y.B.P. and in the last 2000 years, they also interpreted a warming event between ca 7000-5000 y.B.P. The timing of these events correlate with relatively low lake levels (cooling events; ca 10,5000-5000 y.B.P. and ca 3500 y.B.P.) and a relatively high lake level (warming event; ca 5000-3500 y.B.P.) from eastern Lake Erie. Edwards and Fritz, (1987) have also suggested a warm and very moist hypsithermal period from paleoclimatic evidence

for southern Ontario between ca 6000 and 2000 y.B.P. This period correlates with the timing of the onset of the Nipissing Flood (ca 5000) when lake levels rose by as much as 5 m.a.d. in the Erie basin (see Fig 4.12). They have also suggested a cool and very dry event prior to ca 8000 y.B.P. and another cool and moist event after ca 2000 y.B.P., which may partially explain relative low lake levels during these times (see Fig 4.12). These climate/lake level correlations are only preliminary and more investigation is needed but they may be evidence for at least partial climatic control over lake levels.

Differential uplift of the North Bay outlet rerouted Upper Great Lakes drainage through the Port Huron outlet to Lake Erie and Lake Ontario, finishing just after ca 5000 y.B.P. (Lewis and Anderson, 1989). The return of drainage to the Lower Great Lakes which corresponds to the attainment of Nipissing levels in the Upper Great Lakes initiated high lake levels in the Erie basin. The Nipissing "flood" raised lake levels, between ca 5000 and ca 3900 y.B.P., to as much as 5 m.a.d. (Coakley and Lewis, 1985) (see figs. 4.9 and 4.12). Nearshore areas (less than 10 m.b.d.) often are dominated by coarse sediment and bedrock outcrop (St. Jacques and Rukavina, 1973 and Rukavina and St. Jacques, 1971, Thomas, et al., 1976).

Sediment studies (from cores PC-1 and PC-9) and seismic data suggest that a depositional hiatus occurred between ca

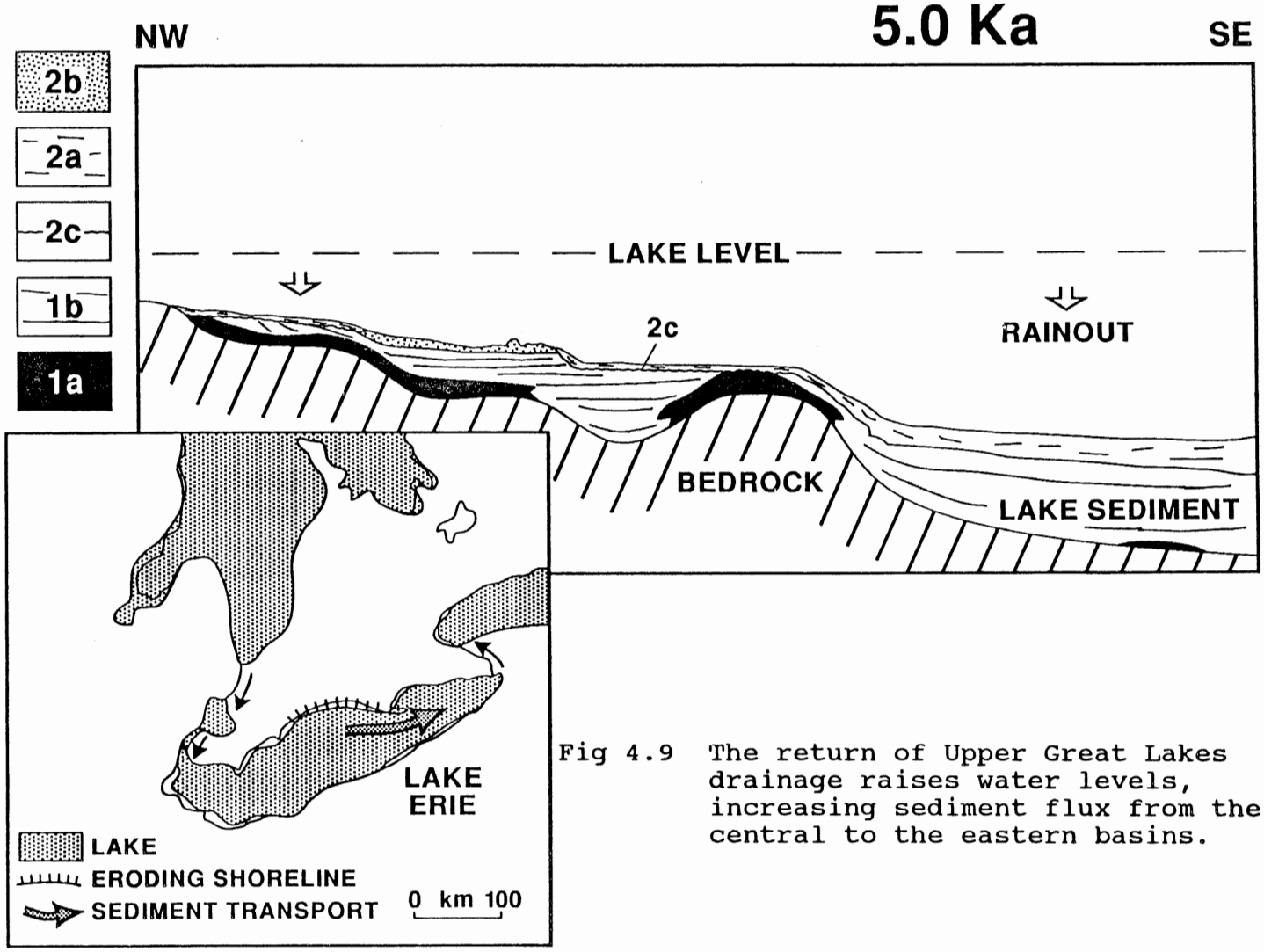

Fig 4.9 The return of Upper Great Lakes drainage raises water levels, increasing sediment flux from the central to the eastern basins.

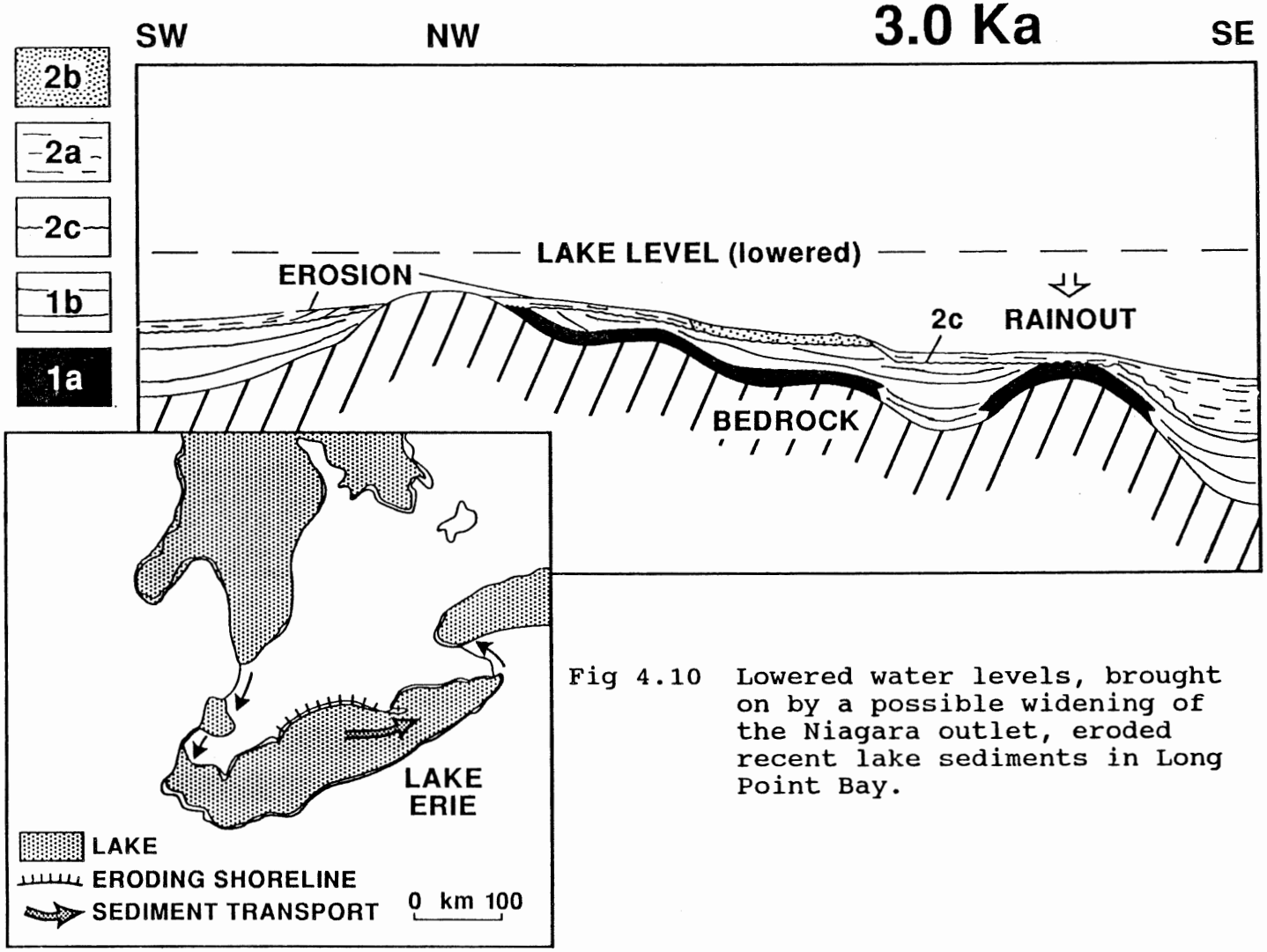

Fig 4.10 Lowered water levels, brought on by a possible widening of the Niagara outlet, eroded recent lake sediments in Long Point Bay.

4800 y.B.P. and ca 3600 y.B.P. This is interpreted as a fall in lake level, by as much as 10 m.b.d. (figs. 4.10 and 4.12). Coakley and Lewis (1985) have also suggested that a drop in lake levels must have occurred sometime after ca 3900 ka, based on reliable C^{14} dates from the western basin and Point Pelee. They propose that the drop in lake levels was brought on by a widening of the Niagara outlet due to higher post-Nipissing outflow.

Pollen data from piston core PC-9, in Long Point Bay, suggest that sedimentation there did not re-occur until ca 150 years ago; this would support a slow rise in lake levels from ca 3500 ka to the present (figs. 4.11 and 4.12), which was also suggested by Coakley and Lewis (1985). They suggest that the lake level rise was due to postglacial isostatic adjustment. The resumption of sedimentation in Long Point Bay may have been aided by increased wave sheltering of the area afforded by the progradation of Long Point.

The Erie basin was dominated by high proglacial lake sedimentation between 13,000 and 12,500 y.B.P. (fig. 4.12). Linear sediment accumulation rates of 30 mm/yr or greater occurred during this time. Sedimentation rates decreased to ca 8-9 mm/yr. between ca 12,500-10,500 y.B.P. as direct glacial influence ended in the Erie basin. Low sedimentation rates of <1mm/yr occurred between 10,500 and 5000 y.B.P. due to a drop in lake level brought on by the

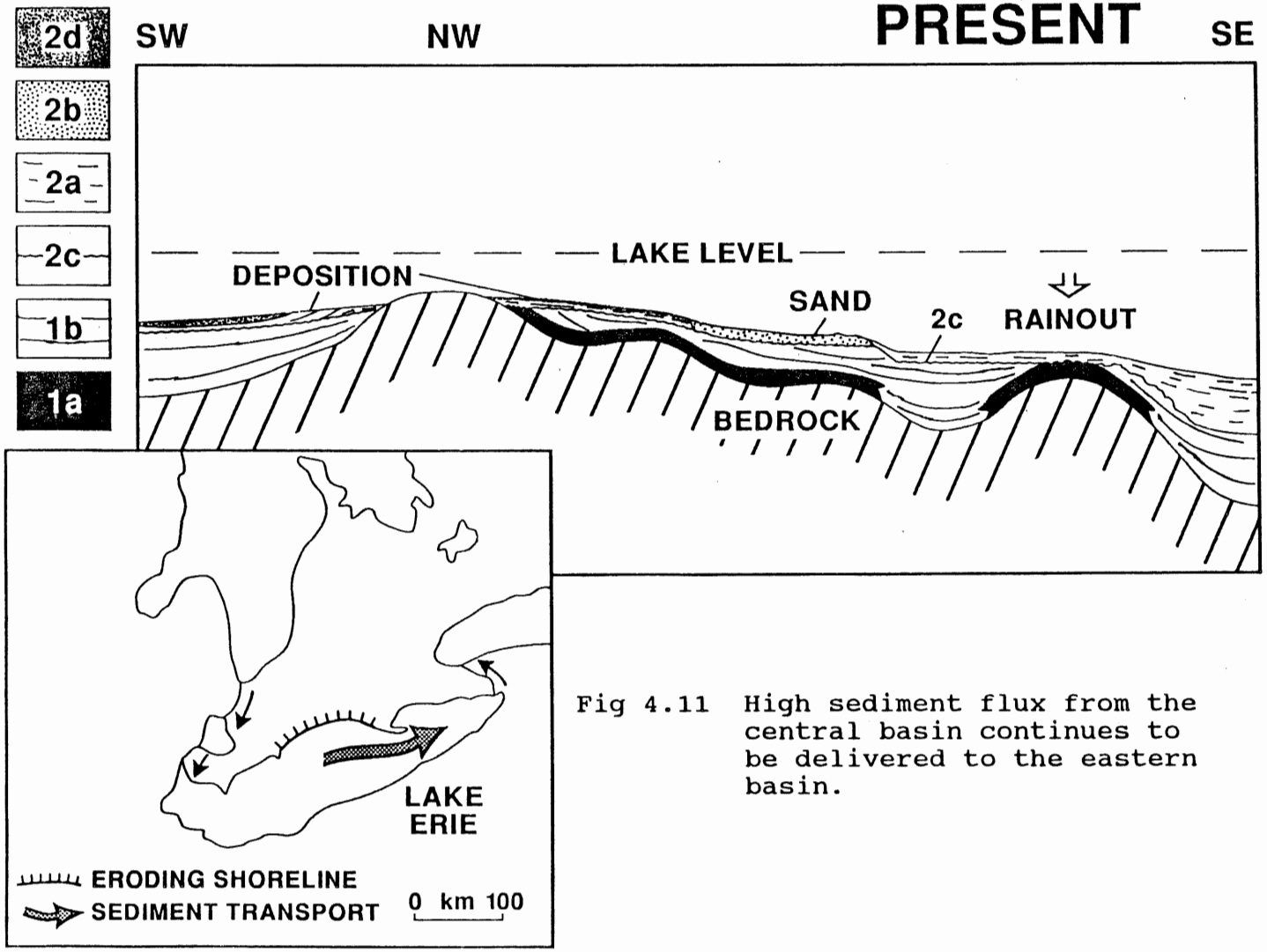

Fig 4.11 High sediment flux from the central basin continues to be delivered to the eastern basin.

diversion of Upper Great Lakes drainage away from the Erie basin. Sedimentation rates increased to ca 2mm/yr during the Nipissing flood and return of Upper Great Lakes drainage. Sedimentation rates dropped to <1mm/yr after lake levels fell ca 3600 y.B.P. Modern sediment accumulation rates of nearly 4 mm/yr. occur in offshore areas of the Erie basin. When postglacial levels rose above the Norfolk Moraine, coalescing eastern and central basin water bodies, products of rapid shore erosion in the central basin were transported by wavedrift eastward, contributing to increased sedimentation in the eastern basin.

Soft sediment faulting, as described in Chapter 2, has been interpreted to be possibly controlled by bedrock structures and/or dewatering of sediments brought on by seismic shaking, normal consolidation or differential sediment compaction. Deformed sediments in facies 1b and acoustically bright or reflection free areas in this sediment section (see Chapter 2) may also be evidence of previous seismic activity. Adams and Basham (1989) have documented seismic activity in the continental part of south eastern Canada and have suggested a westward extension of the Paleozoic rift system of the St. Lawrence Valley into the Ontario and Erie basins. Neotectonic investigations by Thomas et al. (in prep.) and Thomas et al. (1991) in Lake Ontario have documented lake bottom features (plumose structures and aligned ridges) which they suggest are

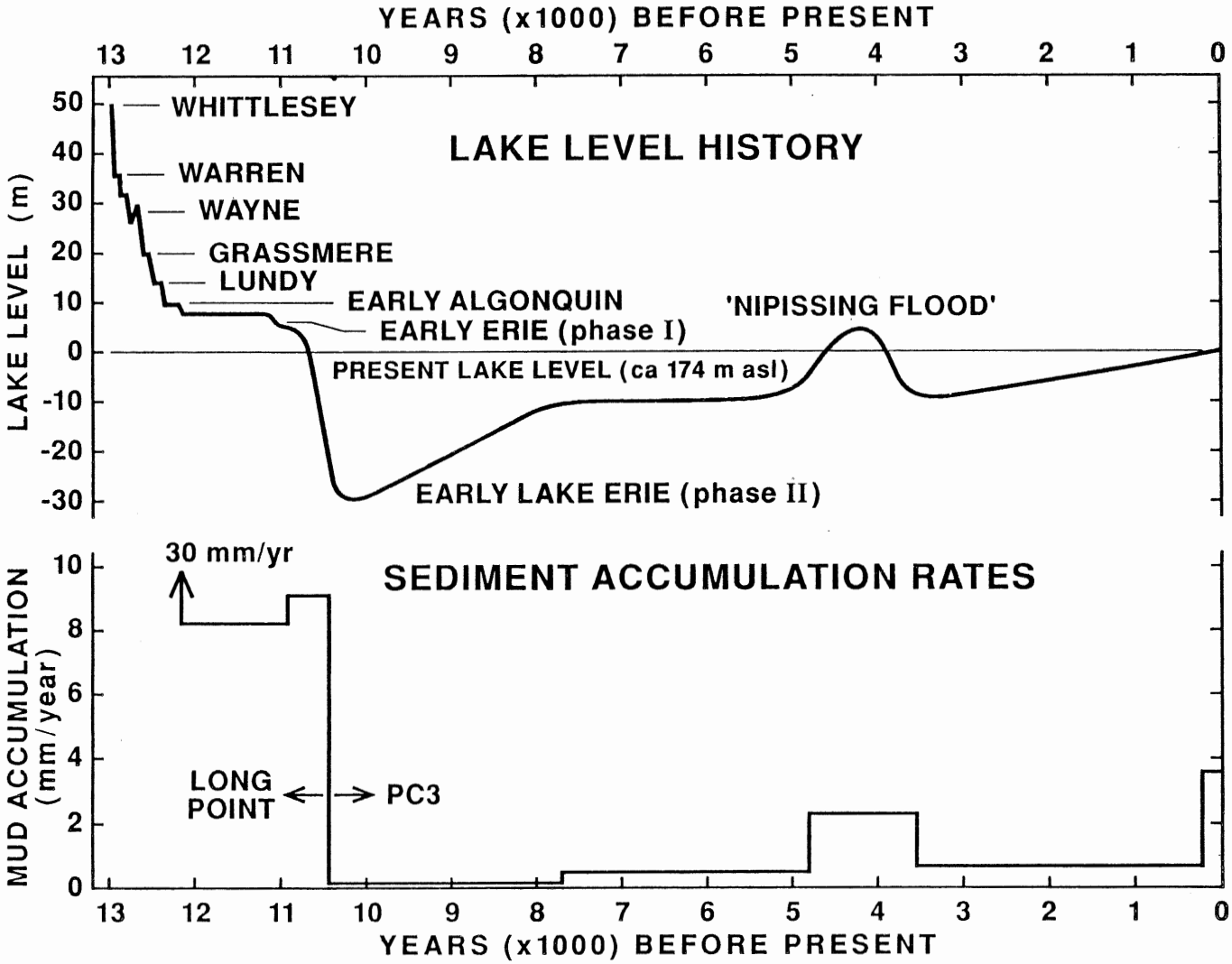

Fig 4.12 Lake levels and mean sedimentation rates, eastern Lake Erie.

evidence for recent crustal movement. They have also defined a structural zone extending into the Erie basin, which they have interpreted to be part of the rift complex proposed by Adams and Basham (1989). The traditional isostatic rebound model for the Great Lakes is based on discontinuous warped terraces and water level indicators and proposes a simple relaxation process of the crust following unloading by retreat of the Laurentide Ice (Walcott, 1972). However, this may be an oversimplification of the crustal response to postglacial isostatic adjustment. Faulting resulting from postglacial isostatic adjustment, rift zone instabilities and fracturing and crustal block tilting (as described by Sanford et al., 1985) may all have contributed to lake level trends and lake outlet controls after glacial unloading.

Conclusions:

The seismic stratigraphy of the eastern Lake Erie basin consists of two seismic sequences separated by the regional R2 reflector, (commonly an erosional unconformity above 35m present water depth). The seismic stratigraphy is supported by observations of lithofacies and sediment physical properties in cores. The lower seismic sequence 1 contains seismic facies 1a (glacial till) and 1b (laminated mud) and has been influenced by glacial ice (Port Huron advance), proglacial lakes and postglacial lake levels, between ca 13,000 y.B.P. and ca 10,500 y.B.P. based on a radiocarbon-dated pollen chronology. The uppermost sequence 2, comprising seismofacies 2a (consisting of laminated, massive or muddy sand) and seismofacies 2b (brown or gray sand), has been influenced by fluctuating postglacial lake levels between ca 10,500 y.B.P. and the present.

The last ice advance (Port Huron) reached into the eastern Erie basin, (at least as far as Long Point Bay), forming a series of high westward-draining proglacial lakes, depositing glacial drift on the basin flanks and bedrock highs and delivering fine grained proglacial lake sediments to deeper portions of the basin. Turbidity currents and rainout sedimentation, as well as ice meltout deposition, are interpreted to be important depositional mechanisms during glacial times in this basin. Ice retreat (ca 12,500 y.B.P.) lowered lake levels and allowed eastward drainage

over the Niagara Escarpment into Ontario basin.

High lake levels (ca 181 m.a.s.l. as compared with ca 174 m for the present lake level) were maintained in the eastern basin, between ca 12,500 y.B.P. and ca 10,500 y.B.P., by continued Upper Great Lakes flow and by partial damming by glacial end moraines which restricted outflow over the Niagara Escarpment. This allowed the continued widespread deposition (predominantly by rainout sedimentation) of seismofacies 1b in the Erie basin. Upper Great Lakes waters were diverted away from the Erie basin by ca 10,500 y.B.P., causing lake levels to fall. Falling waters eroded, subaerially exposed and desiccated the glacial and postglacial sediments in the basin; beach sand deposits developed during this time at the paleo lake shore (ca 30 m.b.d.). Lake muds continued to be deposited beyond the >40 m.b.d isobath. Diversion of the Upper Great Lakes waters and subsequent fall in lake levels brought on modern sedimentation (Holocene) and developed the R2 regional reflector.

Lake levels continued a general upward or stable trend throughout the Holocene, due to isostatic uplift of the Buffalo outlet. Rising water levels may also have eroded lake sediment in areas above the 40 meter isobath. The Nipissing flood (starting ca 5000 y.B.P.) renewed Upper Great Lakes influence in Lake Erie and temporarily raised levels above the present datum (approx. 5 m.a.d.). Water

levels continued an upward trend, after falling below (ca 10 m.b.d., ca 3900 y.B.P.) the present datum, from the Nipissing high, due to outlet incision at Buffalo. Rising water levels coalesed the water bodies of the central and eastern basins, allowing recent lake sediments to accumulate more rapidly in the eastern basin due to the eastward flux of sediment from the rapidly eroding shores of the central basin. Fluctuation of lake levels in Lake Erie may also be influenced by climatic change. Soft sediment deformation and faulting found in the unconsolidated lake sediments may be related to neotectonic activities.

Recommendations:

The lake level curve for Lake Erie is more complex than was indicated by previous models (Lewis, 1969 and Coakley and Lewis, 1985). A review of the relationship between the three sub-basins of Lake Erie and many more radiocarbon datings of former water level indicators are necessary and would likely clarify the overall lake level curve. More resolution is needed in the lake level curve especially between ca 12,500 y.B.P. and ca 10,500 y.B.P. and ca 6000 y.B.P. to the present, to resolve the relationship between the sub-basins. More seismic work is needed over the Norfolk Moraine between the central and eastern basins and along the U. S. side of the lake. A renewed focus on the role of glacio-isostatic uplift on lake levels in the Lake Erie basin is important (in light of recent neotectonic

findings in the region) and may be important in revealing mechanisms related to the post glacial uplift. I feel that the approach and analysis of this project were successful and could be applicable to the determination of the sedimentary history in other lake basins, as they are in marine basins. The application of marine geological techniques in the Laurentian Great Lakes will offer great future potential for the solution of many scientific problems.

Appendices

Grain Size Data

Core #	Depth (cm)	Litho Facies	GR %	SA %	Silt %	Clay %	Mean (phi)	SD (phi)	Kurt	Skew
PC-1	20	2b	0	3.9	46.6	49.5	8.3	2.7	2.2	-.21
	230	2a	0	1.6	46.1	52.4	8.6	2.3	2.4	-.08
	325	2c	.75	55.6	22.6	21.1	4.7	3.5	2.4	.79
	330	2c	.10	69.5	26.0	4.4	3.3	2.2	6.6	1.79
	340	1b	.07	11.5	36.0	52.5	8.0	3.0	2.3	-.41
	380	1b	0	.6	12.2	87.2	10.2	1.9	4.7	-.14
PC-3	380	2a	0	1.3	24.7	74.0	9.5	2.1	2.8	-.58
	776	2c	.07	15.4	15.2	69.3	8.8	3.3	2.5	-.91
	830	1b	0	.2	3.1	96.7	10.5	1.5	6.2	-1.39
PC-6	45	2a	0	3.9	28.0	68.1	9.1	2.4	3.4	-.80
	460	1b	0	.2	4.2	95.7	10.6	1.4	4.5	-1.12
PC-7	80	2a	.1	2.6	27.1	70.3	9.3	2.4	3.6	-.83
	170	1b	0	1.1	4.9	94.0	10.7	1.7	9.9	-2.40
	250	1b	.06	1.3	4.8	93.8	10.4	1.7	8.6	-1.98
	280	1b	0	.9	2.9	96.2	10.5	1.6	7.3	-1.67
	385	1a	4.9	11.8	22.0	61.3	8.1	4.0	3.7	-1.19
PC-9	90	2a	0	1.3	13.5	85.3	10.1	2.1	4.9	-1.47
	220	2c	10.2	59.6	9.2	21.0	3.6	4.2	2.5	.71
	236	1b	0	2.8	27.8	69.4	9.3	2.5	3.0	-.80

Physical Property Data

Core#	Depth (m)	Bulk Density (g/cm^3)	Water Content (%)	Porosity (%)	Velocity (m/s)
GC01	0.10			58.4	1460
GC01	0.20	1.683	60.98		
GC01	0.30			60.9	1460
GC01	0.40	1.605	73.36		
GC01	0.50			61.7	1457
GC01	0.60	1.659	60.88		
GC01	0.70			53.2	1488
GC01	0.80	1.870	40.00		
GC01	0.90			47.5	1493
GC01	1.00	1.837	42.92		
GC03	0.15	1.309	187.91	82.4	1442
GC03	0.25	1.347	149.52	79.8	1439
GC03	0.35	1.388	135.34	77.2	1434
GC03	0.45	1.385	138.93	77.4	1435
GC03	0.55	1.377	139.31	77.9	1437
GC03	0.65	1.400	134.45	76.4	1435
GC03	0.75	1.405	130.90	76.1	1435
GC03	0.85	1.394	137.17	76.8	1437
GC03	0.95	1.411	128.76	75.7	1435
GC03	1.05	1.406	127.30	76.1	1435
GC03	1.15	1.424	126.35		
GC04	0.30	1.544	84.75		
GC04	0.50	1.575	76.81		
GC04	0.70	1.663	63.30		
GC05	0.23	1.282	191.95		
GC05	0.53	1.345	159.33		
GC05	0.74	1.342	153.46		
GC05	0.95	1.381	139.87		
GC05	1.15	1.389	135.91		
GC06	0.10	1.380	135.58	77.7	1439
GC06	0.19	1.433	120.32	73.9	1436
GC06	0.30	1.508	121.61	69.6	1435
GC06	0.40	1.413	120.39	75.6	1432
GC06	0.50	1.512	93.81	69.3	1436
GC06	0.60	1.534	88.96	67.9	1436
GC06	0.70	1.598	72.52	63.8	1444
GC06	0.80	1.591	78.17	64.3	1441
GC06	0.90	1.725	53.65	55.7	1473
GC06	1.00	1.656	63.56	60.1	1456
GC06	1.10	1.749	50.58	54.2	1475
GC06	1.20	1.671	63.71	59.2	1458
GC07	0.05	1.378	142.98		
GC07	0.15	1.357	152.14	79.2	1416
GC07	0.25	1.838	126.95	48.5	1403
GC07	0.35	1.398	126.09		
GC07	0.45	1.462	108.74	72.5	1398

Physical Property Data

Core #	Depth (m)	Bulk Density (g/cm^3)	Water Content (%)	Porosity (%)	Velocity (m/s)
GC07	0.55	2.055	97.11		
GC07	0.65	1.494	101.00	70.4	1427
GC07	0.75	1.543	88.18		
GC07	0.85	1.568	81.55	65.7	1429
GC07	0.95	1.757	50.78		
GC07	1.05	1.715	55.67	56.4	1456
GC07	1.15	1.680	60.26	58.6	1452
PC01B	0.20			63.2	1465
PC01B	0.25	1.608	71.74		
PC01B	0.40			51.6	1499
PC01B	0.45	1.851	40.66		
PC01B	0.60			48.5	1497
PC01B	0.65	1.834	43.14		
PC01B	0.80			49.0	1496
PC01B	0.85	1.829	43.52		
PC01B	0.95			49.1	1505
PC01B	1.10	1.829	43.40	49.1	1512
PC01B	1.30			46.4	1503
PC01B	1.40	1.892	37.63		
PC01B	1.50			46.5	1507
PC01B	1.60	1.847	40.99		
PC01B	1.70			48.2	1506
PC01B	1.80	1.839	41.48		
PC01B	1.90			47.4	1504
PC01B	2.00	1.874	39.68		
PC01B	2.10			46.2	1513
PC01B	2.20	1.874	39.69		
PC01B	2.30			45.1	1510
PC01B	2.40	1.911	36.56		
PC01B	2.45			44.6	1514
PC01B	2.55	1.878	38.71		
PC01B	2.58			46.5	1505
PC01B	2.67	1.845	41.88		
PC01B	2.90	1.908	36.41	44.1	1511
PC01B	3.05	1.855	40.84	47.5	1498
PC01B	3.40	3.020	21.25	47.4	1674
PC01B	3.50	3.030	17.54		
PC01B	3.65	2.118	25.69	45.9	1622
PC01B	3.80	3.160	28.11	52.4	1541
PC01B	3.90	3.267	28.61	56.8	1596
PC01B	4.00			50.9	1554
PC01B	4.10	2.930	27.47	45.0	1595
PC03	0.10	1.440	116.27		
PC03	0.20	1.442	115.53	73.8	1395
PC03	0.30	1.445	114.09	73.6	1417
PC03	0.55	1.514	88.71		

Physical Property Data

Core #	Depth (m)	Bulk Density (g/cm^3)	Water Content (%)	Porosity (%)	Velocity (m/s)
PC03	0.75	1.518	95.00		
PC03	0.95	1.512	93.67		
PC03	1.20	1.525	92.60		
PC03	1.50	1.490	98.45		
PC03	1.55			70.6	1413
PC03	1.75	1.501	94.41		
PC03	1.90			69.5	1423
PC03	1.95	1.512	93.06		
PC03	2.20	1.553	82.37		
PC03	2.45	1.567	77.84		
PC03	2.70	1.580	76.52		
PC03	2.95	1.576	76.67		
PC03	3.20	1.597	74.37		
PC03	3.45	1.646	66.69		
PC03	3.75	1.685	59.38		
PC03	4.05	1.661	62.57		
PC03	4.25	1.669	63.26		
PC03	4.50	1.670	63.56		
PC03	4.75	1.646	66.52		
PC03	5.00	1.724	57.24		
PC03	5.25	1.691	59.43		
PC03	5.50	1.709	58.06		
PC03	5.75	1.726	55.45		
PC03	6.00	1.706	56.77		
PC03	6.25	1.724	55.99		
PC03	6.45	1.734	53.10		
PC03	6.75	1.731	53.89		
PC03	7.00	1.731	54.17		
PC03	7.20	1.730	54.96		
PC03	7.45	1.693	58.69		
PC03	7.65	1.693	59.54		
PC03	7.75	1.874	39.17		
PC03	7.85	1.850	42.11		
PC03	7.95	1.722	57.09		
PC03	8.25	1.742	53.91		
PC03	8.40	1.726	55.89		
PC03	8.55	1.732	55.24		
PC03	8.65	1.649	66.41		
PC04	0.20	1.651	64.99		
PC04	0.40	1.763	49.26		
PC04	0.60	1.687	58.86		
PC04	0.80	1.603	71.71		
PC04	1.00	1.528	87.25		
PC04	1.60	1.568	78.10		
PC04	1.80	1.601	73.33		
PC04	2.00	1.649	66.98		

Physical Property Data

Core #	Depth (m)	Bulk Density (g/cm^3)	Water Content (%)	Porosity (%)	Velocity (m/s)
PC04	2.20	1.646	66.93		
PC04	2.40	1.615	71.64		
PC04	2.60	1.602	72.00		
PC04	2.75	1.595	74.61		
PC04	3.10	1.613	69.46		
PC04	3.30	1.609	71.31		
PC04	3.50	1.683	59.18		
PC04	3.70	2.039	28.71		
PC04	3.90	1.927	33.38		
PC04	4.10	1.879	38.60		
PC04	4.25	1.837	41.80		
PC05	0.15	1.340	165.73		
PC05	0.36	1.467	104.58		
PC05	0.56	1.702	56.87		
PC05	0.76	1.696	58.76		
PC05	0.94	1.756	51.29		
PC05	1.21	1.766	50.36		
PC05	1.41	1.795	46.32		
PC05	1.59	1.928	37.01		
PC05	1.80	2.063	30.89		
PC05	2.00	2.031	30.66		
PC05	2.20	2.083	27.77		
PC05	2.40	2.062	29.86		
PC06	0.10	1.485	89.05	71.0	1439
PC06	0.20	1.639	67.30	61.2	1460
PC06	0.30	1.699	56.62	57.4	1465
PC06	0.40	1.694	57.69	57.7	1456
PC06	0.50	1.679	60.80	58.7	1453
PC06	0.61	1.705	56.54	57.2	1463
PC06	0.70	1.748	51.72	54.3	1468
PC06	0.80	1.708	56.00	56.8	1465
PC06	0.90	1.709	55.90	56.8	1465
PC06	1.00	1.532	77.46	64.2	1452
PC06	1.10	1.650	68.20	60.5	1446
PC06	1.30	1.601	71.95	63.6	1423
PC06	1.40	1.661	64.76	59.8	1436
PC06	1.50	1.643	67.18	61.0	1424
PC06	1.60	1.643	67.68	61.0	1432
PC06	1.70	1.653	67.21	60.3	1432
PC06	1.80	1.591	76.35	64.3	1428
PC06	1.90	1.650	66.93	60.5	1427
PC06	2.00	1.614	73.73	62.8	1432
PC06	2.10	1.576	78.18	65.2	1429
PC06	2.20	1.565	82.91	65.9	1426
PC06	2.30	1.591	77.47	64.3	1431
PC06	2.40	1.619	69.88	62.5	1439

Physical Property Data

Core #	Depth (m)	Bulk Density (g/cm^3)	Water Content (%)	Porosity (%)	Velocity (m/s)
PC06	2.50	1.579	79.11	65.0	1435
PC06	2.60	1.597	76.89	63.9	1436
PC06	2.69	1.601	76.28		
PC06	2.80	1.593	77.66	64.1	1422
PC06	2.90	1.579	78.01	65.0	1426
PC06	3.00	1.636	69.85	61.4	1436
PC06	3.10	1.627	66.83	62.0	1437
PC06	3.20	1.643	68.84	61.0	1434
PC06	3.30	1.602	70.76	63.6	1438
PC06	3.40	1.648	68.29	60.6	1440
PC06	3.50	1.615	70.58	62.6	1444
PC06	3.60	1.636	65.47	61.4	1449
PC06	3.70	1.663	65.77	59.7	1445
PC06	3.80	1.658	65.82	60.0	1449
PC06	3.90	1.727	57.90	55.6	1457
PC06	4.00	1.687	61.30	58.2	1464
PC06	4.10	1.637	68.13	61.3	1462
PC06	4.28	1.688	59.93	51.5	1455
PC06	4.35	1.628	69.07	61.0	1428
PC06	4.45	1.667	64.79	59.4	1423
PC06	4.55	1.693	62.69	57.8	1427
PC06	4.65	1.675	62.71	58.9	1427
PC06	4.75	1.662	66.06	59.7	1429
PC06	4.85	1.682	62.39	58.5	1432
PC06	4.95	1.637	67.35	61.3	1433
PC06	5.05	1.657	64.56	60.1	1434
PC06	5.15	1.664	64.10	59.6	1439
PC06	5.25	1.526	64.20	68.4	1440
PC06	5.35	1.674	61.72	59.0	1439
PC06	5.45	1.656	67.64	60.1	1439
PC06	5.55	1.691	60.15	57.9	1444
PC06	5.65	1.652	63.72	60.4	1442
PC06	5.95	1.666	63.22	59.5	1434
PC06	6.05	1.668	62.53	59.4	1429
PC06	6.15	1.645	69.47	60.8	1458
PC06	6.25	1.638	70.53	61.3	1429
PC06	6.35	1.635	67.44	61.5	1430
PC06	6.45	1.671	64.90	59.2	1429
PC06	6.55	1.653	63.91	60.3	1435
PC06	6.65	1.660	64.80	59.9	1435
PC06	6.75	1.662	63.41	59.7	1445
PC06	6.85	1.710	56.95	56.7	1442
PC06	6.95	1.645	63.96	60.8	1433
PC06	7.05	1.686	62.68	58.7	1432
PC06	7.25	1.699	57.89	57.4	1442
PC06	7.35	1.689	60.07	58.0	1443

Physical Property Data

Core #	Depth (m)	Bulk Density (g/cm^3)	Water Content (%)	Porosity (%)	Velocity (m/s)
PC06	7.45	1.682	60.86	58.8	1444
PC06	7.55	1.700	58.65	57.3	1452
PC06	7.65	1.794	48.29	51.3	1455
PC06	7.75	1.711	55.39	56.6	1449
PC06	7.85	1.743	51.58	54.6	1452
PC06	7.95	1.763	50.01	53.3	1460
PC07	0.10	1.509	90.53	69.5	1422
PC07	0.20	2.149	75.05	67.2	1437
PC07	0.30			65.0	1456
PC07	0.60	1.685	61.31	58.3	1443
PC07	0.80			58.4	1441
PC07	0.85	1.683	59.31		
PC07	0.90			57.1	1433
PC07	0.95	1.725	55.61		
PC07	1.00			55.5	1440
PC07	1.05	2.353	56.68		
PC07	1.10			55.1	1450
PC07	1.15	2.267	55.08		
PC07	1.25	1.746	53.82	54.4	1450
PC07	1.35	2.315	79.38	58.7	1439
PC07	1.45	1.610	74.22	63.1	1436
PC07	1.55	1.592	77.70	64.2	1427
PC07	1.65	1.613	70.55	62.9	1433
PC07	1.75	1.614	72.69	62.8	1434
PC07	1.85	1.619	68.78	62.5	1437
PC07	1.95	2.160	61.60	60.0	1444
PC07	2.05	1.696	68.93	57.6	1438
PC07	2.35	2.320	65.62	58.6	1428
PC07	2.45	1.674	63.96	59.0	1433
PC07	2.55	2.289	62.28	59.0	1441
PC07	2.65	1.674	62.81	59.0	1433
PC07	2.75	1.701	58.75	57.3	1436
PC07	2.85	1.672	63.79	59.1	1435
PC07	2.95	1.665	64.50	59.6	1435
PC07	3.05	1.669	63.75	59.3	1436
PC07	3.15	1.677	62.05	58.8	1442
PC07	3.25	1.647	66.51	60.7	1444
PC07	3.50	2.318	66.93	59.1	1441
PC07	3.60	1.683	62.00	58.4	1444
PC07	3.87	1.801	47.39	51.4	1477
PC07	3.95			55.2	1429
PC07	4.07	1.632	70.25		
PC07	4.05			60.6	1428
PC07	4.15	1.635	69.04	61.5	1432
PC07	4.27	1.671	64.30	59.6	1441

Physical Property Data

Core #	Depth (m)	Bulk Density (g/cm^3)	Water Content (%)	Porosity (%)	Velocity (m/s)
PC07	4.35	1.665	63.84	59.6	1426
PC07	4.47	1.627	70.58	61.6	1440
PC07	4.55	1.630	69.88	61.8	1440
PC07	4.67	1.626	70.94	62.0	1465
PC09	0.18	1.824	43.27		
PC09	0.38	1.803	45.18	50.8	1466
PC09	0.53	1.725	56.01		
PC09	0.62	1.777	49.52		
PC09	0.69			51.6	1471
PC09	0.90	1.839	43.91	49.1	1472
PC09	1.10			54.9	1467
PC09	1.15	1.705	57.70		
PC09	1.30			51.5	1477
PC09	1.35	1.821	45.21		
PC09	1.50			52.9	1524
PC09	1.55	1.752	52.95		
PC09	1.70			54.3	1474
PC09	1.75	1.745	52.86		
PC09	1.90			54.1	1476
PC09	1.95	1.752	52.14		
PC09	2.15	2.654	33.02		
PC09	2.20			14.8	1525
PC09	2.40	2.072	26.52	32.2	1528
PC09	2.60	2.039	28.71	37.6	1560
PC09	2.80	1.974	32.08	39.6	1541
PC09	3.00	2.426	41.53		

Physical Property Data

Core # GC01

Shear Strength Data

Depth (m)	Peak (kPa)	Remoulded (kPa)
0.28	4.72	3.00
0.49	11.00	0.00
0.65	14.31	2.58
0.85	13.88	3.58
0.90	2.58	2.29
1.05	15.31	4.01
1.25	21.74	5.15
1.45	11.59	4.01
1.65	12.87	0.00
1.90	14.87	0.00
2.10	9.58	0.00
2.30	42.34	0.00
2.50	90.81	7.07
2.70	39.03	0.00
2.90	12.73	0.00

Physical Property Data

Core # GC03

Shear Strenght Data

Depth (m)	Peak (kPa)	Remoulded (kPa)
0.10	1.00	0.14
0.20	1.86	0.72
0.30	1.43	0.72
0.40	3.72	0.43
0.50	3.72	1.29
0.60	2.00	0.86
0.70	2.86	0.86
0.80	3.15	0.86
0.90	3.58	2.86
1.00	2.57	0.00
1.10	2.43	1.86
1.20	4.01	0.00

Physical Property Data

Core # GC06

Shear Strength Data

Depth (m)	Peak (kPa)	Remoulded (kPa)
0.05	2.00	3.15
0.15	2.72	1.14
0.25	2.00	1.00
0.35	2.15	1.14
0.45	6.01	1.57
0.55	5.44	2.43
0.65	4.01	3.00
0.75	5.15	2.72
0.85	3.43	3.15
0.95	6.29	2.72
1.05	3.58	0.86
1.15	34.19	1.14
1.25	5.58	4.15

Physical Property Data

Core # GC07

Shear Strength Data

Depth (m)	Peak (kPa)	Remoulded (kPa)
0.10	5.15	0.00
0.20	4.72	0.00
0.30	3.43	0.00
0.40	3.72	1.86
0.50	4.58	0.00
0.60	3.29	0.00
0.70	3.58	1.43
0.80	3.43	0.00
0.90	5.01	0.00
1.00	3.86	0.86
1.10	6.72	0.00
1.20	5.72	0.57

Physical Property Data

Core # PC01

Shear Strength Data

Depth (m)	Peak (kPa)	Remoulded (kPa)
0.15	5.87	1.00
0.35	3.43	0.00
0.55	2.57	0.00
0.75	4.29	0.14
1.00	4.57	0.00
1.15	5.01	0.00
1.50	5.58	1.00
1.70	6.58	0.00
1.90	5.58	3.29
2.10	6.01	0.00
2.30	5.87	3.15
2.45	6.29	0.00
2.60	6.72	4.15
2.80	9.58	0.00
3.00	8.15	5.01
3.10	6.44	0.00
3.30	13.59	1.29
3.35	105.24	0.00
3.45	6.58	0.00
3.55	20.93	6.79
3.75	88.47	0.00
3.85	98.75	0.00
3.95	77.67	21.09
4.05	87.44	0.00
4.15	94.13	5.66

Physical Property Data

Core # PC03

Shear Strength Data

Depth (m)	Peak (kPa)	Remoulded (kPa)
0.05	4.01	2.00
0.15	2.29	1.29
0.25	2.43	0.72
0.35	2.43	0.86
0.45	4.58	0.57
0.65	4.15	0.00
0.85	5.15	0.00
1.05	3.72	0.00
1.40	3.43	1.29
1.60	2.86	0.00
1.80	4.58	1.14
1.98	4.86	0.00
2.10	7.30	1.72
2.35	5.29	0.00
2.85	5.72	4.86
3.10	4.57	0.00
3.35	4.72	0.00
3.50	4.72	1.86
3.65	8.73	0.29
3.90	5.56	0.00
4.15	5.15	0.00
4.40	5.01	2.86
4.65	5.44	2.15
4.90	5.15	0.00
5.10	9.30	0.00
5.35	6.01	1.57
5.60	7.15	0.00
5.85	8.44	0.00
6.10	6.29	2.29
6.35	9.01	3.72
6.60	9.30	2.00
6.85	7.15	0.00
7.10	5.58	0.00
7.35	6.15	2.15
7.60	8.58	5.29
7.70	7.87	3.15
7.80	6.87	0.00
7.90	6.01	0.00
8.00	8.73	4.15
8.15	8.30	2.58
8.35	6.44	4.58
8.60	6.72	1.43

Physical Property Data

Core # PC06

Shear Strength Data

Depth (m)	Peak (kPa)	Remoulded (kPa)
0.05	2.86	2.43
0.15	3.72	0.72
0.25	3.86	0.57
0.35	3.86	1.14
0.45	4.15	1.57
0.55	4.01	2.00
0.65	5.58	3.86
0.75	4.29	2.58
0.85	4.58	2.00
0.95	3.86	1.14
1.05	25.61	3.72
1.15	6.72	4.15
1.30	6.29	1.29
1.40	3.72	2.00
1.50	4.25	2.86
1.60	5.29	3.72
1.70	4.86	1.72
1.80	6.15	2.58
1.90	5.87	2.00
2.00	7.01	2.15
2.10	6.01	1.86
2.20	6.72	1.57
2.30	7.87	2.43
2.40	8.01	1.86
2.50	6.87	1.43
2.60	7.87	2.00
2.80	6.87	2.72
2.90	7.30	2.43
3.00	7.15	2.00
3.10	6.87	2.00
3.20	8.01	1.72
3.30	8.44	1.72
3.40	7.87	2.43
3.50	7.87	1.72
3.60	7.30	1.86
3.70	9.01	3.15
3.80	8.73	3.00
3.90	7.58	4.01
4.00	10.59	3.00
4.10	6.58	1.14
4.20	7.15	3.00
4.31	8.01	2.00

Physical Property Data

Core # PC06 (continued)

Shear Strength Data

Depth (m)	Peak (kPa)	Remoulded (kPa)
4.40	6.01	2.58
4.50	7.30	3.00
4.60	7.58	2.86
4.70	8.44	4.15
4.80	7.58	3.58
4.90	9.16	3.15
5.00	7.30	2.86
5.10	36.48	2.58
5.20	15.45	2.29
5.30	8.15	1.86
5.40	7.87	2.15
5.50	9.16	1.00
5.60	8.01	1.86
5.70	8.15	2.86
5.90	8.15	3.72
6.00	8.44	1.00
6.10	10.44	1.00
6.20	9.44	1.57
6.30	44.78	1.29
6.40	8.44	2.00
6.50	9.73	1.43
6.60	7.72	2.43
6.70	10.30	2.86
6.80	10.44	3.58
6.90	8.44	1.57
7.00	43.35	3.15
7.20	8.73	0.86
7.30	7.58	0.72
7.40	8.30	1.57
7.50	8.58	2.72
7.60	46.20	3.43
7.70	8.44	2.15
7.80	7.72	2.00
7.90	9.01	1.86
8.00	10.01	1.72

Physical Property Data

Core # PC07

Shear Strength Data

Depth (m)	Peak (kPa)	Remoulded (kPa)
0.15	2.15	0.86
0.25	3.58	0.00
0.35	4.15	0.00
0.55	2.43	0.00
0.80	6.15	0.43
0.90	4.57	0.00
1.00	4.72	0.00
1.10	4.58	1.43
1.20	5.72	0.00
1.30	5.01	0.00
1.40	7.58	3.43
1.50	8.58	0.00
1.60	6.58	0.00
1.70	8.44	3.29
1.80	7.44	3.43
1.90	9.01	2.58
2.00	9.16	2.58
2.10	11.87	2.86
2.30	7.87	2.72
2.40	8.30	5.58
2.50	7.87	3.00
2.60	7.01	4.01
2.70	8.01	0.00
2.80	7.87	0.00
2.90	8.73	2.86
3.00	8.15	0.00
3.10	7.30	0.00
3.20	8.30	3.29
3.45	7.30	2.86
3.55	8.73	0.00
3.65	8.30	0.00
3.85	13.16	5.87
4.05	12.45	3.00
4.25	10.87	2.58
4.45	9.30	3.00
4.65	10.01	3.86

Physical Property Data

Core # PC09

Shear Strenght Data

Depth (m)	Peak (kPa)	Remoulded (kPa)
0.28	4.72	3.00
0.49	11.00	0.00
0.65	14.31	2.58
0.85	13.88	3.58
0.90	2.58	2.29
1.05	15.31	4.01
1.25	21.74	5.15
1.45	11.59	4.01
1.65	12.87	0.00
1.90	14.87	0.00
2.10	9.58	0.00
2.30	42.34	0.00
2.50	90.81	7.07
2.70	39.03	0.00
2.90	12.73	0.00

REFERENCES

Adams, J., and Basham, P. 1989. The seismicity and seismotectonics of Canada east of the Cordillera. Geoscience Canada, Vol. 16, No.1, p. 3-16.

Anderson, T.W. 1982. Pollen and plant macrofossil analyses on late Quaternary sediments at Kitchener, Ontario. In Current Research, Geol, Survey Can., Paper 82-1A, p. 131-136.

Anderson, T.W. 1984. Palynological studies in Lake Erie. Geological Survey of Canada. Unpublished manuscript, p.16.

Barnett, P.J. 1978a. Glacial Lake Whittlesey: the probable ice frontal position in the eastern end of the Erie Basin. Can. J. Earth Sci., Vol. 16, p. 568-574.

Barnett, P.J. 1978b. Quaternary geology of the Simcoe area, Southern Ontario. Ontario Div. of Mines, Geoscience Report 162, p. 74.

Barnett, P.J. 1983. Quaternary Geology of the Long Point map area, Southern Ontario. Unpublished manuscript.

Barnett, P.J. 1985. Glacial retreat and lake levels, north central Lake Erie, Ontario. In: Quaternary Evolution of the Great Lakes. Eds., P.F. Karrow and P.E.Calkin. Geological Association of Canada Special Paper 30. p.185-194.

Brodzikowski, K., and Van Loon, A.J. 1987. A systematic classification of glacial and periglacial environments, facies and deposits. Earth-Science Reviews, Vol. 24, p.297-381.

Calkin, P.E., and Feenstra, B.H. 1985. Evolution of the Erie-basin, Great Lakes. In: Quaternary Evolution of the Great Lakes. Eds., P.F. Karrow and P.E. Calkin. Geological Association of Canada, Special Paper 30, p.149-169.

Coakley, J.P. 1977. Processes in sediment deposition and shoreline changes in the Point Pelee to Port Burwell, Ontario, Inland Waters Directorate, Environment Canada, Scientific Series, No.79, p.76.

Coakley, J.P. 1985. Evolution of Lake Erie based on the postglacial sedimentary record below the Long Point, Point Pelee, and Pionte-Aux-Pins Forelands. Unpub. Phd. thesis, University of Waterloo, p.362.

Coakley, J.P., and Lewis, C.F.M. 1985. Postglacial lake levels in the Erie basin. In: Quaternary Evolution of the Great Lakes. Eds., P.F. Karrow, and P.E. Calkin, Geological Association of Canada Special Paper 30, p.195-212.

Creer, K.M., Anderson, T.W., and Lewis, C.F.M. 1976. Late Quaternary geomagnetic stratigraphy recorded in lake sediments. Earth and Planetary Science Letters, vol. 31, p.37-47.

Dreimanis, A. and Karrow, P.F. 1972. Glacial history in the Great Lakes-St. Lawerence region and the classification of the Wisconsinan Stage. XXIV International Geol. Congr. Proc. Sec. 12, p. 5-15.

Edwards, T.W.D., and Fritz, P. 1987. Stable-isotope paleoclimate records for southern Ontario, Canada: comparison of results from marl and wood. Can. J. Earth Sci., Vol. 25, p. 1397-1406.

Eyles, N., Eyles, C.H., and Miall, A.D. 1983. Lithofacies types and vertical profile models; an alternative approach to the description and environmental interpretation of glacial diamict and diamictite sequences. Sedimentology, Vol.30, p.393-410.

Eyles, N., and Miall, A.D. 1984. Glacial facies. in: Facies Models. 2nd ed., Geoscience Canada, Reprint Series 1, p. 15-38.

Feenstra, B.H. 1981. Quaternary geology and industrial minerals of the Niagara-Welland area, southern Ontario. Ontario Geological Survey, open file report 5361, p.260.

Folk, R.L. 1974. Petrology of sedimentary rocks. Hemphill Publishing, Austin, Texas, p.182.

Fritz, P., Anderson, T.W., and Lewis, C.F.M. 1975. Late Quaternary climatic trends and history of Lake Erie from stable isotope studies. Science, Vol. 190, p. 267-269.

Grass, J.D. 1984. Ice scour and ice ridging studies in Lake Erie. IAHR Ice Symposium, p. 33-43.

Gelinas, P.J., and Quigley, R.M. 1973. The influence of geology on erosion rates along the north shore of Lake Erie. Proc. 16th Conf. Great Lakes Res., Internat. Assoc. Great Lakes Res., p. 421-430.

Hamilton, E.L. 1970. Sound velocity and related properties of marine sediments, North Pacific. J. of Geophysical Research, Vol.75, No.23, p.4423-4446.

Hartley, R.P. 1968. Bottom currents in Lake Erie. Proc. 11th Conf. Great Lakes Res., International Assoc. of Great Lakes Res., p 398-405.

Hill, P.R., Moran, K.M., and Blasco, S.M. 1982. Creep deformation of slope sediments in the Canadian Beaufort Sea. Geo-Marine Letters, Vol.2, p.163-170.

Hobson, G.D., Herdendorf, C.E., and Lewis, C.F.M. 1969. High-resolution reflection seismic survey in western Lake Erie. Proc. 12th Conf. Great Lakes Research, IAGLR, p.210-224.

Hough, J.L. 1958. Geology of the Great Lakes. University of Illinois Press, Urbana, p.296.

Hough, J.L. 1966. Correlation of glacial lake stages in the Huron-Erie basins. J. of Geology, Vol. 74, p. 62-77.

Kapp, R.O., and Gooding, A.M. 1964. A radiocarbon dated pollen profile from Sunbeam Prairie Bog, Darke County, Ohio. American J. of Sci., V.262, p. 259-266.

Karrow, P.F. 1963. Pleistocene geology of the Hamilton-Galt area. Ont. Dept. of Mines, Geol. Report 16, p. 68.

Kick, J.F. 1962. An analysis of the bottom sediments of Lake Erie. Unpub. MSc. Thesis, University of Toronto, p.174.

Kindle, E.M. 1933. Erosion and sedimentation at Point Pelee. Ontario Dept. of Mines, 42nd Annual Report, part 2, p.22.

King, L.H., and Fader, G.B.J. 1986. Wisconsinan glaciation of the Atlantic Continental Shelf of southeast Canada. GSC Bulletin 363, p. 1-72.

King, L.H., and Fader, G.B.J. 1991. Till-tongue stratigraphy. Geological Society of America Bulletin, Vol. 103, p.637-659.

Lewis, C.F.M. 1966. Sedimentation studies of unconsolidated deposits in Lake Erie basin. Unpublished PhD. Thesis, University of Toronto, p.173.

Lewis, C.F.M. 1969. Late Quaternary history of lake levels in the Huron and Erie basins. Proc. 12th Conf. Great Lakes Res., Internat. Assoc. Great Lakes Res., p.250-270.

Lewis, C.F.M. 1984. Lake Erie: post glacial shoreline evolution. Geological Survey of Canada, Unpublished manuscript, p.44.

Lewis, C.F.M., and Anderson, T.W. 1989. Oscillations of levels and cool phases of the Laurentian Great Lakes due to inflow from glacial lakes Agassiz and Barlow-Ojbway. Journal of Paleolimnology, Vol 2, p.99-146.

Lewis, C.F.M., and Anderson, T.W. (1990). Stable isotope and pollen trends in sediments of eastern Lake Erie during the climate reversal (11-10.5). Abstract: International Symposium, Past and Present Climate Dynamics; International Reconstruction of Rates of Change, Locarno,Switzerland, p. 13.

Lewis, C.F.M., and Anderson, T.W. (in press). Stable isotope ($\delta^{18}O$ and $\delta^{13}C$) and pollen trends in eastern Lake Erie, evidence for a locally-induced climate reversal of Younger Dryas age in the Great Lakes basin. J. of Climate Dynamics.

Lewis, C.F.M., Anderson, T.W., and Berti, A.A. 1966. Geological and palynological studies of early Lake Erie deposits. Great Lakes Research Division, The University of Michigan, No.15, p.176-191.

Lewis, C.F.M., Wooton, A.E., and Davis, J.B. 1973. Stratigraphic and engineering studies of unconsolidated sediments in central lake Erie near Erieau, Ontario. Geol. Surv. of Canada Report of Activities, Part A: April to Oct. 1972, GSC Paper 73-1, p.205-209.

Mitchum, R.M.Jr., Vail, P.R., and Sangree, J.B. 1977. Seismic stratigraphy and global changes in sea level. Part 6: Stratigraphic interpretation of seismic reflection patterns in depositional sequences. In: Seismic Stratigraphy - Applications to hydrocarbon exploration. Ed. C.E. Payton, AAPG Memoir 26, p.117-133.

Morgan, N.A. 1969. Physical properties of Marine sediments as related to seismic velocities. 37th Annual International Meeting of SEG, p.529-545.

Mudie, P.J., et al. 1984. Standard method for collecting, describing and sampling Quaternary cores for stratigraphy at A.G.C. Geological Survey of Canada, open file.

Nafe, F.E., and Drake, C.L. 1957. Variation with depth in shallow and deep water marine sediments of porosity, density and the velocities of compressional and shear waves. Geophysics, Vol.22, No.3, p.523-552.

Pincus, H.J. 1953. Investigations into Lake Erie sediments, vicinity of Sandusky, Ohio. Div. Geol. Survey, Ohio Dept. Nat. Res., Report of Investigations, No. 18, p.18.

Ross, A.R. 1950. Pleistocene and recent sediments in western Lake Erie. Unpublished PhD. Thesis, University of Michigan, p.57.

Rukavina, N.A., and St.Jacques, D.A. 1971. Lake Erie nearshore sediments Fort Erie to Mohawk Point, Ontario. Proc. 14th Conf. Great Lakes Res., Internat. Assoc. Great Lakes Res., p.387-393.

Rukavina, N.A., and St.Jacques, D.A. 1978. Lake Erie nearshore sediments, Point Pelee to Port Burwell, Ontario. Inland Waters Directorate, Enviroment Canada, Scientific Series, No.99, p.44.

Rukavina, N.A., and Zeman, A.J. 1987. Erosion and sedimentation along a cohesive shoreline, the north-central shore of Lake Erie. Journal of Great Lakes Res., Internat. Assoc. of Great Lakes Res., Vol.13, No.2, p. 202-217.

Sanford, B.V., Thompson, F.J. and McFall, G.H. 1985. Plate Tectonics-a possible controlling mechanism in the development of hydrocarbon traps in southwestern Ontario. Bulletin of Canadian Petroleum Geology, Vol. 33, No.1, p.55-71.

Scott, D.B., Mudie, P.J., Vilks, G., and Younger, D.C. 1984. Latest Pleistocene-Holocene paleoceanographic trends on the continental margin of eastern Canada: foraminiferal, dinoflagellate and pollen evidence. Elsevier Science Pub., Marine Micropaleontology, Vol. 9, p. 181-218.

Shane, L.C.K. 1987. Late glacial vegetational and climatic history of the Allegheny Plateau and the till plains of Ohio and Indiana, U.S.A. Boreas, Vol.16, p.1-20.

Sly, P.G. 1976. Lake Erie and its basin. J. Fisheries Res. Board Canada, Vol. 33, p.355-370.

Sly, P.G., and Lewis, C.F.M. 1972. The Great Lakes of Canada-Quaternary geology and limnology. 24th Int. Geol. Congress, Montreal, Quebec, Guidebook for Field Excursion, A43, p.92.

St.Jacques, D.A., and Rukavina, N.A. 1973. Lake Erie nearshore sediments-Mohawk Point to Port Burwell, Ontario. Proc. 16th Conf. Great Lakes Res., Internat. Assoc. Great Lakes Res., p.454-467.

Tinkler, K.J., Pengelly, J., and Paerkins, W. (in prep."A") Meters matter: lake levels for living along the Erie shoreline.

Tinkler, K.J., Pengelly, J., Paerkins, W., and Terasmae, J. (in prep. "B") Agassiz waters in the Erie basin.

Thomas, R.L., Jacquet, J.M., Kemp, A.L.W., and Lewis, C.F.M. 1976. Surficial sediments of Lake Erie. J. Fisheries Res. Board Canada, Vol 33, No.3, p.385-403.

Thomas, R.L., McMillan, R.K., and Keyes, D. 1991. Evidence of neotectonic activity in Lake Ontario. GAC/MAC program with abstract, Toronto, Canada.

Thomas, R.L., McMillan, R.K., Keyes, D., Bowlby, J.R., Lewis, C.F.M., and Mohajer, A.A. (in prep.). Recent faulting along the postulated extension of the St. Lawerence rift system in Lake Ontario.

Walcott, R.I. 1972. Late Quaternary vertical movements in eastern North America: quantitative evidence of glacio-isostatic rebound. Reviews of Geophysics and Space Physics, Vol. 10, No.4, p. 849-884.

Wall, R.E. 1968. A sub-bottom reflection survey in the central basin of Lake Erie. Geo. Soc. Amer. Bull., Vol.79, No.1. p.91-106.

Wilson, A.W.G. 1908. Shoreline studies on Lake Ontario and Erie. Geological Society of America Bulletin, Vol. 19, p.471-500.

Wood, H.A.M. 1951. Erosion of the shore of Lake Erie, Point-aux- Pins to Long Point. M.A. Thesis, McMaster University, p. 209.

Zeman, A.J. 1976. Geotechnical properties of Lake Erie clays. Unpublished M.Sc. Thesis, McGill Unversity, p.133.